

**HYDROGEOLOGIC INVESTIGATION OF THE UPPER JEFFERSON RIVER  
VALLEY, MADISON AND JEFFERSON COUNTIES, MONTANA:  
WATERLOO GROUNDWATER MODELING REPORT**



**Ali F. Gebril and Andrew L. Bobst**

**Montana Bureau of Mines and Geology  
Ground Water Investigation Program**



**HYDROGEOLOGIC INVESTIGATION OF THE UPPER JEFFERSON RIVER  
VALLEY, MADISON AND JEFFERSON COUNTIES, MONTANA:  
WATERLOO GROUNDWATER MODELING REPORT**

**August 2021**

**Ali F. Gebril and Andrew L. Bobst**

**Montana Bureau of Mines and Geology  
Ground Water Investigation Program**

**Montana Bureau of Mines and Geology Report of Investigation 29**





## TABLE OF CONTENTS

Abstract.....	1
Introduction.....	1
Background.....	1
Purpose and Scope.....	2
Previous Studies.....	2
Study Area Overview.....	2
Physiography.....	2
Climate.....	4
Vegetation.....	4
Land Use.....	5
Water Infrastructure.....	5
Conceptual Model.....	6
Geologic Framework.....	6
Hydrogeologic Setting.....	6
Groundwater Flow System.....	6
Hydrologic Boundaries.....	7
Aquifer Properties.....	9
Groundwater Budget.....	9
Model Design and Construction.....	10
Mathematical Framework (Governing Equation).....	10
Numerical Model Approximation and Computer Codes.....	10
Spatial Discretization.....	10
Temporal Discretization.....	11
Hydraulic Parameters.....	12
Boundary Conditions.....	12
Head-Dependent Flux Boundaries.....	12
Jefferson River.....	13
Groundwater-Fed Streams.....	16
Evapotranspiration.....	16
Specified Flux Boundaries.....	16
Alluvial Groundwater Influx and Outflux.....	16
Lateral Groundwater Influx, Upgradient Irrigation Recharge, and Canal Leakage.....	16
Jefferson Canal.....	16
Irrigation Recharge.....	17
Pumping Wells.....	17
No-Flow.....	19
Model Calibration.....	19
Initial Heads.....	19
Steady-State Calibration.....	20
Calibration Targets.....	20
Calibration Methods.....	20
Steady-State Calibration Results.....	22
Transient Calibration.....	24
Calibration Targets.....	24
Transient Calibration Methods.....	26
Stress Periods.....	26
Aquifer Storage Estimation Using PEST.....	26
Irrigation Recharge Estimation.....	27

Evapotranspiration Estimation.....	27
Canal Leakage and Lateral Groundwater Inflow .....	30
Jefferson River Flows .....	30
Jefferson River Diversions.....	30
Calibration Results.....	30
Model Verification.....	37
Sensitivity Analysis.....	37
Model Predictions (Future Scenarios) .....	41
Canal Lining Scenarios.....	46
Flood to Pivot Irrigation Scenarios.....	47
Canal Lining and Conversion to Pivot Scenario (CF) .....	48
Split Season Irrigation Scenarios .....	48
Model Prediction Results.....	48
Uncertainty Analysis.....	49
Model Limitations .....	52
Summary and Conclusions .....	53
References.....	54
Appendix A: Waterloo Area Conceptual Water Budget.....	57
Appendix B: Jefferson River Slope Calculations.....	69
Appendix C: Hunt Aquifer Test Results .....	71
Appendix D: Model Construction.....	75
Appendix E: Model Results .....	85
Appendix F: Model Sensitivity Analysis .....	97

## FIGURES

Figure 1. Upper Jefferson River project area.....	3
Figure 2. Model area—main surface-water features.....	4
Figure 3. Model area—groundwater and surface-water monitoring network .....	5
Figure 4. Model area—simplified geologic map .....	7
Figure 5. Model area—April 2015 potentiometric surface.....	8
Figure 6. Conceptual water-budget components.....	8
Figure 7. Model grid—plan view.....	11
Figure 8. Model initial horizontal hydraulic conductivity ( $K_h$ ) .....	13
Figure 9. Model boundaries .....	14
Figure 10. Model riparian evapotranspiration rates ( $ET_r$ ).....	17
Figure 11. Model segmentation of the Parrot and Creeklyn irrigation canals .....	18
Figure 12. Calibrated steady-state annual irrigation recharge rates.....	19
Figure 13. Steady-state model calibration groundwater targets.....	21
Figure 14. PEST pilot points and calibrated steady state residuals .....	22
Figure 15. Simulated steady-state potentiometric surface .....	23
Figure 16. Steady-state model computed heads versus observed heads.....	24
Figure 17. Steady-state model groundwater budget .....	25
Figure 18. Steady-state calibrated horizontal hydraulic conductivity ( $Kh$ ) .....	26
Figure 19. Transient model calibrated aquifer storage coefficients ( $S_y$ ).....	27
Figure 20. Transient model calibrated irrigation recharge.....	29
Figure 21. Transient model calibrated specified flux per well along Parrot Canal.....	30
Figure 22. Transient model calibrated specified flux per well along Creeklyn and Jefferson Canals .....	31
Figure 23. Transient model average monthly input flows at the upstream end of the Jefferson River.....	31
Figure 24. Transient model average monthly input diversions from Jefferson River.....	32
Figure 25. Transient model calibrated groundwater hydrographs (Group 1) .....	33

Figure 26. Transient model calibrated groundwater hydrographs (Group 2) .....	34
Figure 27. Transient model calibrated groundwater hydrographs (Group 3) .....	35
Figure 28. Transient model calibrated groundwater hydrographs (Group 4) .....	36
Figure 29. Transient model calibrated average monthly flows in Jefferson River at Corbett's station .....	37
Figure 30. Transient model verification results.....	38
Figure 31. Sensitivity analysis results—groundwater-fed streams (drains) .....	40
Figure 32. Sensitivity analysis results—Jefferson River flow at Corbett's station .....	41
Figure 33. Sensitivity analysis results—calibration statistic RMS .....	42
Figure 34. Sensitivity analysis results—calibration statistics RSS.....	43
Figure 35. Schematic of groundwater and surface-water interactions in the Upper Jefferson River area.....	44
Figure 36. Predictive scenarios results—groundwater-fed streams.....	46
Figure 37. Predictive scenario results—Jefferson River flow at Corbett's station .....	47
Figure 38. Water table elevations at Willow well 9 (GWIC 276285).....	49
Figure 39. Uncertainty analysis—groundwater-fed streams.....	52
Figure 40. Uncertainty analysis—Jefferson River flow at Corbett's station.....	53

## TABLES

Table 1. General stratigraphy, hydrostratigraphy, and model layers.....	6
Table 2. Preliminary conceptual groundwater budget .....	10
Table 3. Simulations applied to the Waterloo model .....	12
Table 4. Transient model—Jefferson River inflows to the model domain and diversion rates.....	15
Table 5. Irrigation recharge rates initially applied to the Waterloo model.....	18
Table 6. Transient calibration—Recharge rates applied to the Waterloo model.....	28
Table 7. Evapotranspiration rates applied to the transient calibration .....	29
Table 8. Sensitivity analysis setup and results .....	39
Table 9. Summary of extreme predictive scenarios for July and August 2024.....	44
Table 10. Summary of predictive scenarios for July and August 2024.....	45
Table 11. Uncertainty analysis parameters.....	50
Table 12. Uncertainty analysis for scenarios C1, F1, and CF .....	51



## ABSTRACT

This modeling study focuses on the area near Waterloo in the Upper Jefferson River Valley. Groundwater discharges to the Jefferson River in this area, and is important during late summer, low-flow conditions. Willow Springs and Parson's Slough also rely on groundwater discharge; these streams provide late summer flows of 40 to 60 cubic feet per second (cfs) of cool water to the Jefferson River.

Leakage from the Parrot, Creeklyn, and Jefferson Canals contributes groundwater recharge to the alluvial aquifer. Excess water applied to irrigated fields also provides substantial groundwater recharge. This irrigation-related recharge eventually discharges to the Jefferson River, Willow Springs, and Parson's Slough. There are concerns that changes in irrigation management practices, such as lining canals or changing from flood to center-pivot irrigation, may alter the volume and timing of groundwater discharge to this river and streams.

We developed a numerical groundwater flow model to evaluate the effects of changing irrigation practices on surface waters during low-flow periods. The model design was based on a conceptual model derived from the analysis of groundwater and surface-water monitoring data, aquifer tests, well logs, and GIS analysis of soil, climate, vegetation, land-use, and water-rights data.

A steady-state version of the model replicated the long-term average groundwater and surface-water flow conditions in the study area. This model was most sensitive to aquifer transmissivity and the streambed conductance assigned to Parson's Slough and Willow Springs. A transient version of the groundwater model was calibrated to conditions observed from 2013 to 2015, using time-dependent stresses (seasonal irrigation activities and changes in Jefferson River flow).

Following calibration, the transient model simulation time was extended from 2005 to 2025 to (a) verify model-simulated groundwater heads compared to data collected in 2005, and (b) run predictive scenarios. The scenarios included lining irrigation canals, converting fields from flood to pivot irrigation, and split season irrigation techniques (apply flood irrigation recharge through the middle of the irrigation season followed by pivot irrigation). The estimated reduction in groundwater discharge to Willow Springs and Parson's Slough in late summer ranged from 6 to 12 cfs (12% to 24% percent of the 50 cfs of average baseflow). More severe effects are expected in drought years. Model results demonstrate that split season irrigation would augment aquifer storage for later release to surface water; however, the timing of this additional groundwater discharge to streams is influenced by the proximity of fields to surface waters, hydraulic gradient, and aquifer transmissivity.

---

## INTRODUCTION

The Jefferson River, located in southwest Montana, regularly experiences low-flow conditions (JRWC, 2013; MTFWP, 2012). The lowest flows and highest temperatures occur during the irrigation season, triggering irrigation water shortages and trout population declines—especially in drought years. Evaluating the water resources in the Upper Jefferson River Valley can inform decisions about future development and conservation efforts in the valley. This involves understanding and quantifying the complex interactions between surface water and groundwater. One of the objectives of the Upper Jefferson Groundwater Investigation (Bobst and Gebril, 2021) is to evaluate the effects of changes in irrigation practices in the area near Waterloo on groundwater discharge

to surface water, particularly Parson's Slough, Willow Springs, and the Jefferson River. The Waterloo groundwater flow model, documented in this report, directly addresses this objective.

### Background

The Jefferson River begins at the confluence of the Beaverhead, Big Hole, and Ruby Rivers near Twin Bridges, Montana. The largest use of surface water in the Upper Jefferson River Valley is irrigated agriculture; residents of the valley rely on groundwater from the alluvial aquifer for potable water. The river is also important for the sport fishing industry. This modeling effort focuses on the area near Waterloo, a region that is critical to providing groundwater baseflow to the

Upper Jefferson River. The Waterloo model area, also referred to in this report as the Waterloo area, begins approximately 3.2 mi north of Silver Star, and extends to approximately 2.7 mi downstream from Parson's Bridge (fig. 1).

The model area, at about 2.5 mi wide by 5 mi long, covers a total area of 12.4 mi<sup>2</sup>. The Highland and Tobacco Root Mountains bound the valley on the west and east, respectively. The Creeklyn and Parrot Canals bound the model area on the west and east, respectively. The Jefferson River runs through the middle of the model area, and water is diverted from the Jefferson River into the Jefferson Canal, between Parson's Bridge and the mouth of Parson's Slough (fig. 2).

### Purpose and Scope

The Montana Bureau of Mines and Geology (MBMG) developed a numerical groundwater model to understand and quantify interactions between surface water and groundwater in the Waterloo area. This model is a field-validated tool that will allow managers and planners to simulate various water management practices and examine the effects on the area water resources, such as the Jefferson River. Hydrogeologic conditions during critical low flow periods—late summer months or drought years—are of particular interest. This report complements the Upper Jefferson Interpretive Report, which presents additional detail on the hydrogeology and geological settings of the study area (Bobst and Gebril, 2021).

### Previous Studies

Water and Environmental Technologies (WET) characterized groundwater/surface-water interactions in the Waterloo area (WET, 2006). WET collected water levels monthly from 13 private wells and 22 piezometers from December 2004 through November 2005. Stage and discharge measurements were collected from 11 surface-water sites located on the Jefferson River, Parrot Canal, Parson's Slough, and Willow Springs. Periodic discharge measurements were made on several ephemeral tributaries (Dry Boulder Creek, Beall Creek, Spring Creek, and Mill Creek) in the Tobacco Root Mountains. A surface-water budget was developed from these data. Analysis of aquifer test data conducted in alluvial deposits yielded a hydraulic conductivity of 634 ft/d. Groundwater and surface-water monitoring networks were sampled for water quality and temperature. WET concluded that changes in

irrigation practices in the Waterloo area may adversely affect late summer flows in Willow Springs. Flood irrigation recharges the aquifer, which in turn provides delayed recharge to the Jefferson River during critical low-flow periods.

A Montana Tech Master's thesis (Brancheau, 2015) prepared in association with this GWIP investigation evaluated the relationships among surface-water, groundwater, and irrigation practices in the study area. The GWIP investigation included surface-water and groundwater monitoring (water levels, river stage, discharge, and water-quality measurements) using a network of wells and surface-water sites (fig. 3). A groundwater budget was developed to evaluate the components of the flow system, and to estimate the net groundwater discharge to the Jefferson River (table A22, appendix A). Results from the Brancheau work showed that:

- groundwater flow from the aquifer discharges to several groundwater-fed streams and directly to the Jefferson River;
- changing flood irrigation to other types of irrigation applications may lower the water table and reduce groundwater discharge to those streams;
- leakage from the irrigation canals and irrigation recharge increase aquifer recharge; and
- lining the irrigation canals would reduce leakage and therefore reduce recharge to the aquifer.

### Study Area Overview

#### *Physiography*

The Waterloo model area is within the relatively flat alluvial valley of the Jefferson River, with the Tobacco Root Mountains to the east and the Highland Mountains to the west. Surface elevations range from 4,452 ft (amsl) near the northern boundary where the Jefferson River flows out of the model area to 4,525 ft (amsl) along the Creeklyn irrigation canal on the western boundary (fig. 2).

The United States Geological Survey (USGS) maintains gaging stations on the Jefferson near Twin Bridges, approximately 15 mi south of the study area (station 06026500, period of record 1941–2014) and at Parson's Bridge (station 06027600, period of record

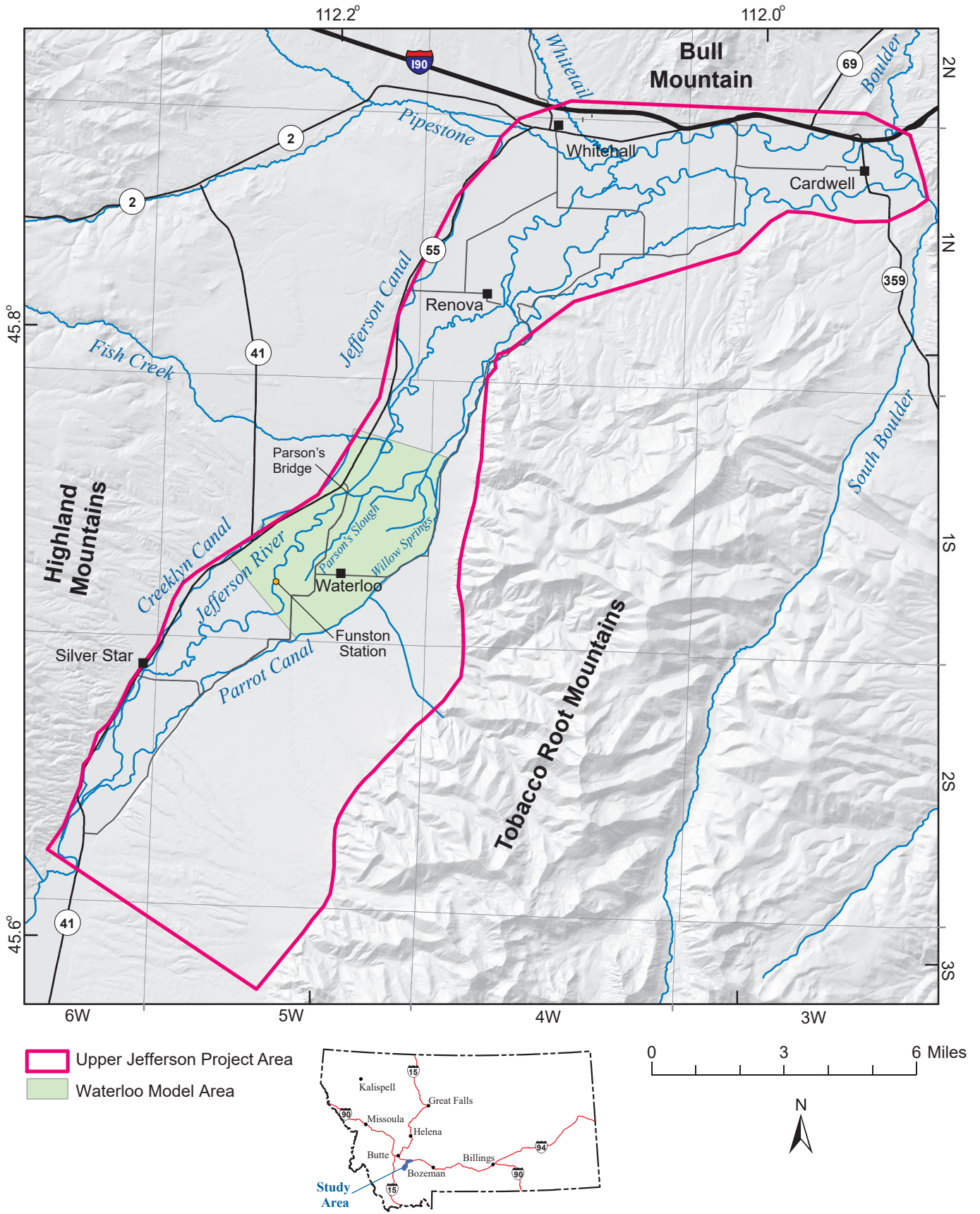


Figure 1. The Waterloo model area is located within the Upper Jefferson River Valley, within the groundwater investigation project area.

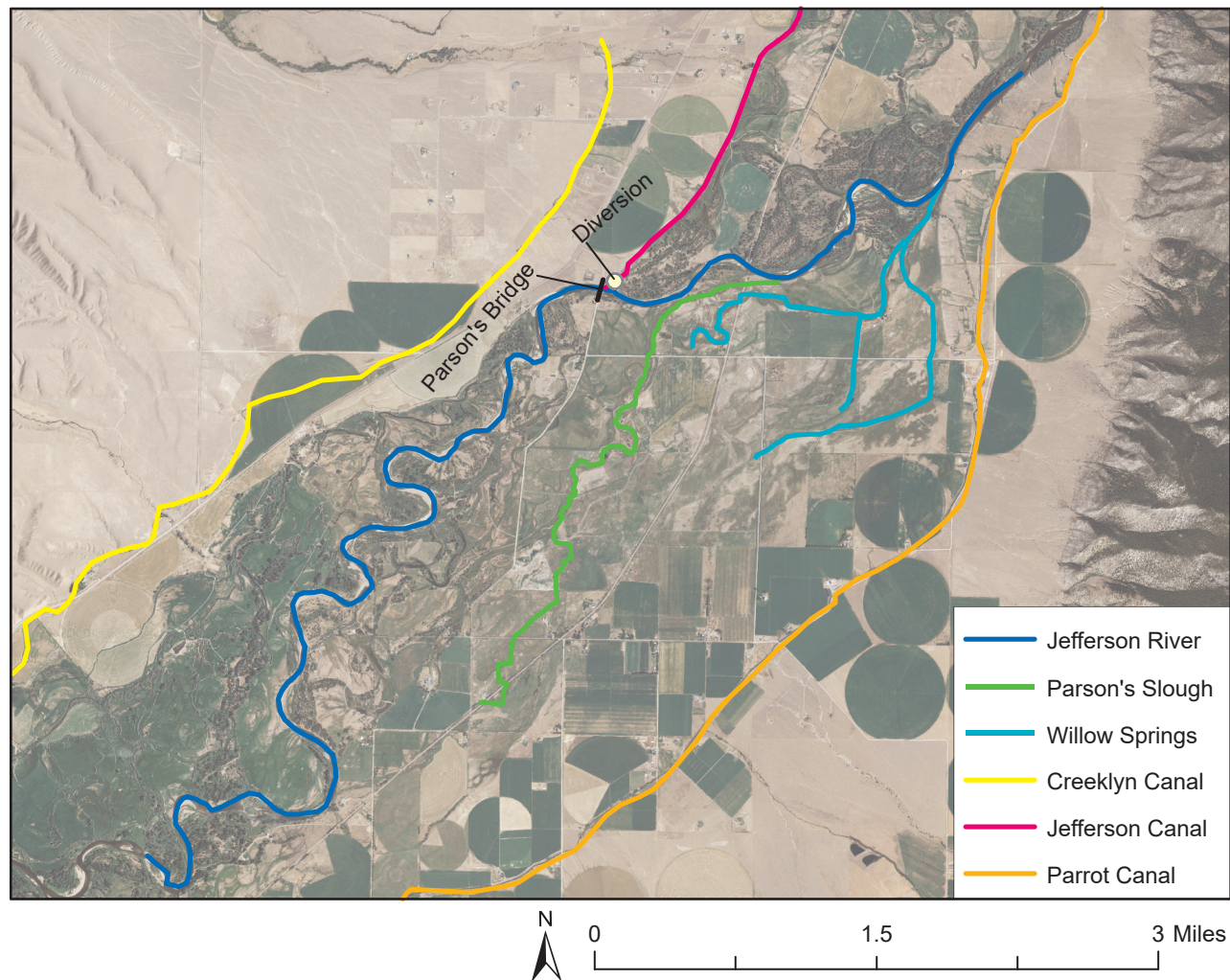


Figure 2. In the Waterloo model area, the main surface-water features include the Jefferson River, Parson's Slough, and Willow Springs (groundwater-fed streams), and the three irrigation canals: Parrot, Creeklyn, and Jefferson.

2006–2020, typically from July to September). The average flow of the Jefferson River near Twin Bridges for the period of record was 1,107 cubic feet per second (cfs), with an average annual peak flow of 9,467 cfs. Low flows occur in August, which has a mean flow of 770 cfs. The lowest mean monthly flow at the Parson's Bridge station, located downstream of the Jefferson Canal diversion and above Parson's Slough (fig. 3), was 40.5 cfs in August 2016; the lowest reported daily mean flow at Parson's Bridge was also in August 2016, at 19.9 cfs.

### Climate

Modeled 30-yr normal precipitation values (PRISM, 2014; Daly and others, 2008) show that the average annual precipitation within the Waterloo study area is about 10 in. The PRISM model indicates that precipitation in this area increases with elevation; the Highland Mountains to the west receive as

much as 32 in per year while the Tobacco Root Mountains to the east receive as much as 42 in per year. Approximately 15 mi south of the study area, in Twin Bridges, the average annual precipitation is 9.55 in (NWS Cooperative Network Station 248430-2; period of record 1950–2016); June is the wettest month in Twin Bridges (1.9 in), and February is the driest (0.2 in).

### Vegetation

Vegetation within the Waterloo area varies based on water availability. Within the alluvial floodplain and along some tributaries, riparian vegetation includes willows, cottonwoods, and wetland grasses. These phreatophyte vegetation types grow where roots can access shallow groundwater. Grass and sagebrush cover non-irrigated areas of the valley bottom and adjacent benches. Forests in the adjacent mountains include ponderosa pine, Douglas fir, lodgepole pine,

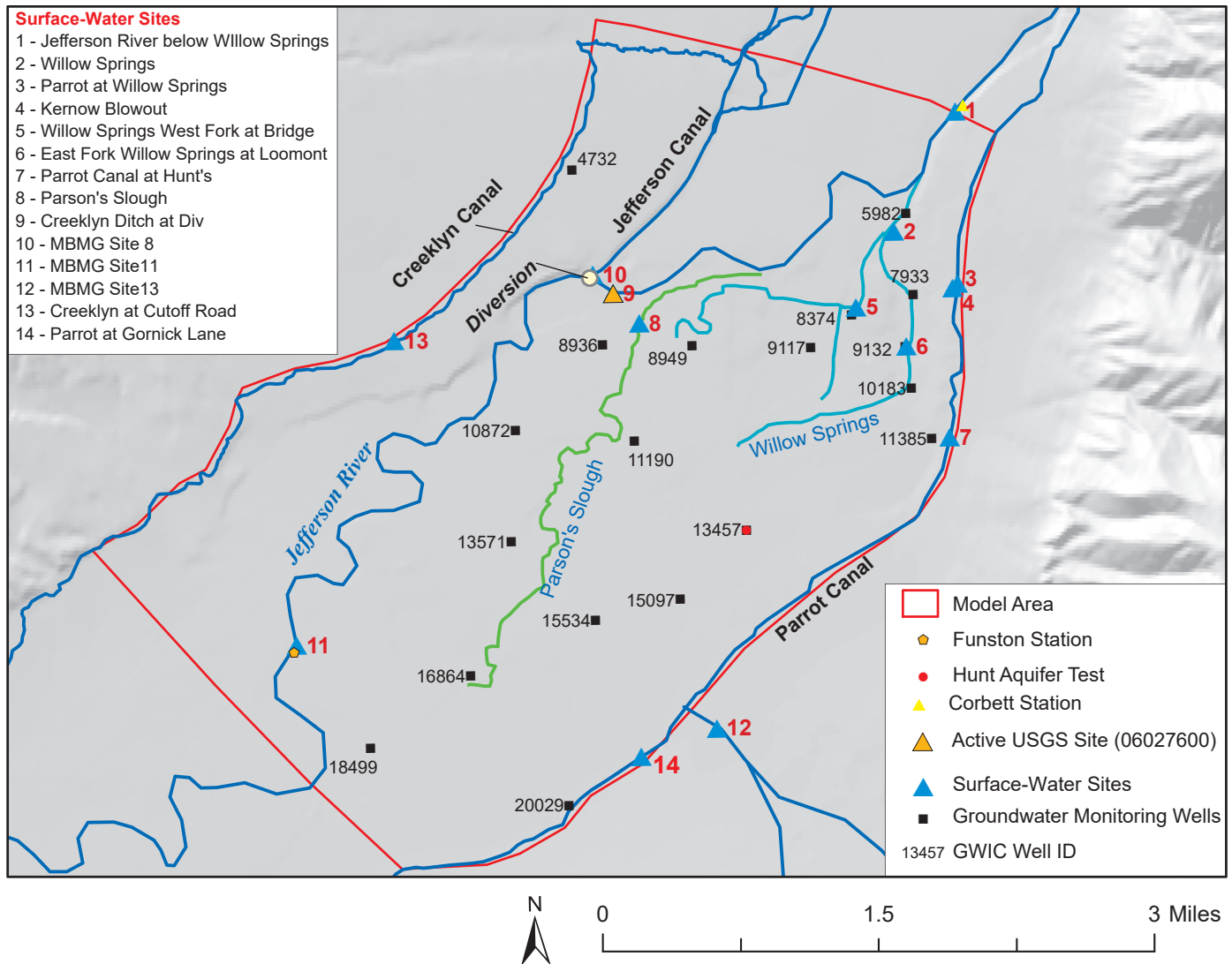


Figure 3. Groundwater and surface-water monitoring network within the model area.

Engleman spruce, and whitebark pine. Irrigated agricultural areas support mainly alfalfa and grass hay. Information from the LANDFIRE Existing Vegetation Type database (USGS, 2010a), the National Land Cover database (USGS, 2011), air photographs, field visits, and landowner interviews were used to develop a simplified map of vegetation for the study area (Brancheau, 2015).

### Land Use

About 60% of the land in the Waterloo area supports irrigated agriculture. Of the irrigated area, approximately 44% is flood irrigated, and 56% is pivot or sprinkler irrigated. Most irrigated fields use surface water diverted from the Jefferson River (via the irrigation canals). The major crops are alfalfa and grass hay. A large portion of the non-irrigated land is used for cattle grazing.

### Water Infrastructure

Within the Waterloo model area, water infrastructure includes irrigation canals (fig. 2), irrigation wells, domestic and stock wells, and septic systems. There are no public water supply or wastewater systems within the model area. The Jefferson River provides water for irrigation canals, and most irrigated fields.

Three major irrigation canals run through the model area (fig. 2). All of these canals receive water diverted from the Jefferson River. Diversions to the Parrot and Creeklyn Canals are approximately 2.8 and 4.4 mi upstream (south) of Silver Star, respectively (fig. 1). The Jefferson Canal, which runs through the north-central portion of the model area, receives diverted water immediately downstream of Parson's Bridge. Irrigation is an important source of groundwater recharge, particularly during low-flow periods (summer months

from July to September; WET, 2006). Canal leakage recharges the underlying alluvial aquifer; in addition, irrigated fields provide infiltration recharge when water is applied in excess of crop demand.

There are 61 domestic wells in the study area. In general, wells extract (pump) groundwater and septic systems return domestic wastewater to the groundwater system. For this study, we estimated domestic well pumping rates based on their net consumptive use rates; that is, the pumping rate less the amount of water returned to the groundwater system via septic systems. In addition to these domestic wells, there are 15 stock wells and 3 irrigation wells completed in the alluvial aquifer.

## CONCEPTUAL MODEL

The conceptual model for the study area describes the characteristics and dynamics of the physical process within the groundwater and surface-water flow system, based on available hydrogeologic information. The conceptual model includes the system's geologic framework, aquifer properties, groundwater flow directions, locations and rates of recharge and discharge, and the locations and hydraulic characteristics of natural boundaries (ASTM, 1995; Mandle, 2002).

### Geologic Framework

The Upper Jefferson Valley is an intermontane basin, filled with sediment transported from surrounding mountains and from the Jefferson River drainage area to the south. Tertiary and Quaternary pediment gravels occur at the base of the mountains, and Quaternary alluvium underlies the modern floodplain (Vuke and others, 2004; fig. 4). Estimates of the thickness of unconsolidated basin-fill material in the valley bottom range from about 2,000 to 10,000 ft (Brancheau, 2015). The depth to bedrock changes dramatically over short distances due to vertical offsets where faults cross the valley. These valley-crossing faults, such as the Waterloo Fault, generally trend northwest (fig. 4).

## Hydrogeologic Setting

Literature review, geologic maps, and well logs contributed to our understanding of the hydrogeologic setting. Eighty-seven well logs were reviewed from the MBMG's Ground Water Information Center (GWIC) and can be accessed through the Groundwater Investigation Program (GWIP) project page, available at <http://mbmg.mtech.edu>. Detailed information on the methods and hydrogeologic interpretation are included in Bobst and Gebril (2021).

The surficial geologic units are classified into the Quaternary alluvium in modern channels and floodplains ( $Q_{al}$ ), Quaternary alluvial terrace ( $Q_{at}$ ), and the Quaternary bench sediments ( $Q_{af}$ ; fig. 4; table 1). Unconsolidated to poorly consolidated Tertiary sediments ( $T_s$ ) underlie these units (fig. 4). Bedrock does not crop out within the model area. There are no geographically extensive confining units in the area, and the Quaternary and Tertiary sediments constitute hydrogeologic units with distinct hydrologic properties within a single alluvial aquifer.

### Groundwater Flow System

A potentiometric surface map was developed from groundwater levels measured in April 2015 (fig. 5). The map shows that on the eastern side of the study area some contours are perpendicular to the model's boundaries, generally following topography. Groundwater flows from the topographic highs—where there is relatively high groundwater recharge (mountain front recharge)—toward the center of the floodplain. The Jefferson River is slightly losing in the upstream portion of the model area, and strongly gaining in the downstream area (Bobst and Gebril, 2021). Groundwater discharges to the Jefferson River if the river is gaining, or flows approximately parallel to the river through the alluvial aquifer where the river is losing. In the floodplain, groundwater in the alluvial aquifer flows from the southwest (southern boundary) to the northeast (northern boundary). To the northeast, the

Table 1. General stratigraphy, hydrostratigraphy, and model layers.

Stratigraphy			Hydrostratigraphy	Model Layers
Quaternary bench sediments ( $Q_{af}$ )	Modern floodplain	Quaternary alluvial terrace ( $Q_{at}$ )	Alluvial aquifer	Layer 1
	Quaternary alluvium ( $Q_{al}$ )			
Tertiary sediment	Tertiary sediment	Tertiary sediment	Base of alluvial aquifer	Not simulated
Bedrock formations	Bedrock formations	Bedrock formations	Bedrock aquifer	Not simulated

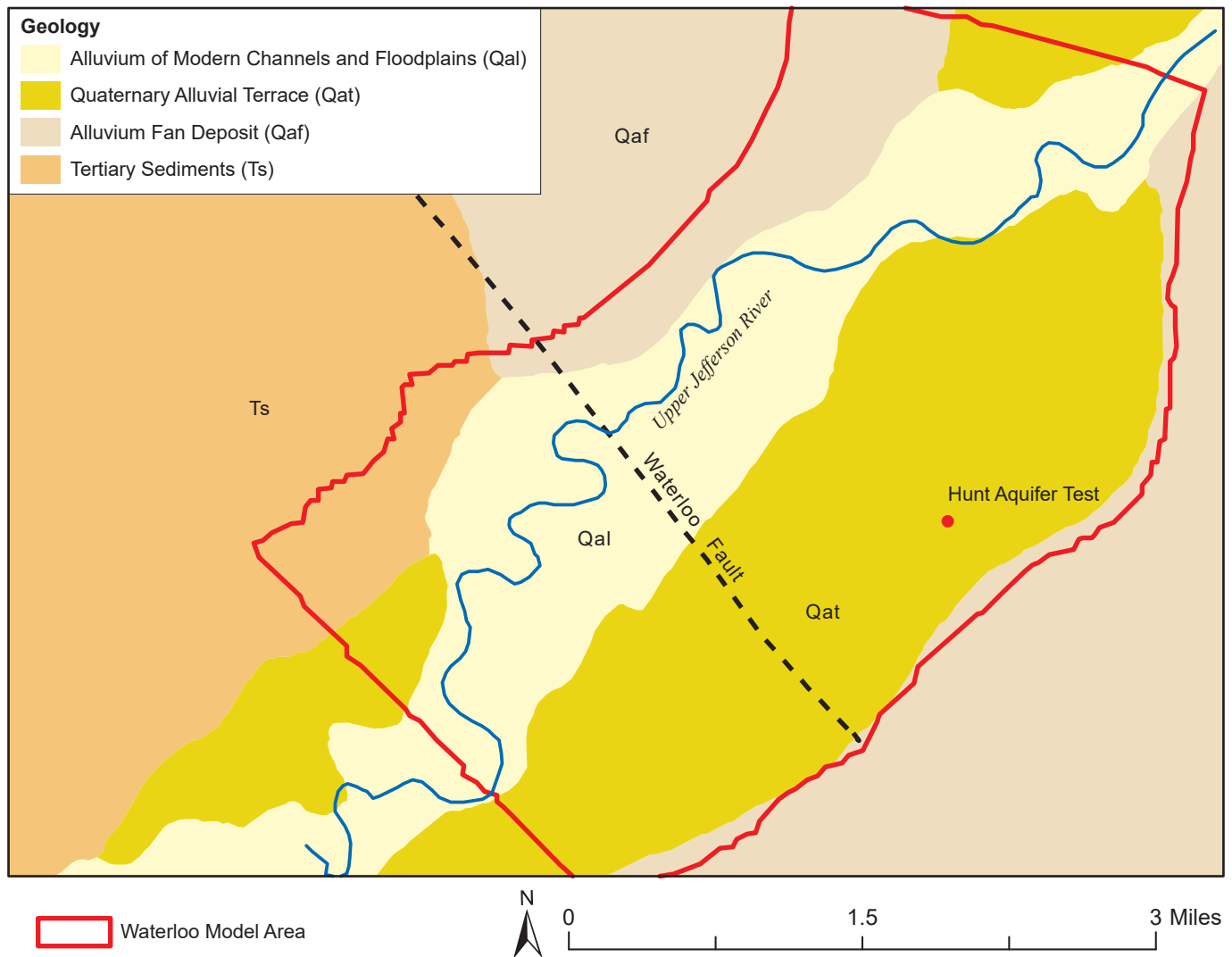


Figure 4. Simplified geologic map of the Upper Jefferson River Valley near Waterloo model area (based on Brancheau, 2015 and Vuke, 2004).

course-grained alluvium (Qal on fig. 4) narrows (fig. 4), and the potentiometric contours become more closely spaced as the hydraulic gradient increases due to decreased cross-sectional transmissivity.

### Hydrologic Boundaries

Hydrologic boundaries are features that convey water into or out of the hydrologic system, in this case, the alluvial aquifer (fig. 6). These boundaries include the Jefferson River, with an average flow of about 1,100 cfs from the southwest to the northeast. The river loses water to the aquifer along a reach upstream from the Jefferson Diversion (fig. 2), while it gains groundwater downstream of the Jefferson Diversion (Bobst and Gebiril, 2021).

The Parrot and Creeklyn irrigation canals form hydrologic boundaries along the east and west sides of the valley, respectively. Leakage from both canals

provides water to the aquifer. Lateral groundwater inflow (influx) and irrigation recharge from irrigated lands upgradient of the canals also contribute water to the model area along these boundaries.

Groundwater also flows into the alluvium on the upgradient (south) side of the model area, and discharges through the alluvium on the downgradient (north) side. These boundaries are perpendicular to the Parrot and Creeklyn Canals (fig. 3) but are limited to the floodplain. Therefore, a no-flow boundary exists perpendicular to potentiometric lines between the floodplain and the canals (along portions of the northeast edge of the model area; fig. 5 and appendix A). Since this is a single-layer model (table 1), the bottom of the alluvial aquifer is also modeled as no-flow due to it being underlain by the less permeable Tertiary Renova Formation (fig. 6; Bobst and Gebiril, 2021).

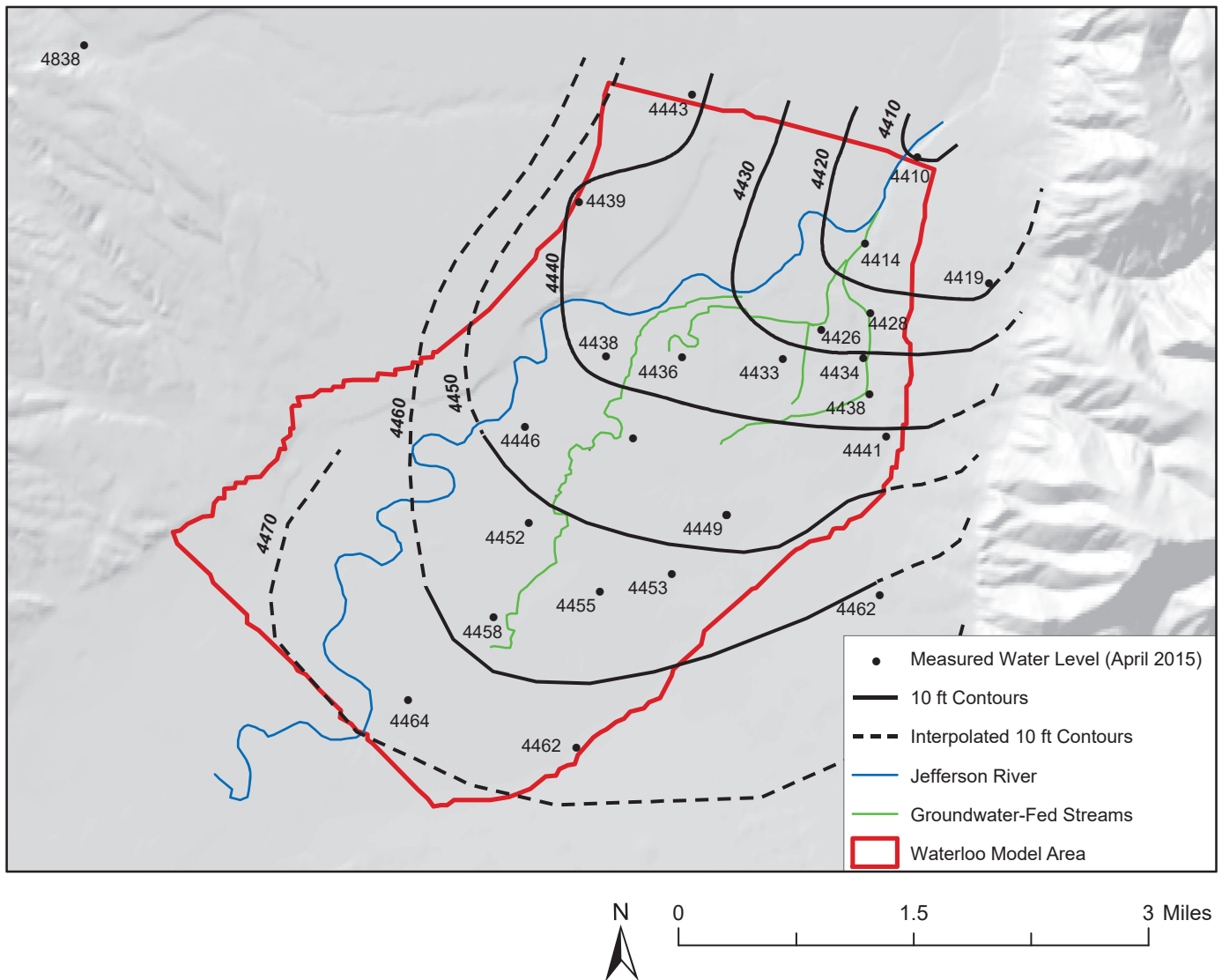


Figure 5. Potentiometric surface of the alluvial aquifer in the model area based on April 2015 groundwater-level measurements.

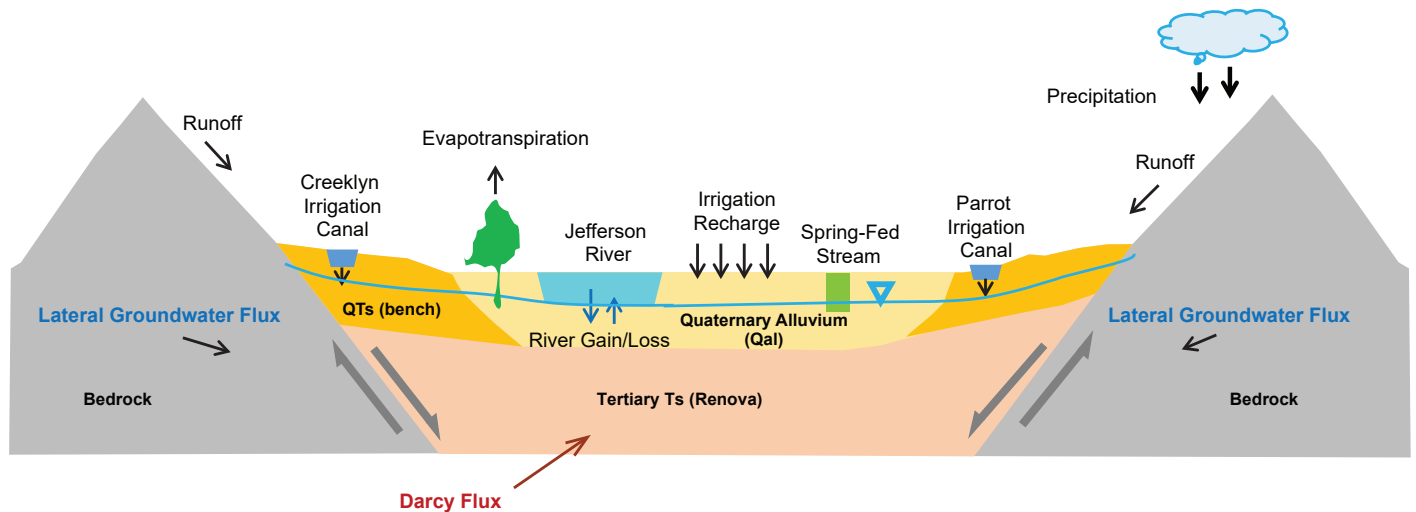


Figure 6. Flow components of the conceptual water budget. The Waterloo model focused on the top Quaternary alluvium and bench Tertiary sediments, where groundwater/surface-water interactions take place. The one-layer model extends from land surface to the bottom of the Quaternary alluvial sediments. Groundwater flow (Darcy flow) is perpendicular to the cross section.

Sources and sinks for water are also located within the model domain. Irrigation recharge, and leakage from the Jefferson Canal, add water to the aquifer. Water is lost from the aquifer via extraction wells, evapotranspiration by riparian phreatophytes and wetland grasses, and through discharge to the Jefferson River, Parson's Slough, and Willow Springs.

Storage of water in the alluvial aquifer sustains baseflow to the Jefferson River, Parson's Slough, and Willow Springs, especially during low-flow periods (e.g., late summer). A considerable amount of the water diverted from the Jefferson River to irrigation canals recharges the underlying aquifer via canal leakage and excess applied irrigation. This irrigation-related recharge causes groundwater elevations in the alluvium to rise. In low-flow periods, the aquifer discharges more water to the Jefferson River and to the groundwater-fed streams than in other periods. The rate and timing of the groundwater's release from storage depends on the gradient between the aquifer and boundaries, the transmissivity of the aquifer, and the distance between recharge areas and discharge areas.

### Aquifer Properties

Aquifer test analysis provides a range of aquifer properties such as transmissivity ( $T$ ), hydraulic conductivity ( $K$ ), and storativity ( $S$ ). We conducted one aquifer test in the alluvial aquifer within the floodplain at the Hunt Ranch, 1.6 mi southeast of Parson's Bridge (Bobst and Gebril, 2020). The wells were screened in the gravel deposits within the floodplain alluvium (Qal; table 1; fig. 4). Data analysis indicated an unconfined aquifer with a  $K$  of about 2,225 ft/d, and a specific yield  $S_y$  of 0.14 (appendix C). This hydraulic conductivity is representative of clean gravel in the floodplain alluvium (Qal). Variations in aquifer properties are expected within each hydrogeologic unit, and this value may be on the high end of the overall range for the alluvium since specific capacity data indicate these wells were more productive than other wells completed in the alluvium (GWIC, 2019). WET (2006) estimated a  $K$  of 634 ft/d for alluvium in this area. We used published values (Freeze and Cherry, 1979; Heath, 1983; Driscoll, 1986; Fetter, 2001) and aquifer test results from outside the model domain (Bobst and Gebril, 2020) to estimate the aquifer properties of the bench sediments. These values were set as the model's initial hydraulic conductivities.

### Groundwater Budget

We developed a preliminary groundwater budget for the Waterloo area to constrain the steady-state model. We based this on modifications from previous work (WET, 2006; Brancheau, 2015; appendix A). The preliminary water budget has total inflows and outflows comparable to those calculated by Brancheau (2015). Our preliminary water budget assumed quasi-steady-state conditions (no change in storage) based on groundwater-level monitoring from 2005 to 2015 (Bobst and Gebril, 2021). In addition, we calculated a monthly groundwater budget to compare it with the transient model's monthly budget (appendix A).

Inflows to the aquifer include groundwater influx from the alluvium in the south, groundwater influx from the adjacent mountain blocks, irrigation recharge, and canal leakage. Outflows are groundwater outflow through the alluvium in the north, evapotranspiration by riparian plants, well pumping, and net discharge to surface waters (Jefferson River, Parson's Slough and Willow Springs; fig. 6). This budget can be expressed as:

$$GW_{in-al} + GW_{in-lat} + CL + IR = GW_{out-al} + ET_r + WEL + SW_{net}$$

where  $GW_{in-al}$  is alluvial groundwater influx;  $GW_{in-lat}$  is lateral groundwater influx;  $CL$  is canal leakage;  $IR$  is irrigation recharge;  $GW_{out-al}$  is alluvial groundwater outflow;  $ET_r$  is riparian evapotranspiration;  $WEL$  is well pumping; and  $SW_{net}$  is net groundwater discharge to surface waters.

These budget components are summarized in table 2, with details provided in appendix A. The "flux" term used in this study refers to the volumetric flux.

Some of the separate components in the water budget were lumped into a single boundary in the model. For instance, a single specified flux boundary that extends along the Parrot Canal represents lateral groundwater inflow, upgradient irrigation recharge, and canal leakage.

## MODEL DESIGN AND CONSTRUCTION

Table 2. Preliminary conceptual groundwater budget.

	INFLOW (acre-ft/yr)		OUTFLOW (acre-ft/yr)		
	Preliminary Budget	Water-Budget Study (Brancheau, 2015)	Preliminary Budget	Water-Budget Study (Brancheau, 2015)	
Irrigation Recharge (IR)	11,096	11,595	Evapotranspiration (ET)	501	957
Groundwater Influx <sup>1</sup>	45,947	23,371	Net discharge to surface waters*	38,556	38,323
Canal Leakage (CL)	5,600	13,406	Groundwater Outflux	27,154	12,963
Lateral Groundwater Influx <sup>2</sup>	3,702	3,869	Pumping Wells (PW)	134	0
Total:	66,345	52,241	Total:	66,345	52,243

<sup>1</sup>Groundwater Influx is the Darcy flow through the southern model boundary.

<sup>2</sup>Lateral Influx is groundwater inflow from the eastern and western model boundaries.

\*Net discharge to surface water is the difference between aquifer recharge from surface water and aquifer discharge to surface water

### Mathematical Framework (Governing Equation)

In saturated groundwater conditions, a combination of continuity (mass conservation) and Darcy's Law leads to the following mathematical description of groundwater flow (Anderson and others, 2015):

$$\frac{\partial}{\partial x} \left( K_x \frac{\partial h}{\partial x} \right) + \frac{\partial}{\partial y} \left( K_y \frac{\partial h}{\partial y} \right) + \frac{\partial}{\partial z} \left( K_z \frac{\partial h}{\partial z} \right) = S \frac{\partial h}{\partial t} - W^* \quad (1)$$

In this equation the dependent variable is the hydraulic head,  $h$ , which is defined in the traditional ( $x$ ,  $y$ ,  $z$ ) Cartesian coordinate system. The horizontal ( $K_x$ ,  $K_y$ ) and vertical hydraulic conductivities ( $K_z$ ) and storage coefficient ( $S$ ) are specified. Boundary conditions ( $W^*$ ) and initial head conditions must also be specified to solve equation 1. The boundary conditions may be specified head (Dirichlet), specified flux (Neumann), or head-dependent flux (Cauchy).

### Numerical Model Approximation and Computer Codes

We used the USGS groundwater flow modeling software MODFLOW-2000 (Harbaugh and others, 2000), which provides a means to solve equation 1 and simulate the groundwater flow. MODFLOW applies the finite-difference method to approximate the solution. Groundwater Vistas (version 6.77, build 9; Environmental Simulations Incorporated, 2011) was used as the graphical-user interface (GUI) for MODFLOW. We relied on PEST, a general-purpose param-

eter estimation utility (Doherty, 2010, 2013a,b), to aid in model calibration.

### Spatial Discretization

The model grid was overlain on a map of the Waterloo area and was set to the North American Datum 1983 Montana State Plane coordinate system, in units of International Feet. The rectangular grid frame encompassed the Jefferson River Valley study area near Waterloo, and cells outside of the model area were inactivated. The model consisted of a single layer representing the unconfined Quaternary aquifer. In single layer, there is no vertical hydraulic gradient ( $\partial h/\partial z$ ), therefore, the *vertical* flow term is not calculated. This approach provides simplicity and maintains reasonable solution stability, and reduces run times for PEST and model execution. The grid consisted of 150 rows and 150 columns (22,500 cells) with uniform grid spacing of 178.18 ft x 188.66 ft (fig. 7). This refined cell size avoided placing multiple boundary conditions (such as a well located close to a stream) in a single cell. The model layer thickness ranged from 199 ft to 215 ft based on topography of the land surface. Additional details on the model grid are in appendix D and table D1.

Initially the top elevation of the grid was set using a Digital Elevation Model (DEM) derived from the USGS 1-arc second National Elevation Dataset (USGS, 2009). The DEM data point spacing was about 98 ft (30 m). Survey data from several wells in

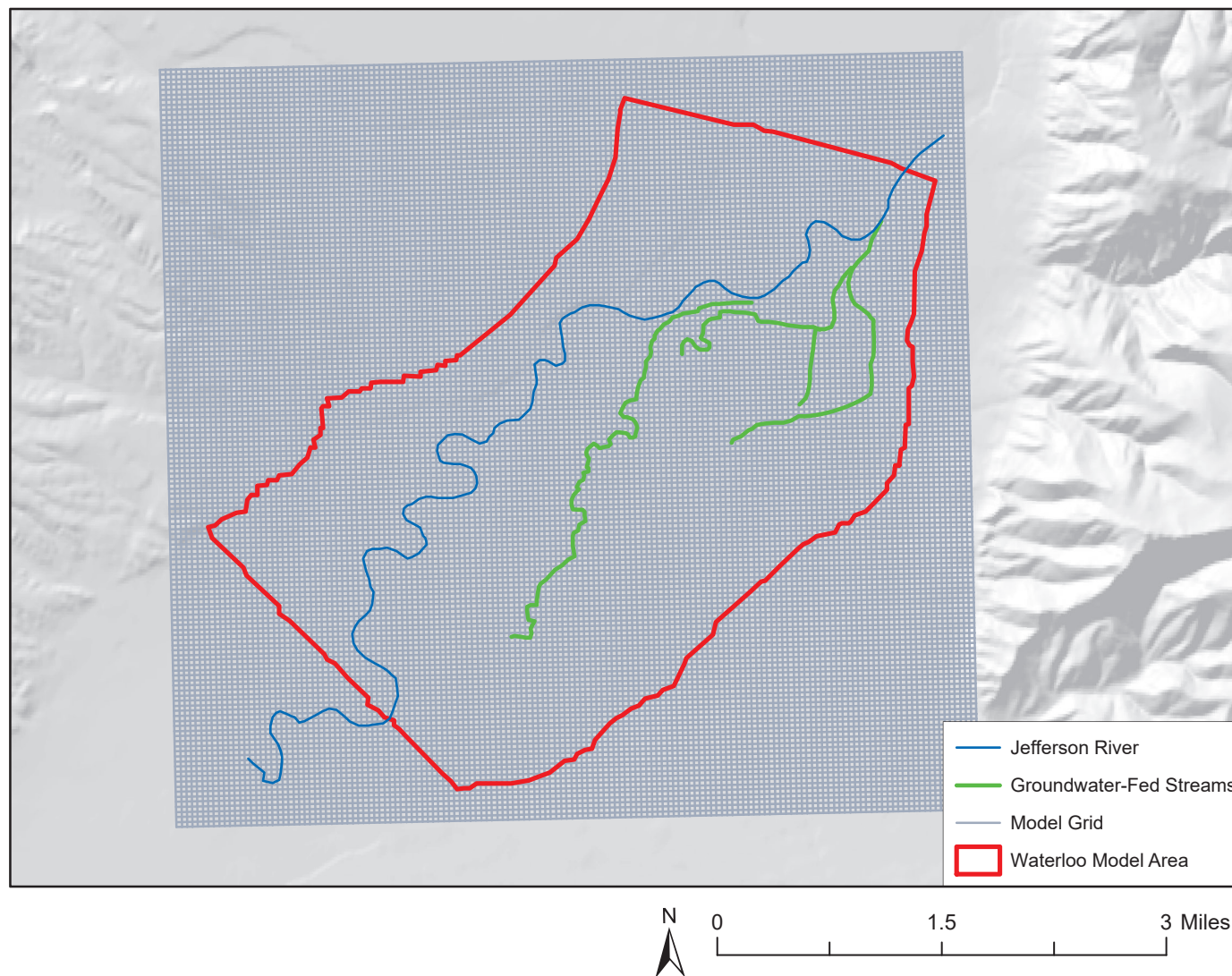


Figure 7. The model grid consisted of 150 rows and 150 columns (22,500 cells) with a cell size of about 178 ft x 188 ft.

the model area were not in agreement with the DEM. To correct the top elevations, the difference between the survey data and the DEM were defined and extrapolated by kriging with linear variogram (using Surfer 9 software). The DEM-based cell-top elevations were adjusted using the extrapolated differences (fig. D1, appendix D).

### Temporal Discretization

Steady-state models generally reflect average conditions and do not consider time-dependent parameters (storage coefficient, pumping schedules, seasonality of incoming boundary fluxes, irrigation rate changes, etc.). Transient simulations support time-dependent parameters that vary throughout the simulation period. Transient models can be used to verify past conditions and to simulate future predictive scenarios. Table 3 summarizes the Waterloo model simulations.

The transient model imposes monthly stress periods to simulate variations in seasonal stresses, such as irrigation recharge. Each stress period consists of six time steps to accommodate field observations, help numerical stability, and minimize run times. The duration of each time step depends on the length of the month, and ranges from 4.7 to 5.2 days (table D2, appendix D).

The transient calibration period included 31 monthly stress periods (2 yr and 7 mo) from April 1, 2013 to October 31, 2015. A one-day steady-state simulation was included as the first stress period of the transient simulation, resulting in 32 stress periods in the calibrated model. Thus, the heads from the one-day steady-state model were used as initial heads for the transient model.

Table 3. Simulations applied to the Waterloo model.

Simulation Type	Stress Periods	Duration	Simulation Period	Notes
Steady-State	1	Day	Not applicable	Simulates equilibrium state using average boundary conditions (e.g., pumping rates, recharge, etc.)
Transient Calibration	31	Months	April 2013 through October 2015	Simulate changes in groundwater heads and average monthly river flows for comparison to monitoring data collected during this study (2013–2015)
Model Verification	141	Months	April 2004 through October 2015	Simulates changes in heads for comparison to data collected by WET (2004–2005)
Prediction (future scenarios)	260	Months	April 2005 through October 2025	Simulates changes in groundwater levels, and Jefferson River flow and spring-fed stream discharge caused by different scenarios

### Hydraulic Parameters

Prior to steady-state model calibration, we divided the active grid cells into four aquifer property zones, representing the floodplain alluvium (Qal; zone 1), the alluvial terrace (Qat; zone 2), and the western (zone 3) and eastern (zone 4) bench sediments ( $Q_{at}$ ,  $Q_{af}$  and  $Ts$ ; figs. 4, 8). Anisotropy for this study is assumed equal to 1 ( $K_x = K_y$ ) based on the aquifer test data; we used  $K_h$  to express horizontal hydraulic conductivity and  $K_v$  for vertical hydraulic conductivity instead of  $K_z$ . Initial values for  $K_h$  were assigned to these zones (fig. 8) as described in the Aquifer Properties section. We assumed a vertical hydraulic conductivity ( $K_v$ ) of 10% of the horizontal ( $K_h$ ); however, since there is no vertical hydraulic gradient ( $\partial h/\partial z$ ) within the model cells, the vertical flow term is zero (eq. 1). These initial parameter values were modified during model calibration (see Calibration section).

### Boundary Conditions

Flow model boundary conditions control the addition or removal of water (mass) from the model. Boundary conditions are mathematical expressions of the state of the aquifer system that constrain the model equations; they are assigned to the edges of the model domain and to internal sources and sinks (ASTM,

1995). In the Waterloo model, boundary conditions (fig. 9) follow the conceptual model discussed in the Hydrologic Boundaries section.

### Head-Dependent Flux Boundaries

We applied head-dependent flux boundaries (Cauchy boundary type) to represent surface-water features in contact with groundwater, and the removal of groundwater by plants through evapotranspiration (ET). Assuming the Jefferson River is hydraulically connected with the underlying aquifer, we simulated the Jefferson River with MODFLOW's stream package (STR), and used the drain package (DRN) to simulate Parson's Slough and Willow Springs. Evapotranspiration was calculated with MODFLOW's EVT package.

During model execution, solving the groundwater flow equation involves calculations of the exchanged flow rates between the groundwater and the head-dependent flux boundaries. The STR package allows water to flow from the groundwater to the stream (gaining stream), or from the stream to groundwater (losing stream). The DRN and EVT packages only remove water from the model; groundwater-fed streams simulated with the DRN package cannot lose flow to the groundwater system. In the transient model, the

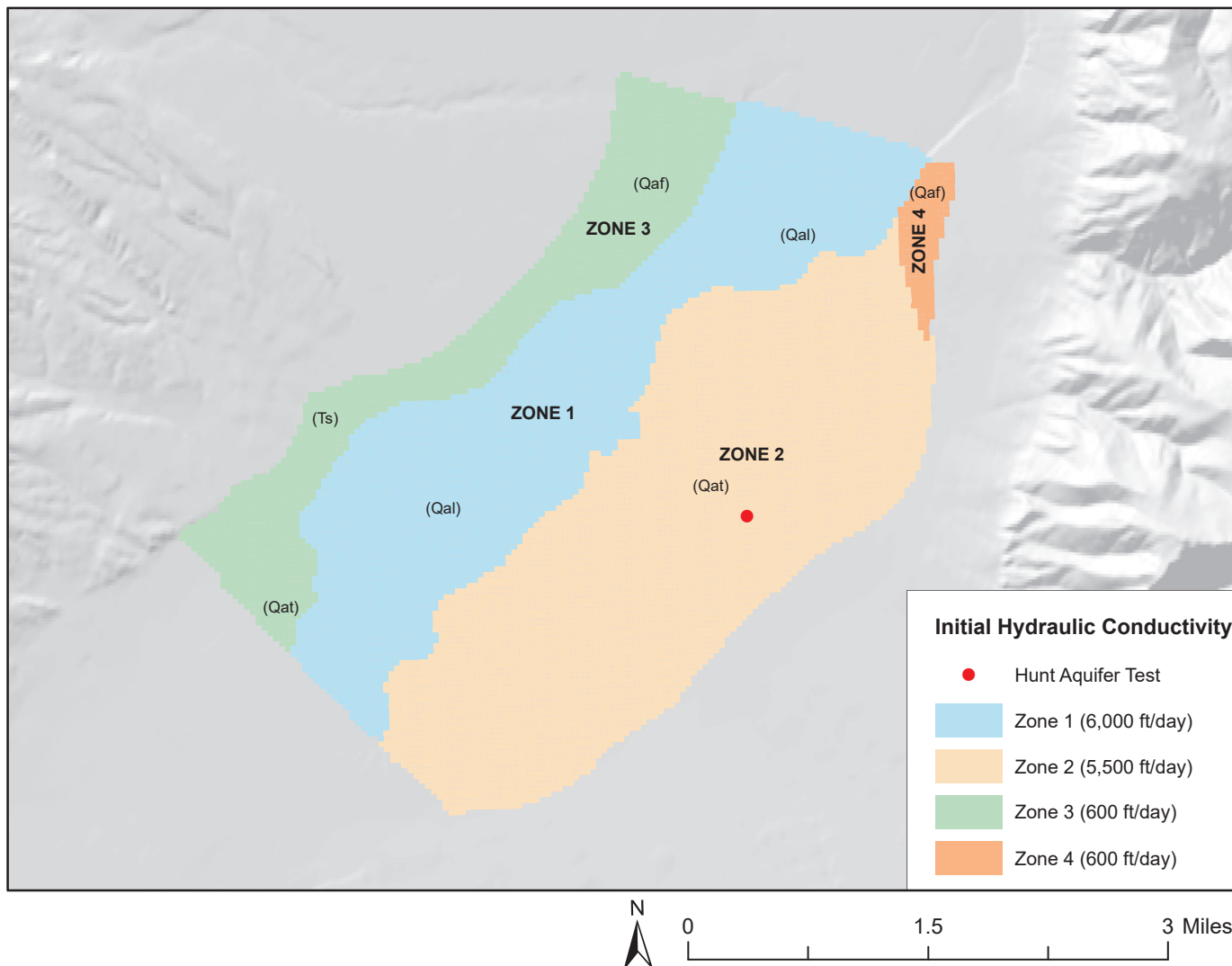


Figure 8. The initial aquifer properties were designated into zones based on horizontal hydraulic conductivity ( $K_h$ ). Figure 4 and table 1 show geologic units.

rates at which water flows to or from these boundaries can change over time as a result of changing stresses. Thus, when head-dependent boundaries are used, the model quantifies changes in flow to one part of the system due to changes in other parts within the model domain. For instance, the model will simulate a reduction in groundwater flow to a stream as a result of a decrease in nearby canal leakage.

Jefferson River

In reality, the Jefferson River loses flow to groundwater in some areas, and gains groundwater as baseflow in other areas. Gaining and losing stretches of the river may also change seasonally. MODFLOW STR package terminology defines a “reach” as the portion of the stream specific to a grid cell (fig. D2, appendix D). A series of connected reaches with uniform or linearly changing properties that have tributary inputs to

the first reach and/or a diversion from the final reach is a “segment.” A group of one or more connected segments is a “network.” In the Waterloo model, the Jefferson River is divided into three stream segments (fig. D3, appendix D).

The STR package requires the specification of several variables, including flow entering the segment, streambed top elevation, hydraulic conductivity ( $K_v$ ) of the riverbed sediments, length ( $L$ ), width ( $W$ ), bed thickness ( $M$ ), streambed roughness, and channel slope ( $S$ ). The STR package does not explicitly account for direct precipitation. Evaporation from the river is assumed negligible.

The STR Package (fig. D4, appendix D) calculates flux across the streambed as:

$$Q_b = C (h_b - h_{ijk}),$$

where  $Q_b$  is the flux across the streambed,  $C$  is the streambed conductance,  $h_b$  is the head in the stream, and  $h_{ijk}$  is the head in the aquifer.  $C$  is a function of riverbed material thickness, riverbed vertical hydraulic conductivity  $K_v$ , stream width, and the length of the stream reach. We set the starting value of the streambed conductance equal to  $K_v$ , about 10% of the initial estimate of aquifer horizontal hydraulic conductivity—these values were later adjusted during model calibration.

The STR package routes water through the stream network by applying Manning’s equation to determine depth as function of flow and assumes rectangular channel dimensions. Manning’s equation requires a roughness coefficient ( $n$ ), which is defined as:

$$n = \frac{\phi}{Q} AR^{2/3} S^{1/2},$$

where  $\phi$  is a constant ( $L^3/T$ ; in English Units 1.486

cfs);  $Q$  is the stream discharge ( $L^3/T$ ; cfs);  $A$  is the cross-sectional area ( $L^2$ ; ft<sup>2</sup>);  $R$  is the hydraulic radius (cross-sectional area divided by the wetted perimeter;  $L$ ; ft); and  $S$  is the channel slope ( $L/L$ ; ft/ft; unitless).

Manning’s coefficient  $n$  was estimated for the Corbett monitoring site on the Jefferson River (GWIC 278156; fig. D3, appendix D) based on survey data and measured stage and flow. The estimated  $n$  value of 0.040 was assigned to all cells representing the river. Our estimate is similar to coefficients developed by the USGS for similar streams, such as the Middle Fork Flathead River near Essex, Montana (0.041; Barnes, 1967).

Streambed elevations were specified for each cell. Surveyed elevations at the Funston (GWIC 278427) and Corbett (GWIC 278156) surface-water stations were applied to calculate an average riverbed slope of 0.001732 ft/ft (appendix B). Applying the same

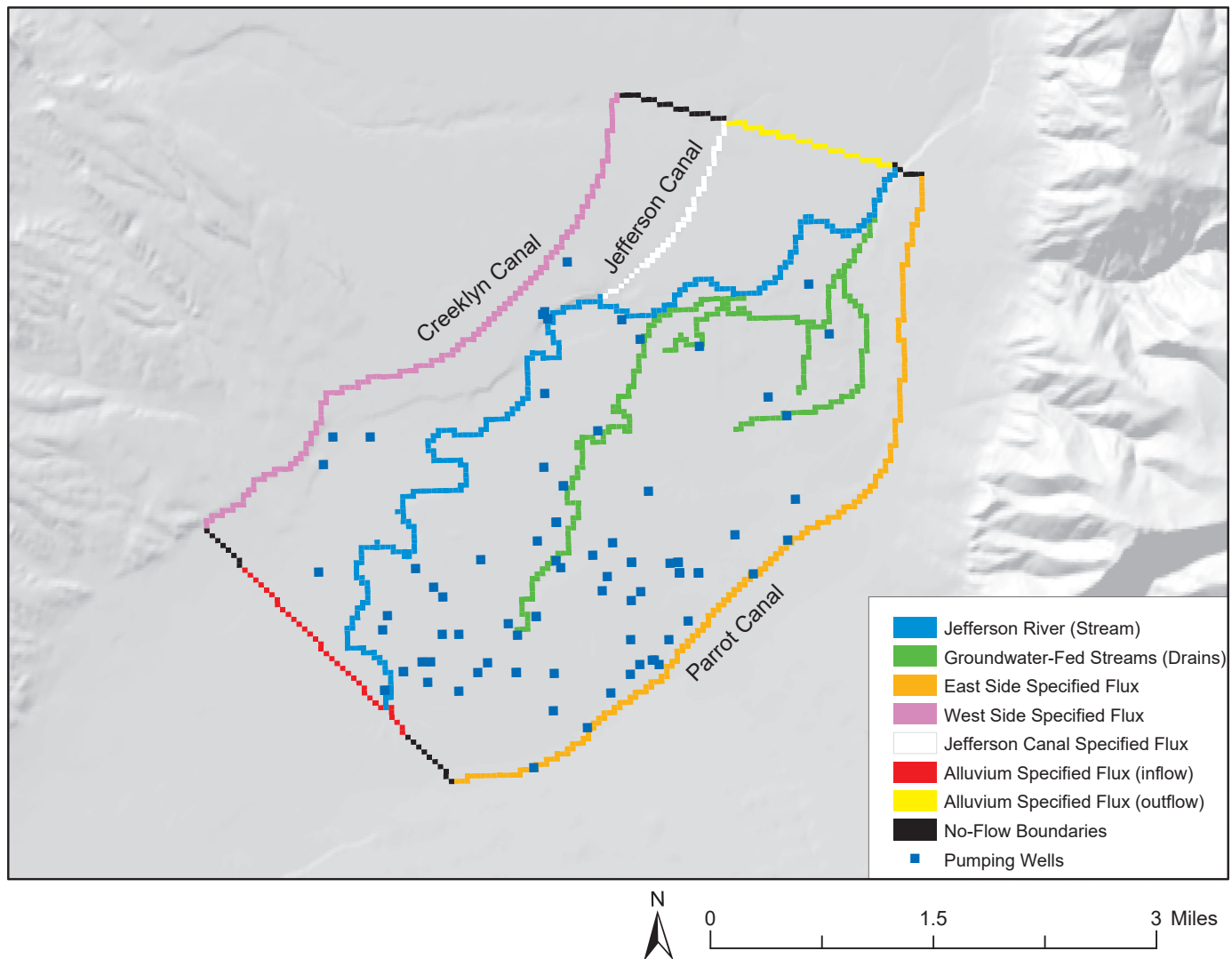


Figure 9. The model boundaries are based on the conceptual model (fig. 6); they include specified heads (drains), mixed specified heads and specified flux (stream), specified flux (wells used to simulate canal leakage and groundwater flux), and no-flow boundaries.

method, the slope between the Funston station and the upstream station near Silver Star (GWIC 277191; fig 1) was estimated as 0.001362 ft/ft (appendix B). These slopes were used to estimate streambed elevations for the Jefferson River through the Waterloo model domain.

Three segments were used in the STR package (fig. D3, appendix D). Segment 1 represents the Jefferson River from the southern model boundary to the Jefferson Canal. Segment 2 was a single cell simulating diversion from the Jefferson River into the Jefferson Canal, at the location of staff gage GWIC 274575. Segment 3 represents the Jefferson River from the Jefferson Canal to the northern model boundary, near Corbett station.

Segments 1 and 3 consist of a number of grid cells (reaches). The STR package calculates surface-water stage in each reach using Manning's equation for open channel flow. STR also calculates the exchange between the stream and groundwater (gain and loss) in each cell based on the head difference between surface-water and groundwater, and streambed conductance. The net surface-water flow is then

routed to the next reach in the segment. The STR package either routes all the water in the last reach (cell) to the next downstream segment, or splits the water between the downstream segment and a diversion.

In the model, flow enters the simulated Jefferson River at the first upstream cell in segment 1. In the steady-state simulation, an average flow of 1,724 cfs was the input flow (table 4). The input goes into the first upstream cell and the STR package calculates how much flow enters the next cells. In transient simulations, the monthly average flow was varied based on estimates from data collected between April 2013 and May 2015 (table 4). At the Jefferson Canal diversion (the downstream end of segment 1) water is diverted to the Jefferson Canal, an outflow through segment 2, or routed to segment 3 (the downstream reach of the Jefferson River), or split between diversion outflow and routed flow through segment 3. Diversion flow at segment 2 is input to the model as the average monthly flow obtained from available diversion records at GWIC 274575 (table 4).

Table 4. Transient model—Jefferson River inflows to the model domain and diversion rates.

Month	Multiplier	Monthly Inflow		Month	Diversion**	
		(cfs)	Inflow* (ft <sup>3</sup> /d)		(cfs)	Diversion (ft <sup>3</sup> /d)
Jan	0.80	1,031	7.13E+07	Jan	0	0
Feb	0.80	1,072	7.41E+07	Feb	0	0
Mar	0.80	1,256	8.68E+07	Mar	0	0
Apr	1.10	2,130	2.02E+08	Apr	13	1.09E+06
May	1.10	3,442	3.27E+08	May	64	5.50E+06
June	1.00	4,690	4.05E+08	June	59	5.11E+06
July	1.00	1,742	1.51E+08	July	77	6.61E+06
Aug	1.05	664	6.02E+07	Aug	93	8.00E+06
Sept	1.15	835	8.29E+07	Sept	47	4.05E+06
Oct	1.00	1,286	1.11E+08	Oct	0	0
Nov	0.90	1,378	1.07E+08	Nov	0	0
Dec	0.80	1,164	8.04E+07	Dec	0	0

Note. Average Monthly Inflow(cfs)\*\* = 1,724. Average Monthly Diversion (cfs)\*\* = 29. The average monthly flow of 1,724 cfs and diversion of 29 cfs are applied in the steady-state model.

\*Inflow, the monthly inflow in cfs adjusted by a multiplier and converted to CFD.

\*\*Flows obtained from GWIC 274575.

## Groundwater-Fed Streams

Groundwater-fed streams were modeled using the Drain Package (DRN). Drains remove water from a model cell whenever the groundwater elevation is higher than the elevation of the drain bed. The drainage flux is calculated from the drain conductance and the difference between the groundwater and drain elevations (fig. D5, appendix D). This flux calculation is the same as in the STR package, except that drains never add water to the aquifer, whereas the STR package allows streams to lose flow to the aquifer.

We modeled Parson's Slough and Willow Springs as drains (285 drain cells; fig. D3, appendix D) since they are formed by groundwater discharge, and there is no evidence that they lose water to the aquifer. The drain cells were grouped into nine reaches. Parson's Slough has two reaches (1 and 9) and Willow Springs has seven reaches (2 to 8). Note that the STR and DRN packages both use the term "reach," but in the STR package a reach is a single cell, while in the DRN package a reach denotes a group of cells.

Drain elevations were set initially at 2 ft below ground surface based on air photos and survey data. These elevations were adjusted during steady-state calibration. The DRN package calculates bed conductance in the same way the STR package calculates the streambed conductance. Initial  $K_v$  values were 10% of the initial estimate of  $K_h$  and were later adjusted during model calibration.

## Evapotranspiration

The MODFLOW EVT Package simulates riparian evapotranspiration ( $ET_r$ ) as a flux equal to the portion of groundwater consumed by riparian vegetation. This flux depends on the head in the cell and on three user-specified variables: maximum extinction depth, the  $ET_r$  surface elevation, and maximum  $ET_r$  rates. The extinction depth was set to 10 ft below ground surface in cells with riparian vegetation land cover (phreatophytes and grasses; Leenhouts and others, 2006; Scott and others, 2004; Shah and others, 2007). The  $ET_r$  surface elevation was set equal to the land surface elevation (the top) of each cell. As shown in figure 10, maximum  $ET_r$  rates were set to 22 in/yr for woody plants and 3 in/yr for riparian grasses (similar to Bobst and others, 2016).

## **Specified Flux Boundaries**

Specified flux boundaries add or remove a specified amount of water. In this model specified flux boundaries were implemented as injection or extraction wells (WEL package), or recharge (RCH package). These boundaries simulated alluvial groundwater flow into and out of the model along portions of the southern and northern edges, respectively, lateral groundwater inflows from east side and west side boundaries, irrigation recharge, leakage from irrigation canals, and pumping from wells.

## Alluvial Groundwater Influx and Outflux

As discussed in appendix A (appendix A, fig A1, tables A5, A6, A11, and A12), groundwater flow into and out of the alluvial aquifer was calculated using Darcy's Law. At the southern model boundary, inflow was initially set as 46,742 acre-ft/yr and later reduced to 37,781 acre-ft/yr during calibration. This adjusted value was within the range of the uncertainty inherent in this calculation. The outflow at the northern model boundary was set as 25,962 acre-ft/yr, based on the preliminary water budget (appendix A). These rates were used in both the steady-state and the transient models.

## Lateral Groundwater Influx, Upgradient Irrigation Recharge, and Canal Leakage

Along the eastern and western edges of the model, specified flux boundaries (injection wells) supplied water to the model along the Creeklyn and Parrot Canals. These boundary flows combine lateral groundwater inflow, upgradient irrigation recharge, and canal leakage. The combined inflow was estimated in the preliminary water budget. The long-term average inflow was used in the steady-state simulation, while the rates varied monthly according to changes in canal leakage and irrigation recharge in the transient simulation. We divided the Parrot Canal boundary into five segments, and the Creeklyn Canal into three segments to account for spatial variation in both canal leakage and irrigation recharge from upgradient irrigated fields (fig. 11).

## Jefferson Canal

Canal leakage from the Jefferson Canal was also simulated as specified flux, using injection wells (fig. 11). This canal differs from the Creeklyn and Parrot Canals, in that it only represented canal leakage. The

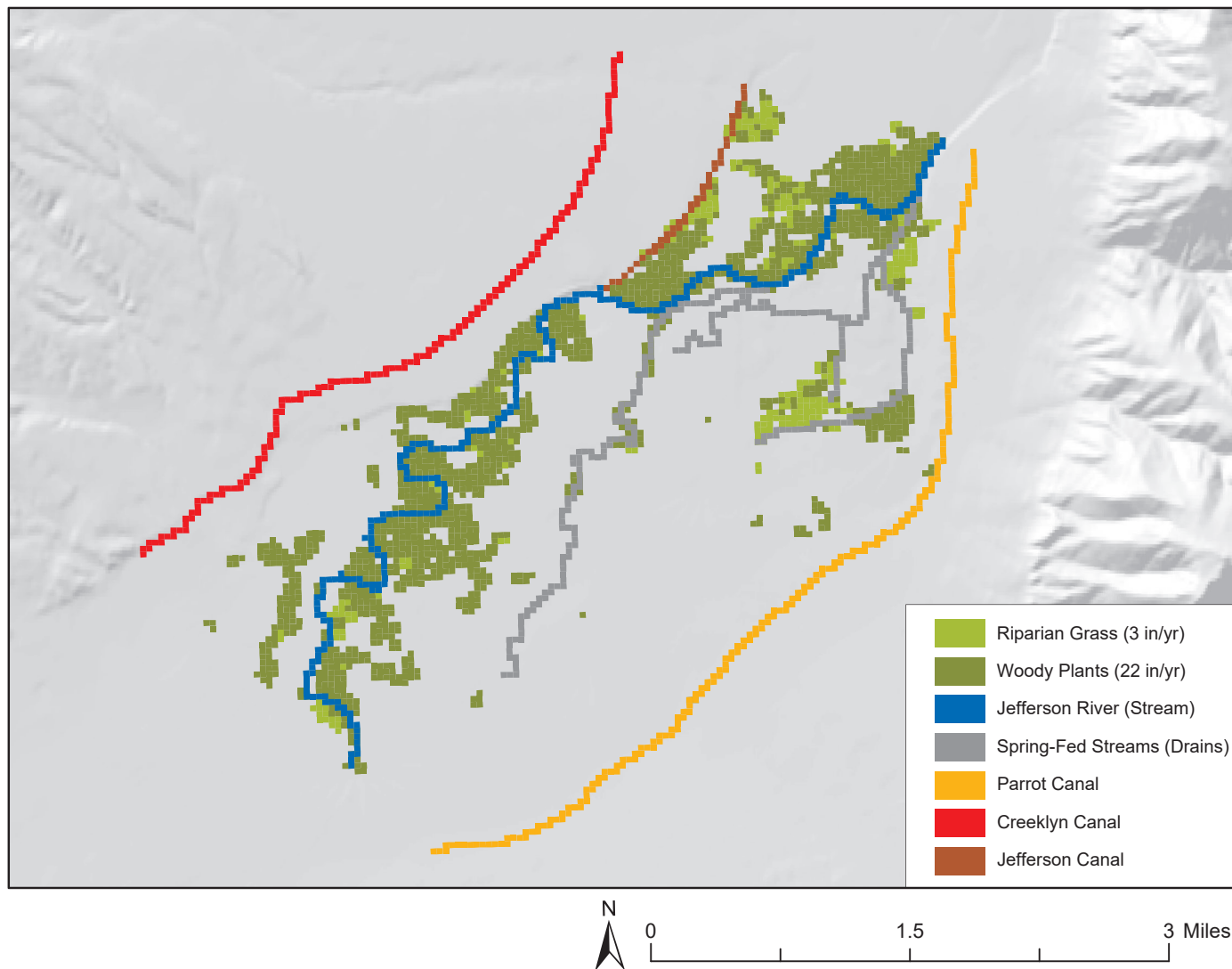


Figure 10. The distribution of the riparian evapotranspiration rates ( $ET_r$ ), limited to areas with riparian grass and woody plants, concentrated along the Jefferson River, Parson’s Slough, and Willow Springs.

Jefferson Canal was assigned the average leakage rate applied to the Parrot and Creeklyn Canals (appendix A).

Irrigation Recharge

Irrigation recharge supplies water to the model through the MODFLOW Recharge package (RCH), which is a specified flux boundary. The RCH package applies flux in units of length over time (L/T) applied over an area (L<sup>2</sup>). We applied irrigation recharge rates to portions of the model where land use was designated as irrigated fields. These areas were derived from the Statewide Final Land Unit classification database [Montana Department of Revenue (MDOR), 2012], field visits, and landowner interviews. The rate applied varied by irrigation method, crop type, and source water (appendix A; tables A9, A10). We estimated an annual recharge rate for each of six irrigation and crop types in the model area; initial values are shown in

table 5. Figure 12 shows the calibrated average irrigation recharge rates for the crop types and application methods. For the transient models, this recharge was only applied during the irrigation season, and the rate was slightly adjusted during calibration (Transient Calibration section).

Pumping Wells

The MODFLOW WEL package simulated pumping from domestic, stock, and irrigation wells (fig. 9) with overall water consumption of about 134 acre-ft/yr. The annual consumption is made of 76% irrigation water, 22% domestic water, and 2% for livestock (appendix A). The domestic well average annual consumptive is 435 gallons per day (gpd; or 58.15 ft<sup>3</sup>/d) per residence, based on rates determined for the North Hills, located near Helena, Montana, with a climate similar to that of the Waterloo area (Waren and others, 2013).

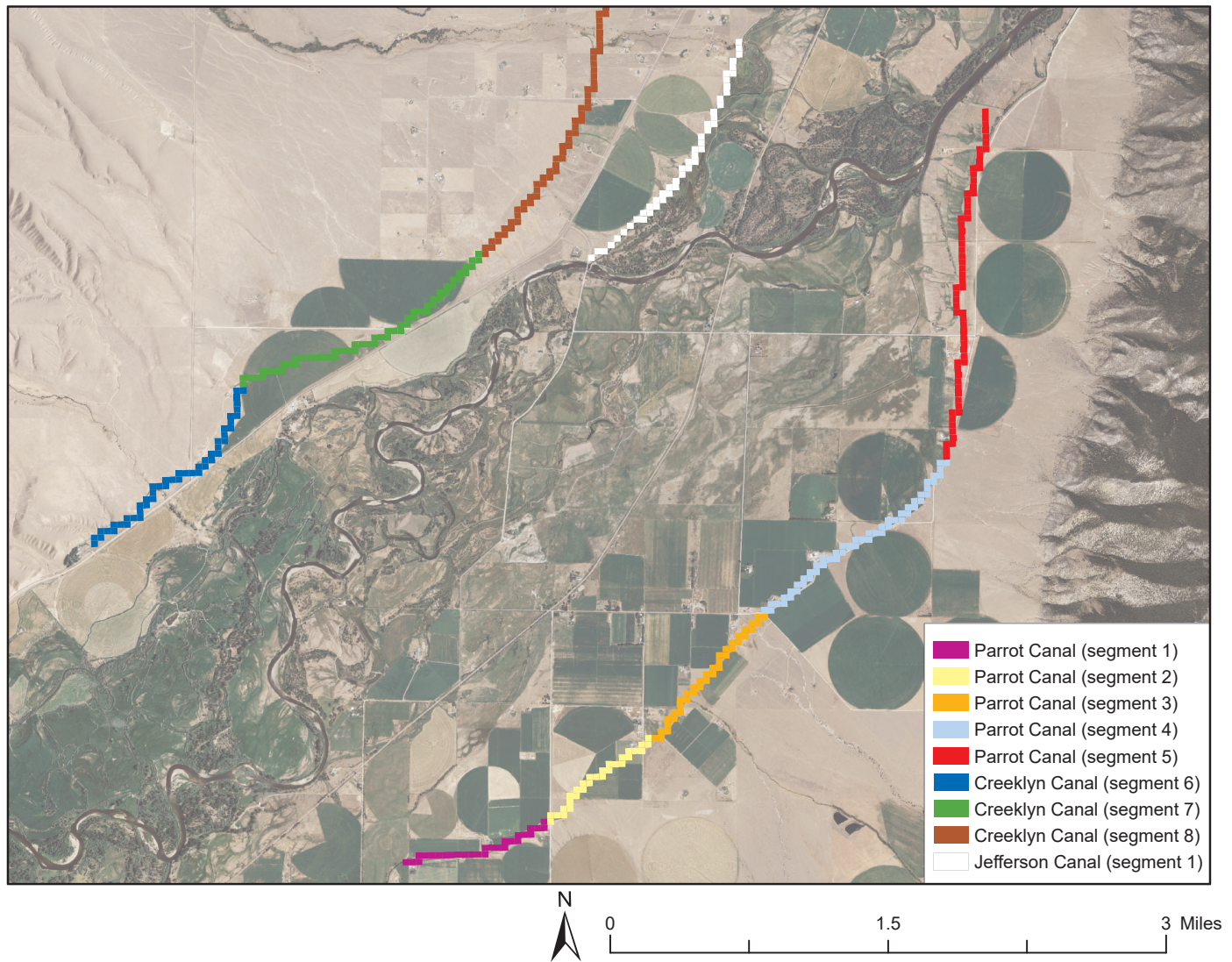


Figure 11. Dividing the Parrot and Creeklyn irrigation canals into segments helped to improve the model transient calibration. Segments correspond to the location and the extent of the irrigated fields outside the model area.

Table 5. Irrigation recharge rates initially applied to the Waterloo model.

Month**	Multiplier	Flood	Sprinkler	Pivot
		Avg. Recharge (ft/d)*	Avg. Recharge (ft/d)*	Avg. Recharge (ft/d)*
		6.33E-03	9.16E-04	5.06E-04
Apr	1	6.33E-03	9.16E-04	5.06E-04
May	2	1.27E-02	1.83E-03	1.01E-03
Jun	2	1.27E-02	1.83E-03	1.01E-03
Jul	2	1.27E-02	1.83E-03	1.01E-03
Aug	2	1.27E-02	1.83E-03	1.01E-03
Sep	2	1.27E-02	1.83E-03	1.01E-03
Oct	1	6.33E-03	9.16E-04	5.06E-04

\*The average recharge for each irrigation type is applied in the steady-state model.

\*\*Recharge rates for each irrigation type are applied from April through October in transient simulations.

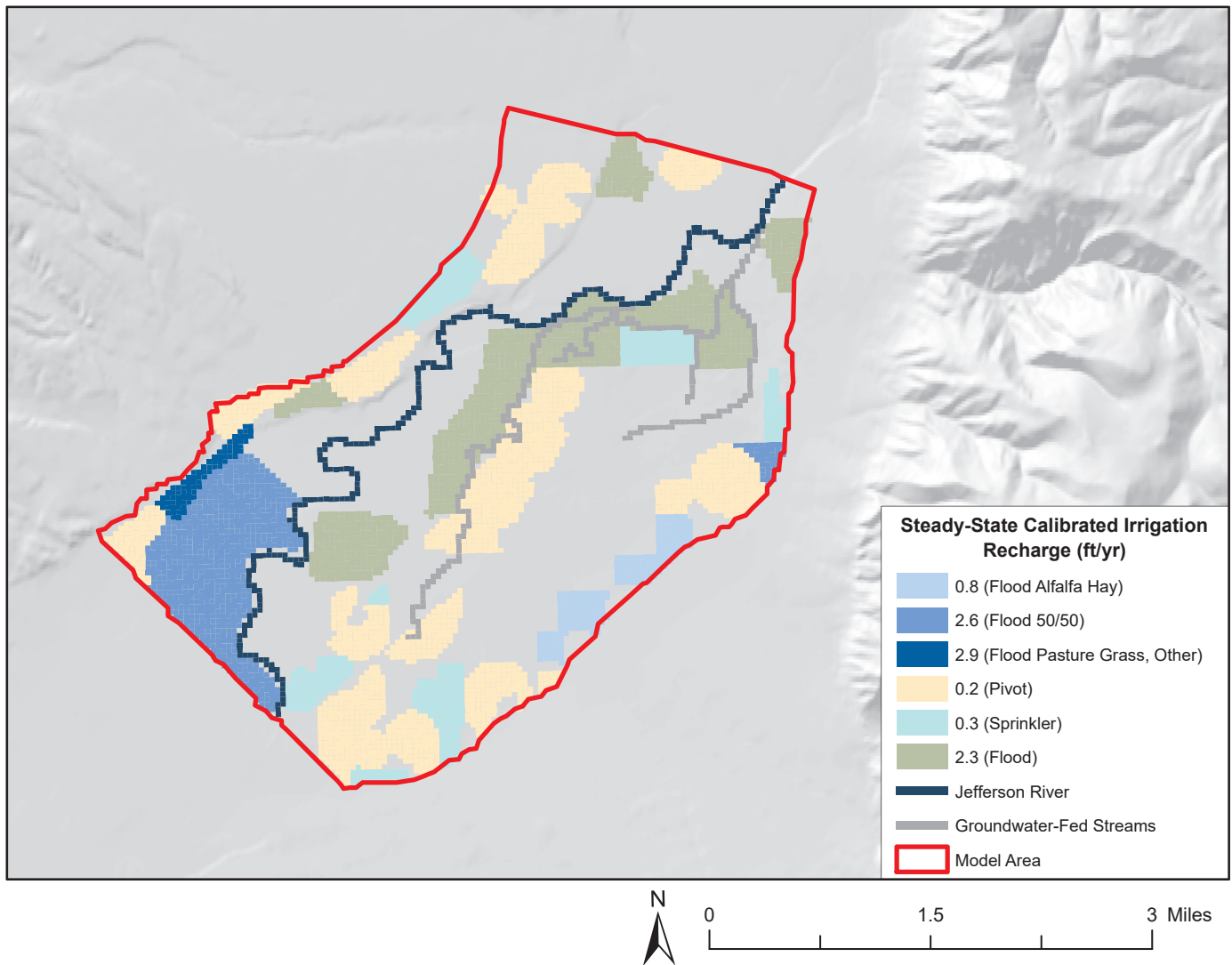


Figure 12. Calibrated steady-state annual irrigation recharge rates.

### No-Flow

No-flow boundaries are a type of specified-flux boundary where the flux is zero. No-flow boundaries were used along portions of the southern and northern sides of the model, where flow lines are parallel to the model boundaries (figs. 5, 9). These boundaries are set in areas where the potentiometric surface suggests little to no flow entering or leaving the model domain. At the southern edge of the model, no-flow boundaries extended from the Parrot and Creeklyn Canals to the alluvium. At the northern edge of the model, they extended from the Creeklyn Canal to the Jefferson Canal and from the Parrot Canal to the Jefferson River (fig. 9).

## MODEL CALIBRATION

In model calibration, changes are systematically made to model parameters in order to match field observations within some acceptable error. For this

model field observations included groundwater elevations, stream elevations, and stream flows. The ultimate goal of model calibration is to find a set of model parameters that make the model useful to predict future system behavior with confidence. One challenge in model calibration is commonly known as the *non-uniqueness problem*: the possibility that different combinations of model parameters may provide an equally good match to field measurements, resulting in another version of the calibrated model. For this model, we used field observations, the settings of the hydrogeologic units, aquifer test results, published values for aquifer properties, and the preliminary groundwater budget (appendix A) to reduce the possibility of creating a non-unique model.

### Initial Heads

April 2015 water levels were the basis for initial heads in the model (fig. 5). The values were extrapo-

lated over the modeling domain using Surfer 9 to make an initial-head surface. During the steady-state calibration, the head results from one run were used as the initial heads for the next run to improve model run times. The final steady-state calibrated heads were set as the initial heads for the transient simulations.

### Steady-State Calibration

A steady-state model simulates the groundwater flow system in equilibrium with its boundary stresses. The goal of the steady-state calibration was to estimate the model's parameters, within a reasonable range of field observations and published values, to simulate the mid-April 2015 heads distribution, while maintaining a water budget consistent with observations (appendix A). A steady-state simulation can be useful in predicting the effect to the groundwater flow system from potential stress changes; quantifying the total groundwater budget; and estimating stream and drain conductance independently from storage parameters (Doherty and Hunt, 2010). In this study, we calibrated the steady-state model by adjusting hydraulic conductivities ( $K_h$ ), streambed conductance, and drain conductance. The steady-state calibrated model produced a set of heads and boundary fluxes applied to the first stress period (1-d steady-state period) in the transient simulations.

### Calibration Targets

Calibration targets included observed groundwater elevations, stream flows, groundwater discharge to the Jefferson River between Parson's Bridge and Corbett's station, and groundwater discharge to Parson's Slough and Willow Springs.

The groundwater-monitoring network initially was composed of 25 wells in the Waterloo area. Groundwater-level data were generally collected monthly from July 2013 through October 2015. To avoid the effects of snowmelt and irrigation, data from April 13, 2015 were selected as the steady-state (average) head calibration targets. Four wells (GWIC 276103, 276127, 276041, 276113) were dry on April 13, 2015; therefore, they were excluded from the target list. Only heads from the remaining 21 wells were used (fig. 13); table E1 in appendix E lists the selected target wells.

The calibration criterion for groundwater head was set as a  $\pm 5$  ft head residual, approximately 10% of the 50 ft range (maximum head - minimum head)

observed in April 2015. We evaluated the steady-state model calibration using overall error statistics of the head residuals, i.e., the residual mean (ME); the mean of the absolute value of the residuals (MAE), and the root mean square (RMS) error.

It is worth noting that there are no calibration targets in the west and southwest regions of the model domain (hachured lines in fig. 13). Although the lack of targets in these areas may have affected the estimation of streambed conductance, the model was insensitive to this parameter (sensitivity analysis section). In addition, the eastern and northeastern portions of the model domain are the primary focus of this modeling study, where Parson's Slough and Willow Springs originate and groundwater discharges to the Jefferson River.

Groundwater flux and streamflow targets facilitated the calibration of the bed and streambed conductance in DRN and STR packages, respectively. A surface-water flow target was set at the last stream cell, representing Corbett's station on the Jefferson River. Groundwater discharge targets were assigned along the stream segments (fig. 13). During calibration, discharge to the stream segments was compared to the average net groundwater discharge to the river that was calculated in the preliminary water budget.

The ability of the model to simulate the average groundwater discharge to Parson's Slough and Willow Springs was important for evaluating the steady-state calibration. We compared the simulated steady-state discharge to the drains (Parson's Slough and Willow Springs) to their average flow (from field data); the average target ranged between 35 cfs and 60 cfs.

### Calibration Methods

Calibration of the steady-state model involved the use of the automated parameter estimation software PEST and limited manual adjustments of hydraulic conductivity ( $K_h$ ). PEST is executed independently of MODFLOW, and it is not involved in solving the governing flow equation. In order to determine the quality of fit to observed data, PEST automatically varies one—or a group—of the model's input parameters (e.g., hydraulic conductivity, conductance, recharge, etc.) within a specified range, runs the MODFLOW flow model, and then evaluates the model's output (e.g., heads) by minimizing an objective function (ME, RSS, RMS, etc.).

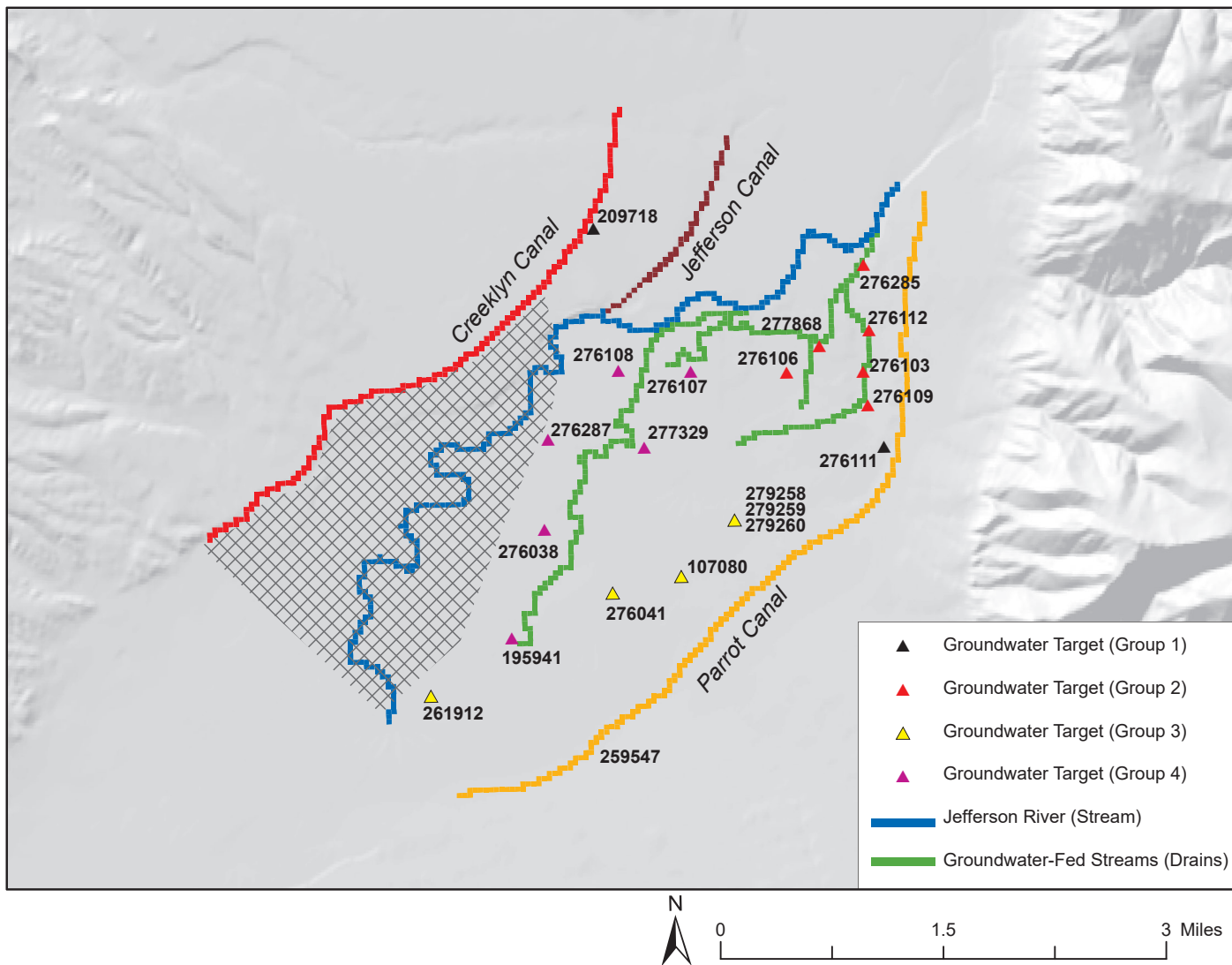


Figure 13. Model calibration groundwater wells (targets) divided into four groups based on location. The hachured lines show the part of the model domain without target wells.

The objective of calibration is to minimize the difference between the model output and observed values (i.e., to minimize the residuals). For groundwater heads, the goal was to minimize the sum of squared residuals (RSS), consequently reducing the average simulation error, typically presented as the root mean squared error (RMS). For Jefferson River flows, the goal was to minimize the difference between simulated average monthly flow and the measured average monthly flow at Corbett’s station. For the groundwater-fed streams, the objective was reducing the difference between the simulated discharge to the drains and the measured combined average discharge for Parson’s Slough and Willow Springs.

In the steady-state model calibration, we applied PEST to estimate the horizontal hydraulic conductivity distribution ( $K_h$ ), Jefferson River bed conductance (segments 1 and 3), and Parson’s Slough and Willow

Springs bed conductance. The  $K_h$  was initially divided into four zones determined by the geology (figs. 4, 8). However, with this set up, PEST could not produce a calibrated model; simulated heads did not meet calibration criteria even within the same hydraulic zone, suggesting a greater heterogeneity in aquifer properties. Therefore, the calibration was repeated using the PEST pilot points method. The pilot points method generates parameter values at selected points (pilot points) within the model grid, which in turn serve as surrogate parameters, and their values are interpolated onto the model domain. The interpolation method is specified by the user. For this model, we selected the ordinary kriging interpolation method with an exponential variogram, utilizing default values provided by Groundwater Vistas, and an applied search radius of 2,500 ft. A uniform grid was initially used to create PEST ( $K_h$ ) pilot points. Additional pilot points were

added in areas near the drain to enhance calibration in those areas. Seventy-eight pilot points helped to achieve the calibrated steady-state model (fig. 14). Pilot point values were constrained by upper and lower bounds established for the geologic setting in the area (floodplain, bench, etc.). The bounds established for each area were typically within an order of magnitude of those defined by the aquifer test data (Bobst and Gebril, 2020), the conceptual model, and by published values (Freeze and Cherry, 1979; Fetter, 2001). Most pilot points in the floodplain alluvium fell within hydraulic conductivity values of 1,000 and 6,000 ft/d. However, pilot points near Parson’s Slough and Willow Springs (drains) had a lower range (100 to 500 ft/d); for the bench sediments (within zone 3, fig. 8), the range was from 1 to 285 ft/d.

### Steady-State Calibration Results

The calibrated model simulates the Jefferson River with a steady-state flow of 1,727 cfs at segment 3, comparable to the long-term average flow at Corbett’s station (~1,690 cfs). The average simulated net groundwater discharge to the Jefferson River (stream segments 1 and 3) was 8 cfs, which is about 70% of 12 cfs, the average groundwater discharge estimated for 2014 (Broncheau, 2015). Streambed conductance averaged  $1.3 \times 10^7$  ft<sup>2</sup>/d in stream segment 1, and  $5.6 \times 10^6$  ft<sup>2</sup>/d in segment 3. Simulated discharge to Parson’s Slough and Willow Springs (combined) was 47 cfs, which is within the established range of 35 to 60 cfs.

The model reasonably simulated the potentiometric surface in the model area (fig. 15). Qualitatively, the potentiometric contours show the expected in-

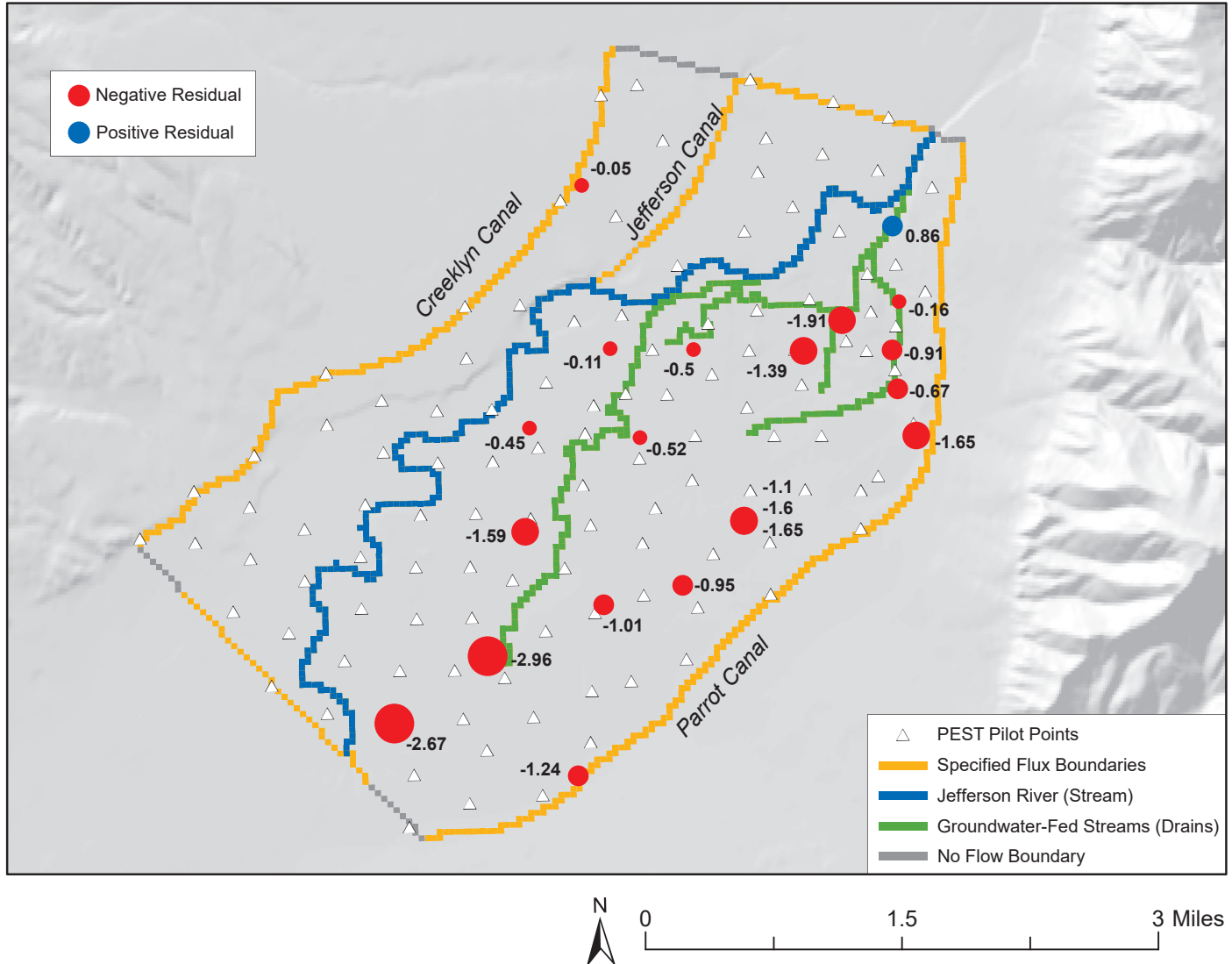


Figure 14. PEST pilot points and calibrated steady-state residuals. Placing 78 pilot points enabled PEST to estimate the heterogeneous hydraulic conductivity within the model domain. The steady-state calibrated head residuals from 21 target wells were all below 5 ft (calibration criteria).

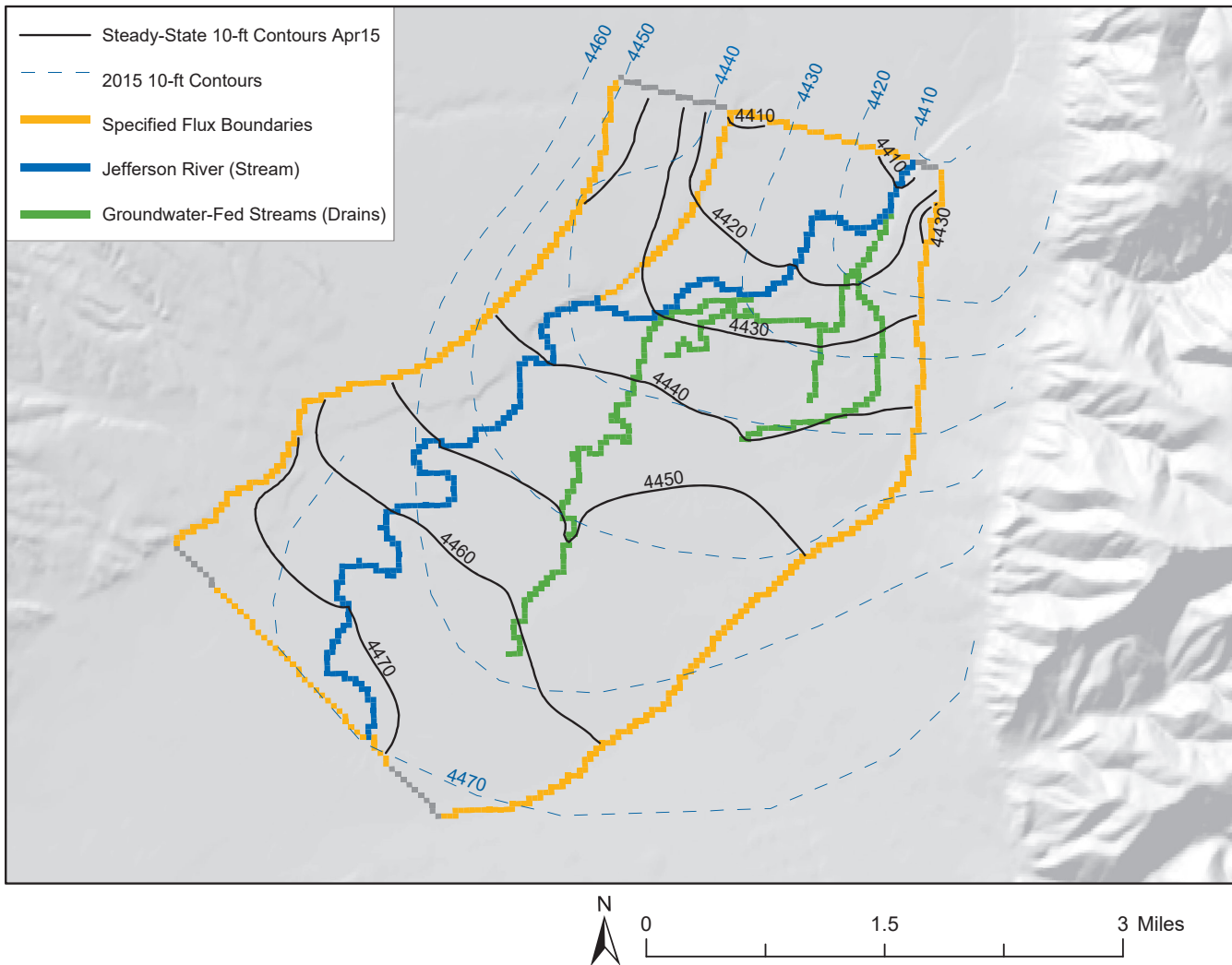


Figure 15. Calibrated steady-state potentiometric surface compared to conditions observed in April 2015. The potentiometric contours display interaction among the alluvial aquifer and surface water, Jefferson River, Parson's Slough, and Willow Springs, and demonstrate the gaining and losing segments of the river and the groundwater-fed streams.

teraction among groundwater and Parson's Slough and Willow Springs (drains), and the Jefferson River (stream); i.e., reaches of gaining and losing are consistent with the conceptual model. The modeled heads closely match the observed values in the 21 target wells (fig. 16). Head residuals (the difference between observed and modeled heads) were all below the 5 ft criteria (fig. 14; table E1, appendix E); however, they are slightly on the high side almost everywhere in the domain, still not affecting the quality of the calibration. Thirteen head residuals (61.9%) were less than 1 ft, six residuals (28.6%) were between 1 and 2 ft, and two residuals (9.5%) were between 2 and 3 ft. The RMS calibration statistic was 1.38 ft, a much lower value than the 5 ft error criteria.

As shown in figure 17, the steady-state model water budget is generally comparable to the Waterloo preliminary water budget. The numerical model

simulated more canal leakage and lateral groundwater influx than initially estimated, and less irrigation recharge and groundwater influx. The calibrated model discharged less groundwater to the Jefferson River than estimated, but discharged more to Parson's Slough and Willow Springs. Overall, the calibrated model simulated less net groundwater discharge to surface waters than the preliminary budget.

The distribution of calibrated  $K_h$  indicates a more heterogeneous distribution than was originally conceptualized (fig. 8 vs. fig. 18). The  $K_h$  values in the floodplain alluvium (initially zone 1) ranged from 11 to 6,270 ft/d, with a geometric mean of 1,140 ft/d. The alluvial terrace (initially zone 2) has  $K_h$  values ranging from 15 to 7,620 ft/d, with a geometric mean of 20 ft/d. The western bench (initially zone 3) has  $K_h$  values ranging from 1 to 5,000 ft/d, with a geometric mean of 187 ft/d. The  $K_h$  values in the eastern bench (initially

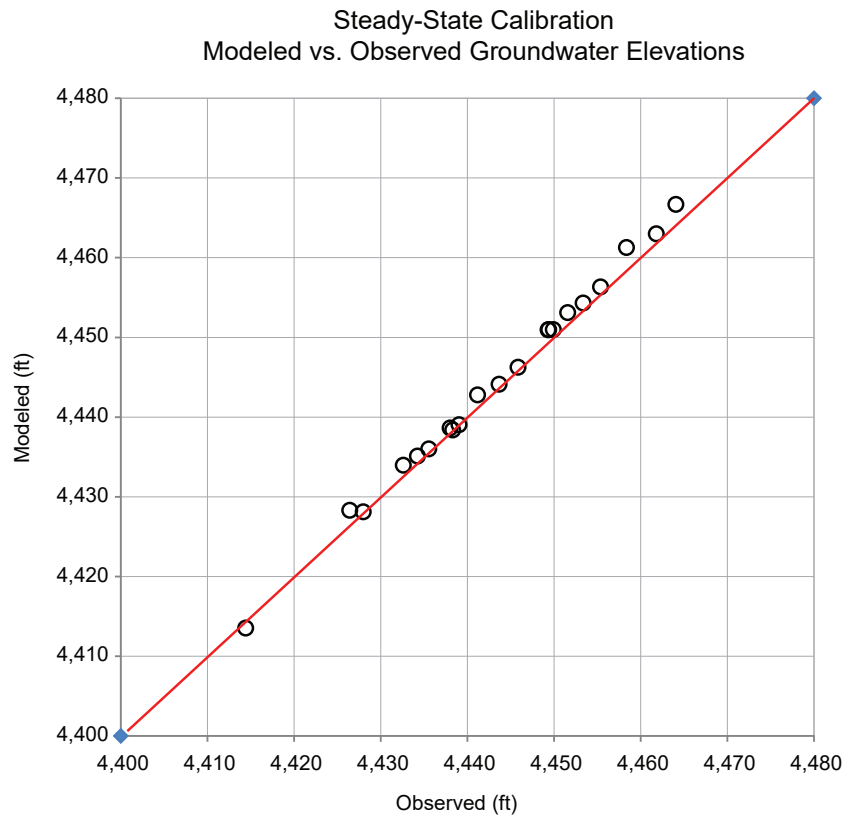


Figure 16. The steady-state calibrated heads closely match the observed heads. Each point represents a target well plotted using its observed head (horizontal axis) and modeled head (vertical axis). Points located along or near the 1:1 line (red) indicate a close match between observed and modeled heads.

zone 4) ranged from 1 to 345 ft/d, with a geometric mean value of 20 ft/d. From the calibration results, it appears that (a) conductive fluvial sediments underlie some portions of the alluvial terrace, and (b) most of the lower conductivity in zone 2 are near Parson’s Slough and Willow Springs (fig. 18), consistent with field observations of marshy wet conditions, indicating an elevated water table due to a lower transmissivity.

### Transient Calibration

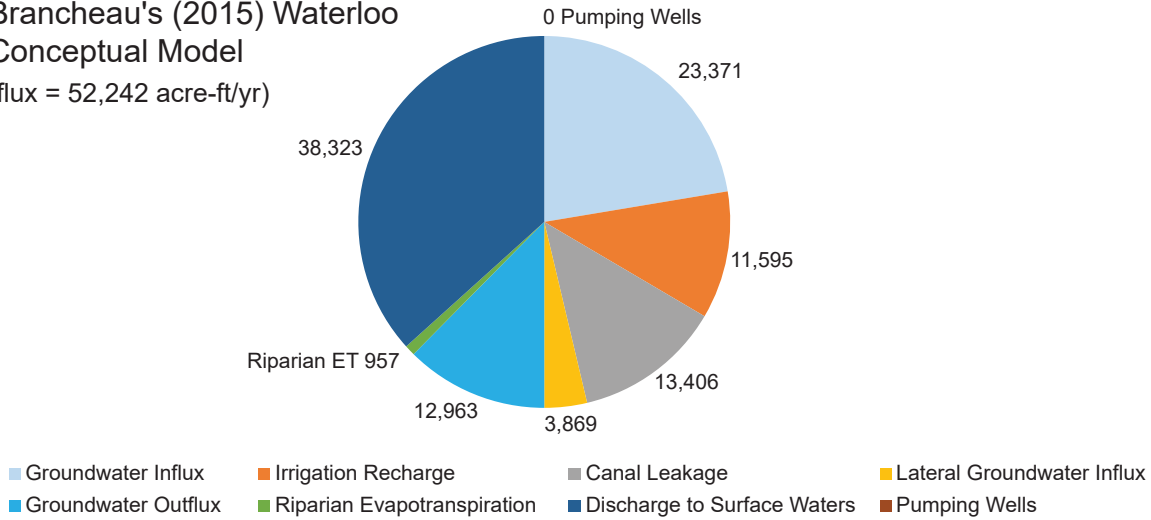
Transient calibration of a groundwater model aims to adjust the model’s time-dependent parameters to reasonably reproduce groundwater heads and fluxes, and surface-water flows that respond to time-dependent changes in boundary conditions and/or applied stresses. Calibration was achieved by adjusting aquifer storage properties and boundary conditions until observed water-level changes were reasonably simulated by the model. We used PEST to estimate the model’s storativity, storage coefficient  $S_s$ , and/or specific yield  $S_y$ ; other boundary parameters (e.g., canal leakage) were modified manually.

### Calibration Targets

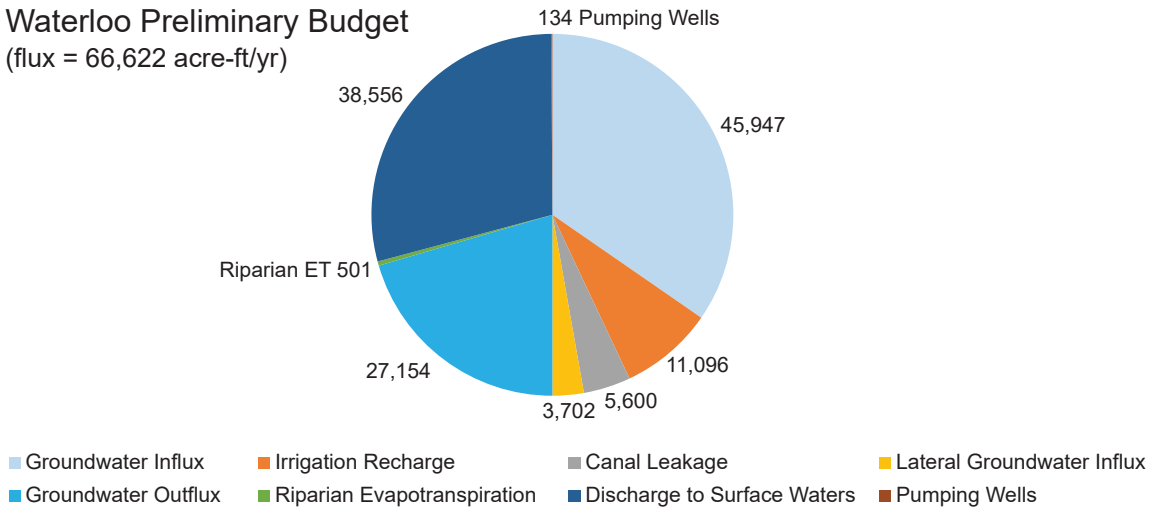
Nineteen target wells had data suitable for the transient calibration. Ten wells have data from 2004 to 2005, with a data gap from 2005 to 2013, and additional data from April 2013 to June 2015. Data from eight wells are limited to April 2013 to June 2015. One well (GWIC 107080) has a continuous record from 2004 to 2015. Due to these data gaps, we calibrated the transient model to the 2013–2015 period, and used data from 2004 to 2005 for model validation.

The three surface-water monitoring sites located on the Jefferson River are the Funston station, USGS station at Parson’s Bridge, and the Corbett station (fig. 3). Corbett station operated from April 29, 2014 to November 11, 2014. Funston station operated from July 9, 2014 to November 10, 2014, and the USGS station at Parson’s Bridge operated from July 1 to September 30 in 2013 and 2014. Corbett station was selected as the surface-water calibration target because (a) it has the longest record in 2014, and (b) it is located at the model’s downstream boundary, where it receives all flows from the Jefferson River, Parson’s Slough, Willow Springs, and the net groundwater discharged to the Jefferson River.

**Brancheau's (2015) Waterloo Conceptual Model**  
(flux = 52,242 acre-ft/yr)



**Waterloo Preliminary Budget**  
(flux = 66,622 acre-ft/yr)



**Waterloo Numerical Model**  
(flux = 50,305 acre-ft/yr)

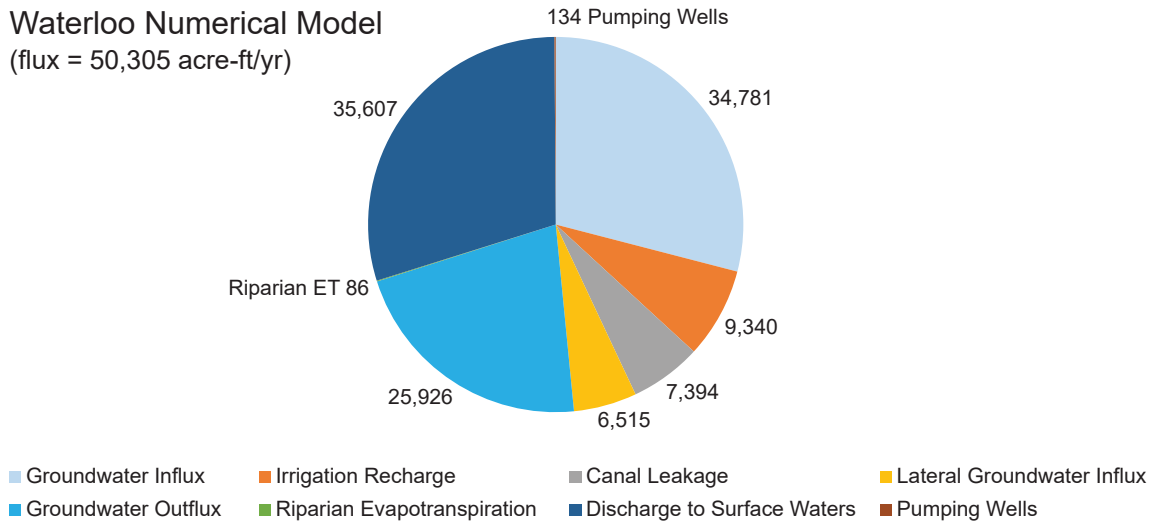


Figure 17. Comparison of three water budgets (Brancheau's 2015 budget, the preliminary budget, and the calibrated steady-state numerical model). The numerical model water budget is comparable to the preliminary water budget with some differences in the distribution of inflow to the aquifer. The three budgets show that outflow is primarily divided between discharge to surface water and groundwater outflow.

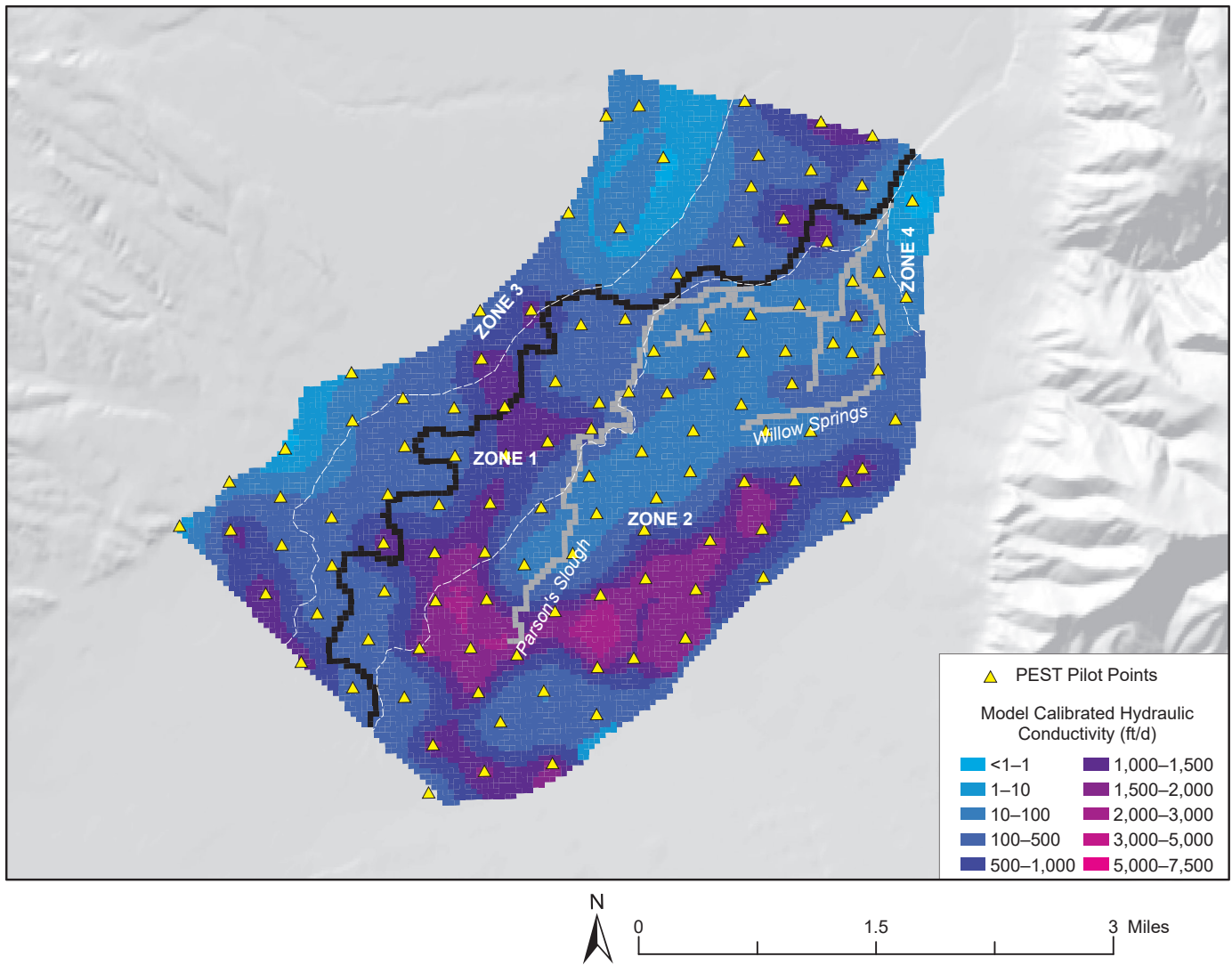


Figure 18. Distribution of horizontal hydraulic conductivity ( $K_h$ ) in the calibrated steady-state model. This distribution of  $K_h$  is more heterogeneous than that based on geologic units (fig. 8).

**Transient Calibration Methods**

Stress Periods

The transient model was initiated with a 1-d stress period (corresponds to March 31, 2013) as a steady-state period, with its output, like the heads and boundary stresses, becoming the initial conditions for the subsequent transient simulation. Starting the simulation in April, the beginning of the irrigation season and 3 mo ahead of the data collection period (July 2013), provided the numerical model with enough time to stabilize and adjust to seasonal changes.

After the first stress period, boundary stresses varied monthly from April 2013 through October 2015 to replicate seasonal changes. These stresses include irrigation recharge rate, canal leakage, lateral groundwater inflow along the Parrot and Creeklyn Canals, evapotranspiration, river flow entering the model

area, diversions, and pumping from irrigation wells. Domestic and stock wells were kept at constant pumping rates (appendix A). The groundwater inflow and outflow through the alluvial aquifer across the southern and northern boundaries remained constant at their steady-state rates throughout the transient simulation.

Aquifer Storage Estimation Using PEST

Storage parameters in MODFLOW were specified using the layer property-flow (LPF) package, with a layer type “LAYCON” equals 1, which is unconfined layer type, applying specific yield ( $S_y$ ) to calculate changes in storage within each cell.

For the transient calibration, we identified four geologic zones for which PEST estimated  $S_y$ : the western bench (zone 1), the alluvial valley (zone 2), and two zones representing the eastern bench (zones 3 and 4, fig. 19). The eastern bench zones were designed

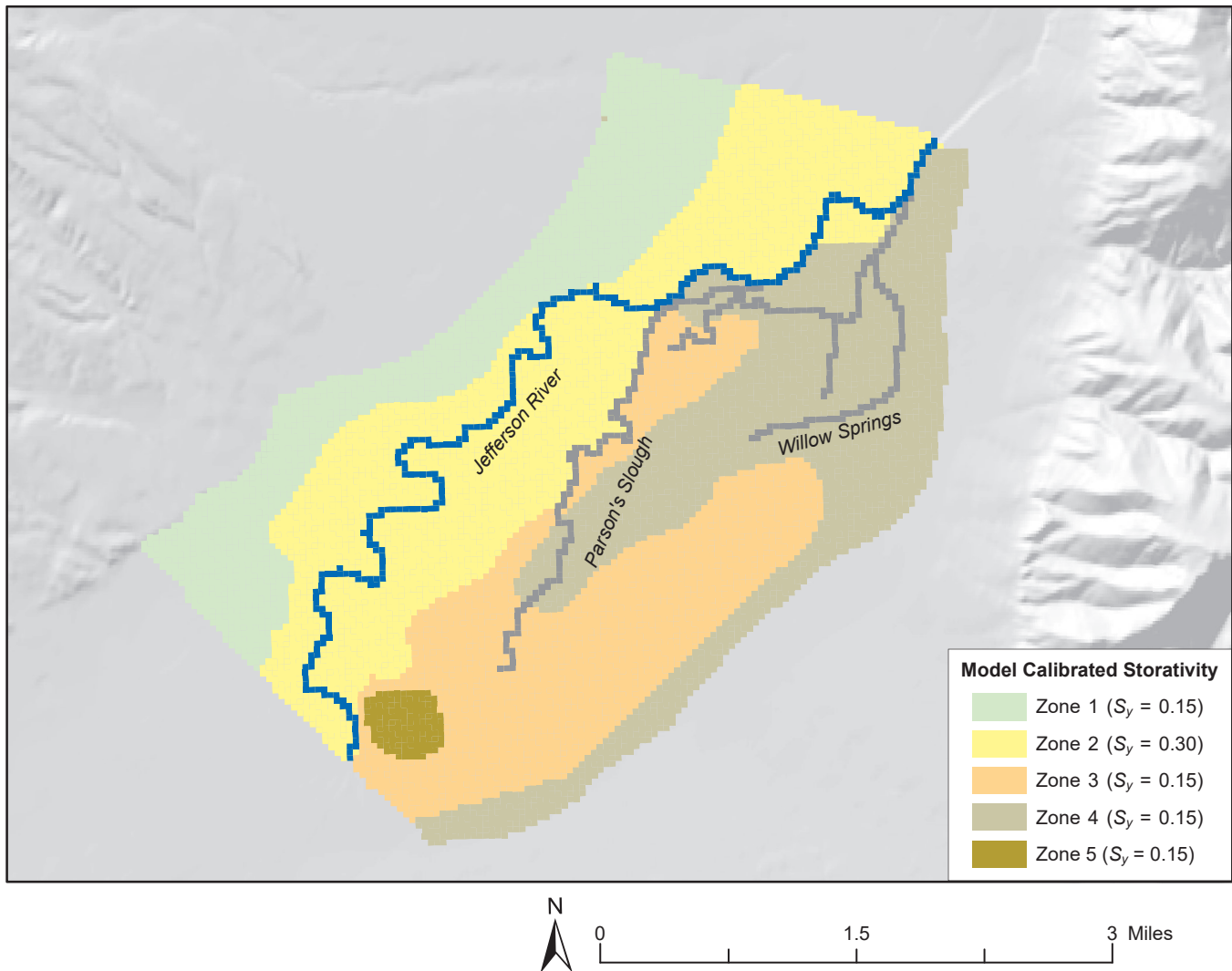


Figure 19. Transient model calibrated aquifer storage coefficients produced by PEST using the zonal approach. The property zones include the western bench (zone 1), the alluvial valley (zone 2), and the eastern bench (zones 3, 4). Zone 5 was added to improve the calibration close to the south (upgradient) end of the Jefferson River.

to generally account for the apparent variation in  $K_h$  distribution in that area. PEST produced similar storage coefficients  $S_y$  for zones 3 and 4, suggesting these act as one zone. Additional adjustment of  $S_y$ , needed to improve the calibration in targets near the southwest boundary of the model, was accomplished by adding a fifth zone within zone 3 (fig. 19), in which  $S_y$  was modified manually.

#### Irrigation Recharge Estimation

As shown in the Model Construction section of this report and documented in appendix A (appendix A, tables A9, A10), several irrigation recharge zones simulated pivot, sprinkler, and flood irrigation. During the transient calibration, the average irrigation recharge rates applied to the steady-state model were systematically changed—with multipliers—to generate monthly irrigation recharge rates over the calendar

year (table 5). The model was run with the adjusted recharge rates and the results were compared to observed head changes at target wells. This process was repeated until there was a good match with observations. Additional recharge zones representing different rates were added during the transient simulation to adjust groundwater levels to match target hydrographs (table 6, fig. 20).

#### Evapotranspiration Estimation

The steady-state evapotranspiration rates were applied to the transient model. A multiplier was applied for the months April through September, and a multiplier of zero was used for the rest of the calendar year. This approach was used for both riparian grass and woody plant zones. The multipliers were adjusted for April through September to produce monthly rates reflecting seasonal variations in  $ET_p$  (table 7). The

Table 6. Transient calibration—Recharge rates applied to the Waterloo model.

Month	Multiplier	Transient Recharge Rates (ft/d)													Multiplier	Transient Recharge Rates (ft/d)		
		Zone 1	Zone 2	Zones 3, 14–18			Zone 4	Zone 5	Zone 6	Zone 7	Zone 8	Zone 9	Zone 10	Zone 11		Zone 12	Zone 13	
Apr	0.9	0	7.38E-05	5.70E-03	4.55E-04	8.24E-04	7.20E-03	6.45E-03	1.94E-03	6.40E-04	1.25	1.00E-02	4.72E-03	2.22E-03	8.10E-03			
May	1.8	0	1.48E-04	1.14E-02	9.10E-04	1.65E-03	1.44E-02	1.29E-02	3.89E-03	1.28E-03	2.5	2.01E-02	9.45E-03	4.44E-03	1.62E-02			
Jun	1.8	0	1.48E-04	1.14E-02	9.10E-04	1.65E-03	1.44E-02	1.29E-02	3.89E-03	1.28E-03	2.5	2.01E-02	9.45E-03	4.44E-03	1.62E-02			
Jul	1.8	0	1.48E-04	1.14E-02	9.10E-04	1.65E-03	1.44E-02	1.29E-02	3.89E-03	1.28E-03	2.5	2.01E-02	9.45E-03	4.44E-03	1.62E-02			
Aug	1.8	0	1.48E-04	1.14E-02	9.10E-04	1.65E-03	1.44E-02	1.29E-02	3.89E-03	1.28E-03	2.5	2.01E-02	9.45E-03	4.44E-03	1.62E-02			
Sep	1.8	0	1.48E-04	1.14E-02	9.10E-04	1.65E-03	1.44E-02	1.29E-02	3.89E-03	1.28E-03	2.5	2.01E-02	9.45E-03	4.44E-03	1.62E-02			
Oct	0.9	0	7.38E-05	5.70E-03	4.55E-04	8.24E-04	7.20E-03	6.45E-03	1.94E-03	6.40E-04	1.25	1.00E-02	4.72E-03	2.22E-03	8.10E-03			
Average Recharge (ft/d)	0.00	8.20E-05	6.33E-03	5.06E-04	9.16E-04	8.00E-03	7.16E-03	2.16E-03	7.11E-04	Average Recharge (ft/d)	8.04E-03	3.78E-03	1.78E-03	6.48E-03				

Note. Zone 1 recharge was zero (not shown in the table). Recharge applied to zones 14 and 18 is identical to zone 3 recharge.

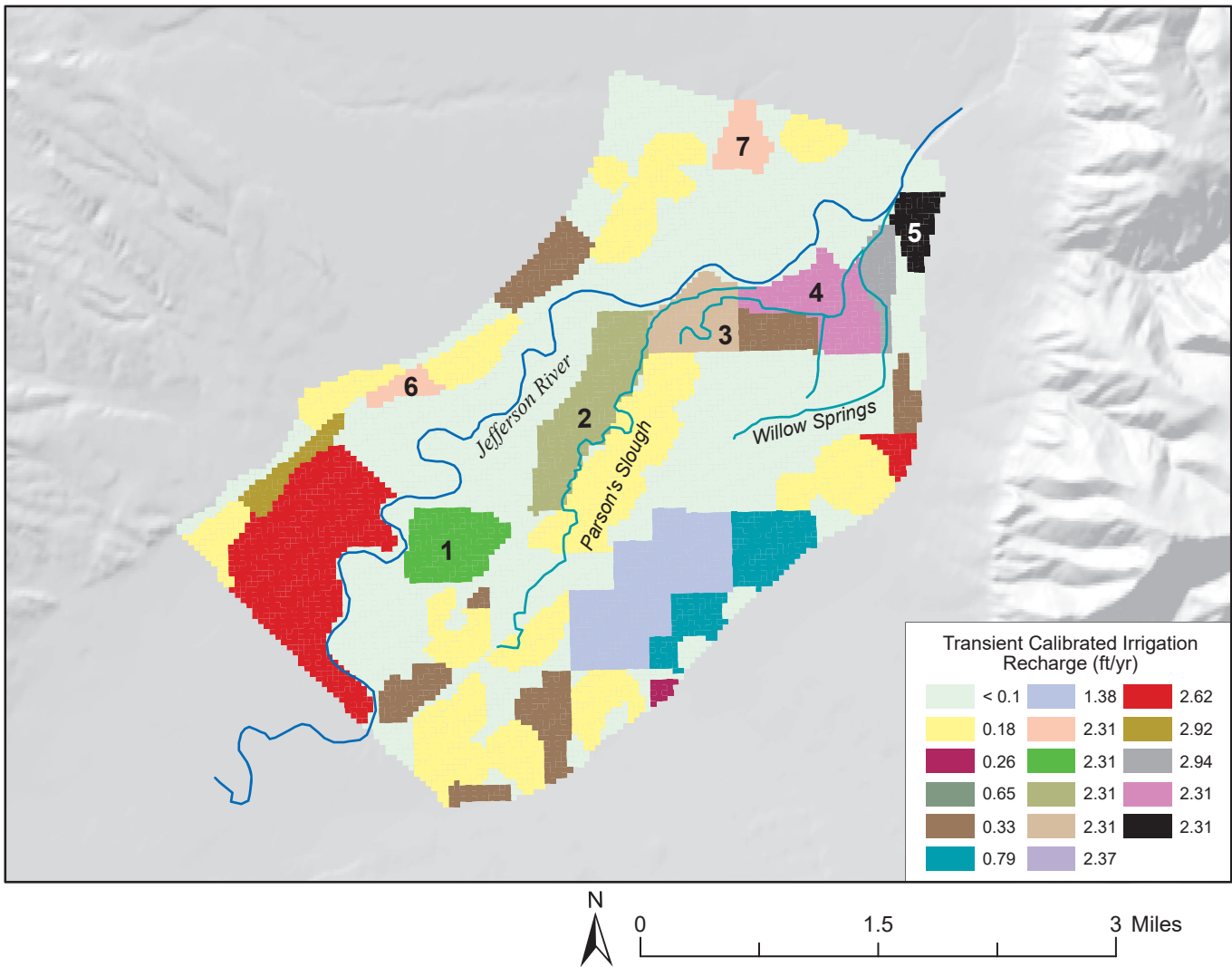


Figure 20. Transient model calibrated irrigation recharge. Areas 1 to 7 are flood-irrigated zones with annual average recharge rate of ~2.3 (ft/yr). These areas were converted to pivot irrigation (~0.2 ft/yr) to simulate effects of changes to irrigation practices.

Table 7. Evapotranspiration rates applied to the transient calibration.

Month	Woody Plants Zone	Riparian Grass Zone
	Average ET (22 in/yr)	Average ET (3 in/yr)
	Multiplier	Multiplier
Apr	0.09	0.00
May	0.21	0.09
Jun	0.30	0.21
Jul	0.27	0.30
Aug	0.14	0.27
Sep	0.00	0.14

Note. ET rates are applied through growing season only, April–September.

model was run with the adjusted  $ET_r$  rates, and the simulated hydrographs at target wells were compared to measured data. This process was repeated until the results were considered satisfactory.

Canal Leakage and Lateral Groundwater Inflow

The Parrot and Creeklyn Canals were initially modeled as single segments with uniform leakage rates, but this yielded a poor match to target hydrographs. We divided both canals into smaller segments (fig. 11) with its own specified flux rate. The rate represents the sum of canal leakage, lateral groundwater inflow, and irrigation recharge from adjacent upgradient irrigated areas outside the model domain (figs. 21, 22). The segments adequately simulate variation in canal leakage along the canal length, and account for changes in lateral groundwater influx and upgradient irrigation recharge. The Jefferson Canal was represented with a single segment because the specified flux represents canal leakage only (figs. 11, 22).

Jefferson River Flows

In the steady-state model, the average monthly flow in the Jefferson River (1,724 cfs) was based on data from the three surface-water stations in the

model domain (fig. 3), and the year-round USGS gage between Twin Bridges and Silver Star (USGS 06026500). During calibration of the transient model, we adjusted monthly multipliers applied to the average flow at the beginning of the Jefferson River (stream reach 1) to improve the model’s match to groundwater head targets and average monthly river flows at Corbett station, at the downgradient end of the river (table 4, fig. 23).

Jefferson River Diversions

The diversion from the Jefferson River to the Jefferson Canal occurs immediately downstream of Parson’s Bridge. For the steady-state model, we estimated a steady-state average diversion rate of 29 cfs based on monitoring records for the Jefferson Canal (GWIC 274575; Jefferson Canal at Diversion). In the transient model, we calculated average monthly diversion rates (table 7, fig. 24) from monitoring data and adjusted them during calibration.

**Calibration Results**

The calibrated transient model simulates head changes with time that matched well with observations (figs. 25–28). Grouping target wells according to their

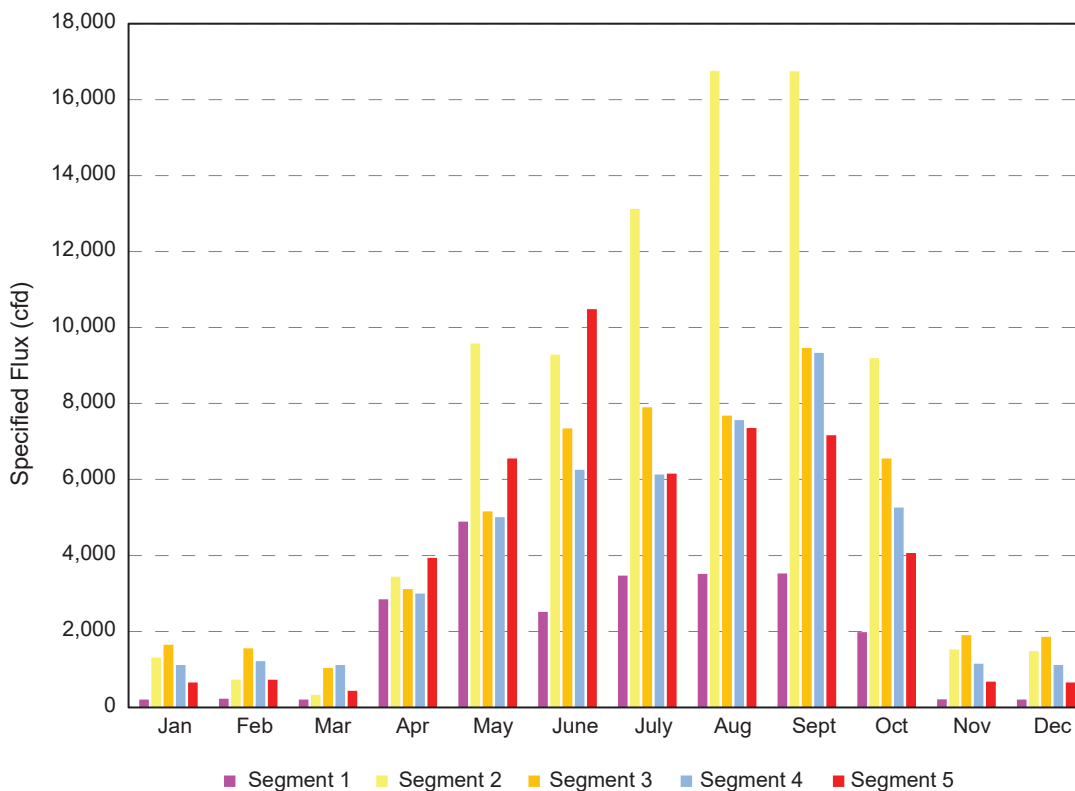


Figure 21. Transient model calibrated specified flux per well along Parrot Canal. The boundary was divided into five segments (fig. 11). The applied flux represents the sum of canal leakage, lateral groundwater inflow, and irrigation recharge from irrigated fields outside of the model domain.

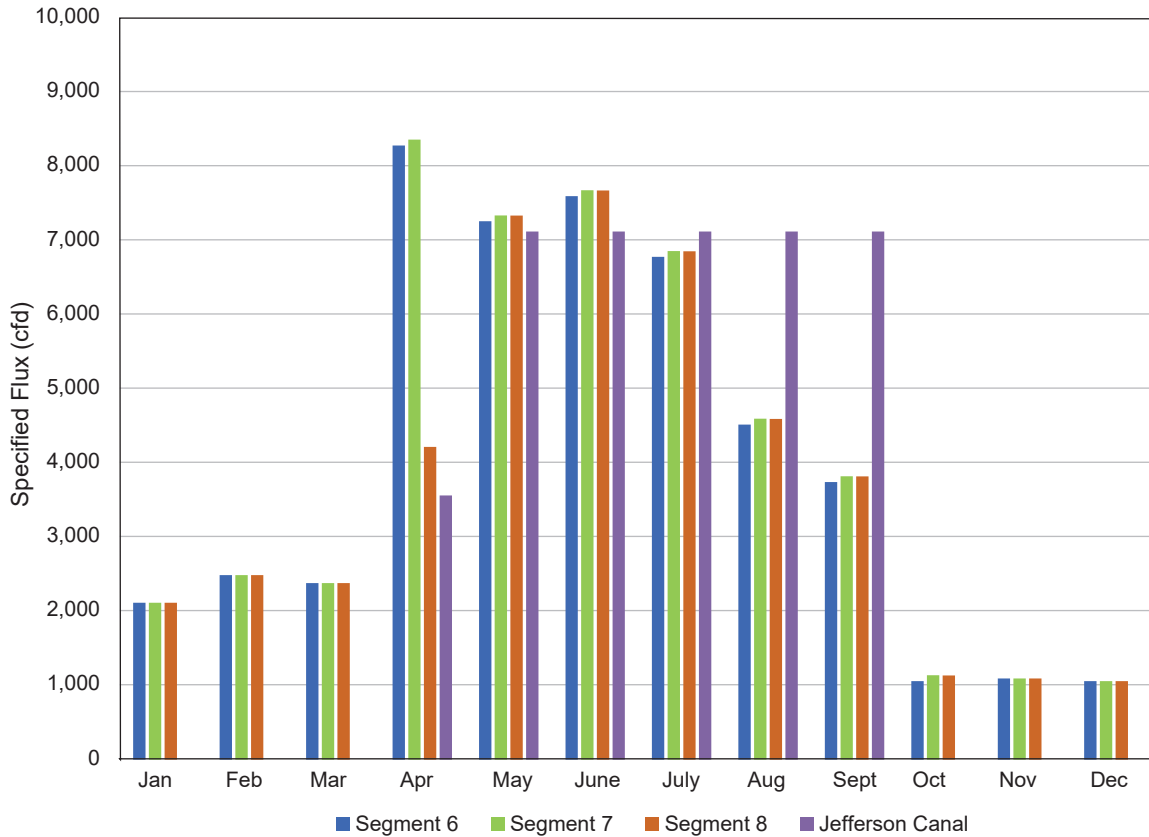


Figure 22. Transient model calibrated specified flux per well along Creekllyn and Jefferson Canals. The canals were divided into segments (fig. 16). For Creekllyn Canal, the applied flux represents the sum of canal leakage, lateral groundwater influx, and irrigation recharge from irrigated fields outside of the model domain. For Jefferson Canal the applied flux represents canal leakage.

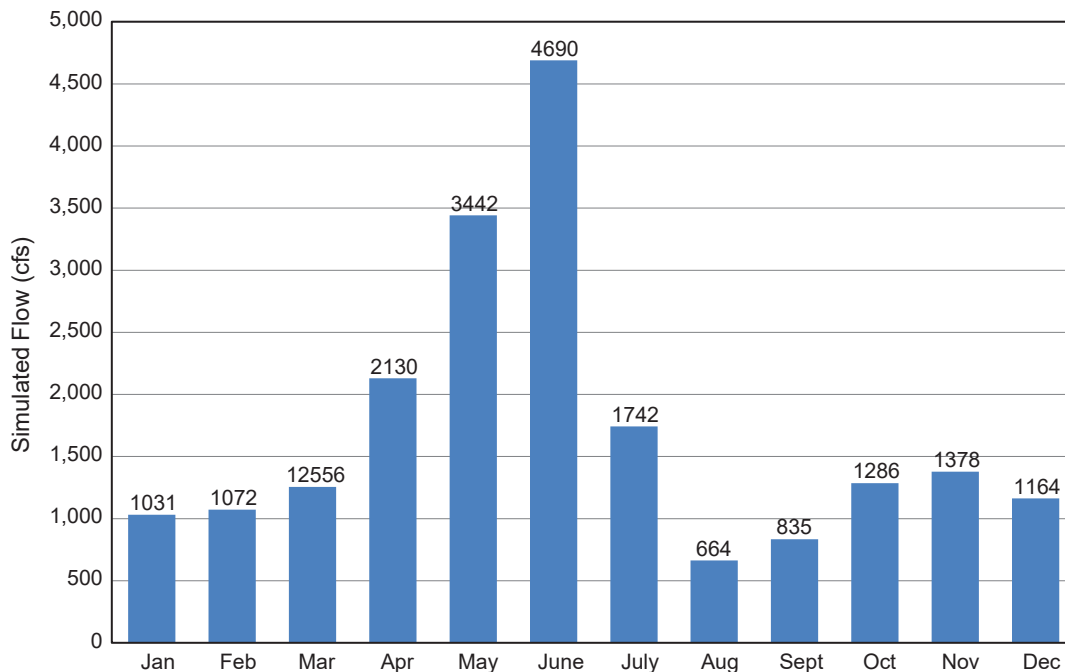


Figure 23. Transient model average monthly flows at the upstream end of the Jefferson River. River input flows were slightly adjusted during calibration with multipliers.

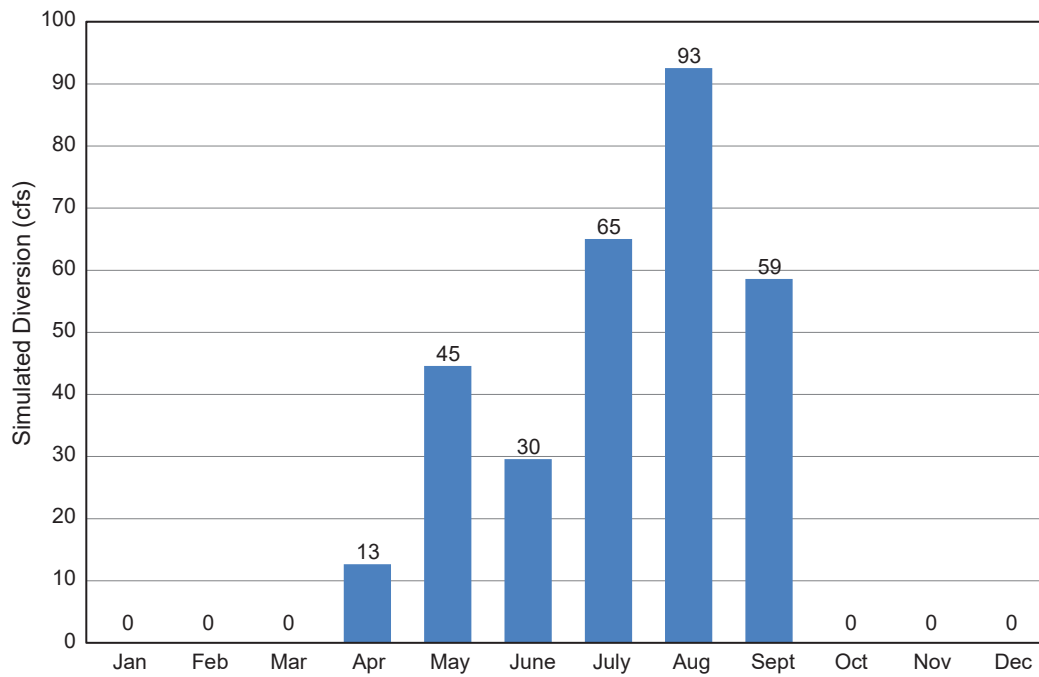


Figure 24. Transient model average monthly diversion from the Jefferson River to the Jefferson Canal during the irrigation season (April through September).

proximity to the model's boundaries (i.e., irrigation canals, groundwater-fed streams, river, etc.) revealed a common response to stresses within each group. Qualitatively, transient calibration results show the following:

1. Simulated groundwater levels at target wells near the Parrot and Creeklyn Canals (group 1) show a good match to observed data and captured seasonal head fluctuations (fig. 25). Canal leakage, lateral groundwater inflow, and irrigation recharge influenced groundwater heads in these areas.
2. Simulated groundwater levels at target wells close to Parson's Slough and Willow Springs (group 2) generally matched the observed hydrographs (fig. 26). They reflect the effect of seasonal recharge and a damping effect of groundwater discharge to the drains that shield them from the river's influence.
3. Target wells located between the Parrot Canal and Parson's Slough (group 3) show a good match to field observations (fig. 27). It appears that irrigation recharge strongly influenced these wells, as demonstrated by mid-summer peaks in hydrographs when the demand for irrigation is high.
4. The hydrographs for target wells in the floodplain, west of Parson's Slough (group 4), show a good match to observed heads, with a capture of seasonal head changes, caused by increased river flow due to snowmelt, and increased irrigation recharge (fig.

28). Hydrographs of wells 276287 and 276108, both located in flood-irrigated areas, demonstrate the combined influence of the Jefferson River and irrigation recharge.

We used the Nash Sutcliffe coefficient of efficiency (Nash and others, 1970) to quantify the fit between simulated and measured heads. The Nash Sutcliffe efficiency coefficient (*NS*) ranges from  $-\infty$  to 1; a positive *NS* means a good fit (1 is the best fit), while a negative *NS* indicates poor matching (Anderson and others, 2015). A detailed example of the *NS* calculation is presented in appendix E. As shown in transient calibration results (figs. 25–28), 13 of 19 hydrographs (68% of the targets) have positive *NS* coefficients, meaning an overall good fit between simulated and observed conditions. Well 277868 and well 276038 in groups 2 and 4, respectively, showed large negative *NS* coefficients. Close proximity of well 277868 to Willow Spring (modeled as a drain) may have caused the higher heads at that well. Heads simulated at well 276038 appear to be influenced by the Jefferson River. Improving the fit to those targets was not possible without degrading the quality of the model calibration.

The simulated Jefferson River flow at the end of stream reach 3 is the sum of instream flow and net groundwater discharge to the river; however, it does not include groundwater discharge to Parson's Slough

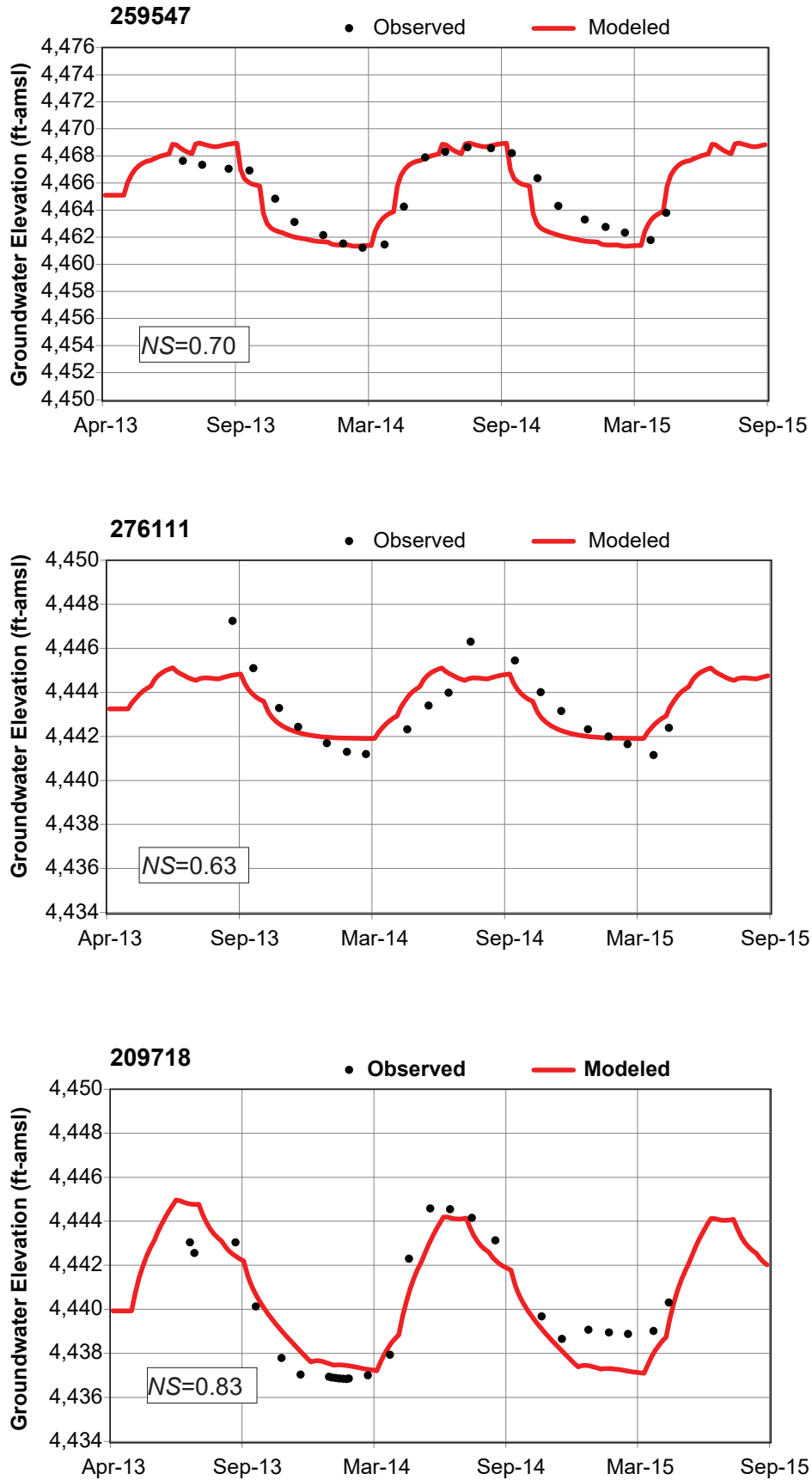


Figure 25. Transient model calibrated groundwater hydrographs (groundwater elevations) for three target wells (Group 1). Results show that the model captured seasonal head changes with a good fit indicated by positive *NS* number (*NS*, Nash Sutcliffe coefficient of efficiency).

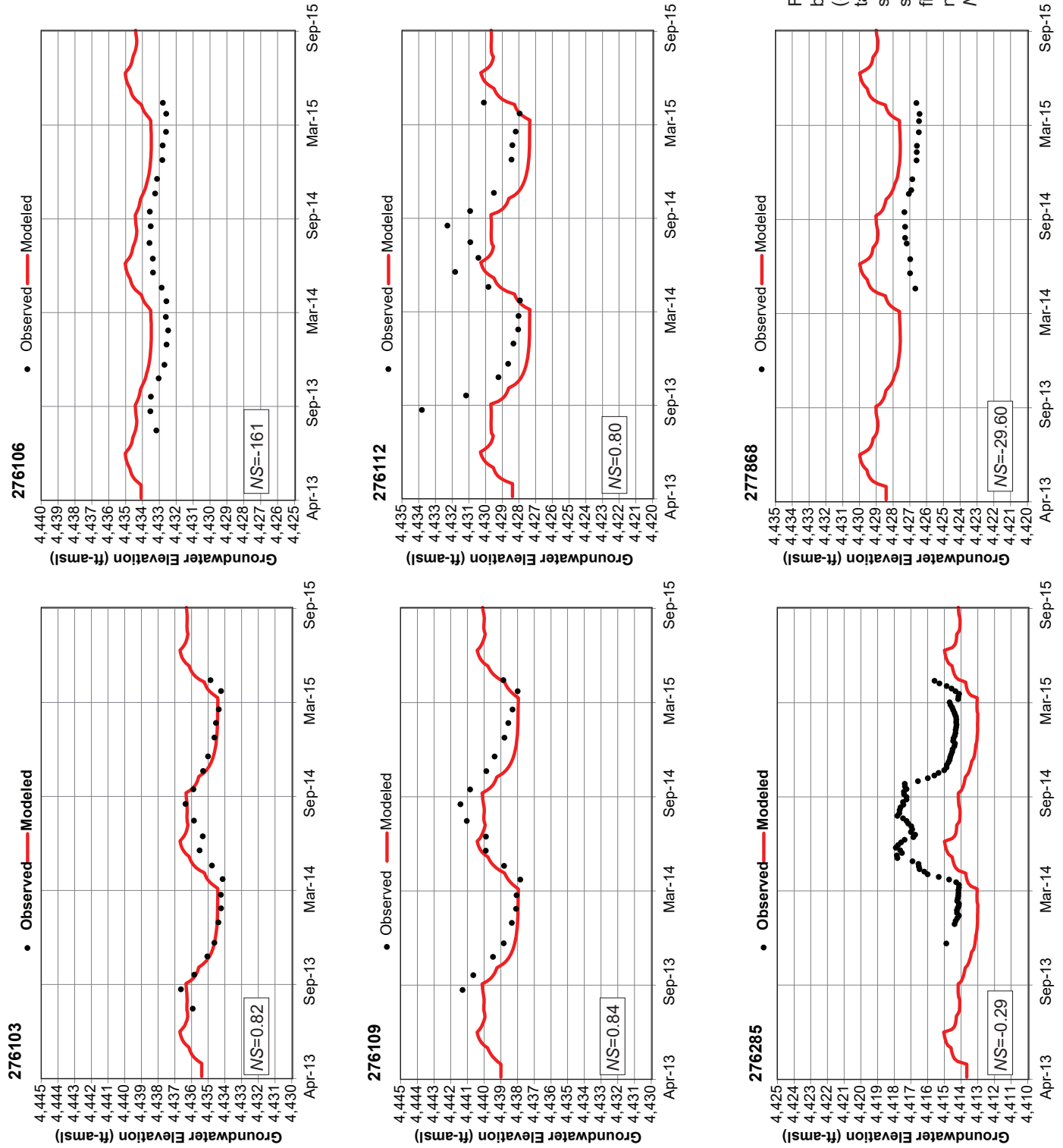


Figure 26. Transient model calibrated groundwater hydrographs (groundwater elevations) for six target wells (Group 2). Results show that the model captured seasonal head changes with a good fit in three of the wells (positive NSE number), and three with negative NSE number (poor fit).

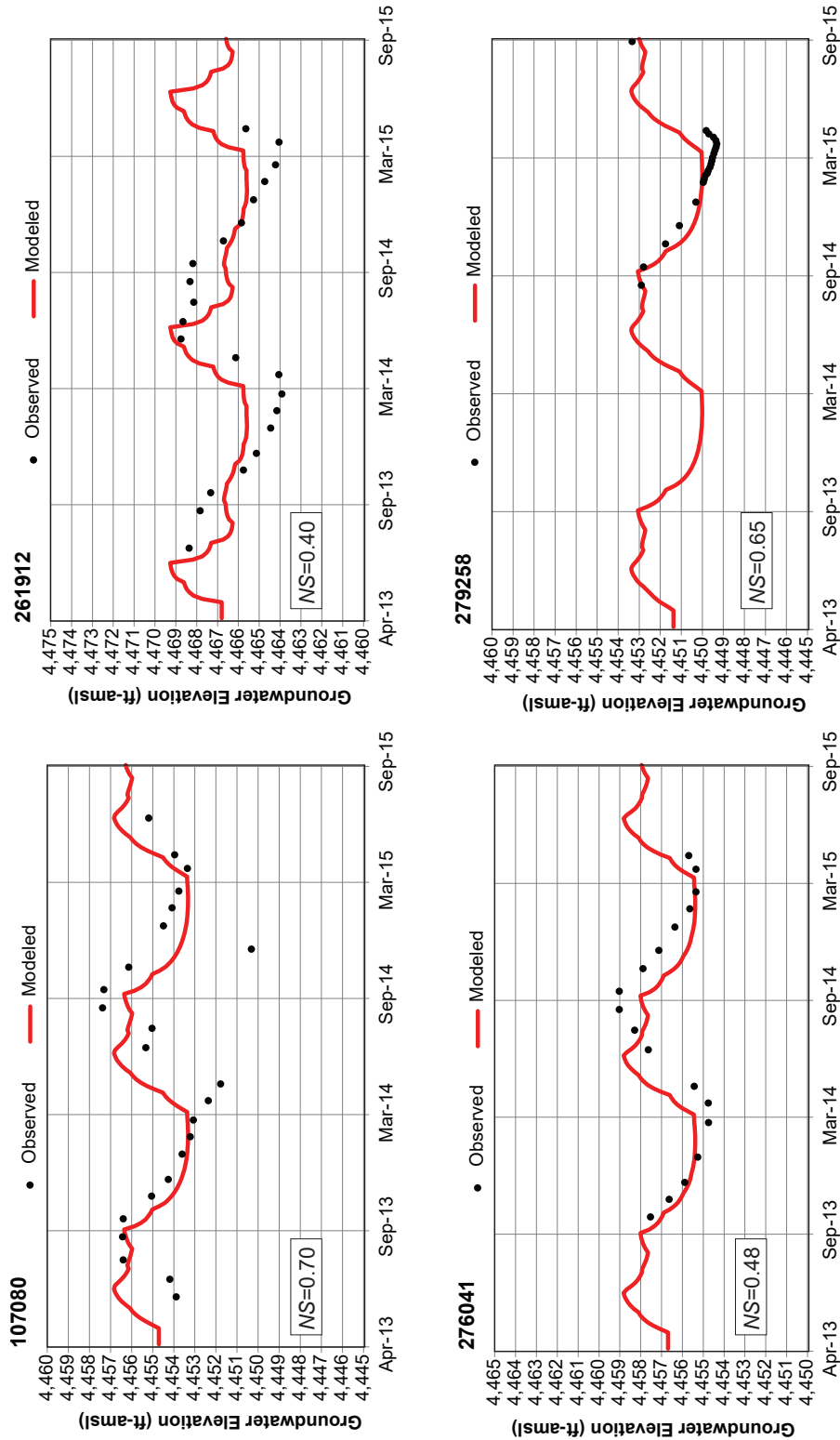


Figure 27. Transient model calibrated groundwater hydrographs (groundwater elevations) for four target wells (Group 3). Results show that the model captured seasonal head changes with a good fit indicated by positive NS number. Effects of boundary (Jefferson River) and irrigation recharge are noticed on the simulated heads (well 261912).

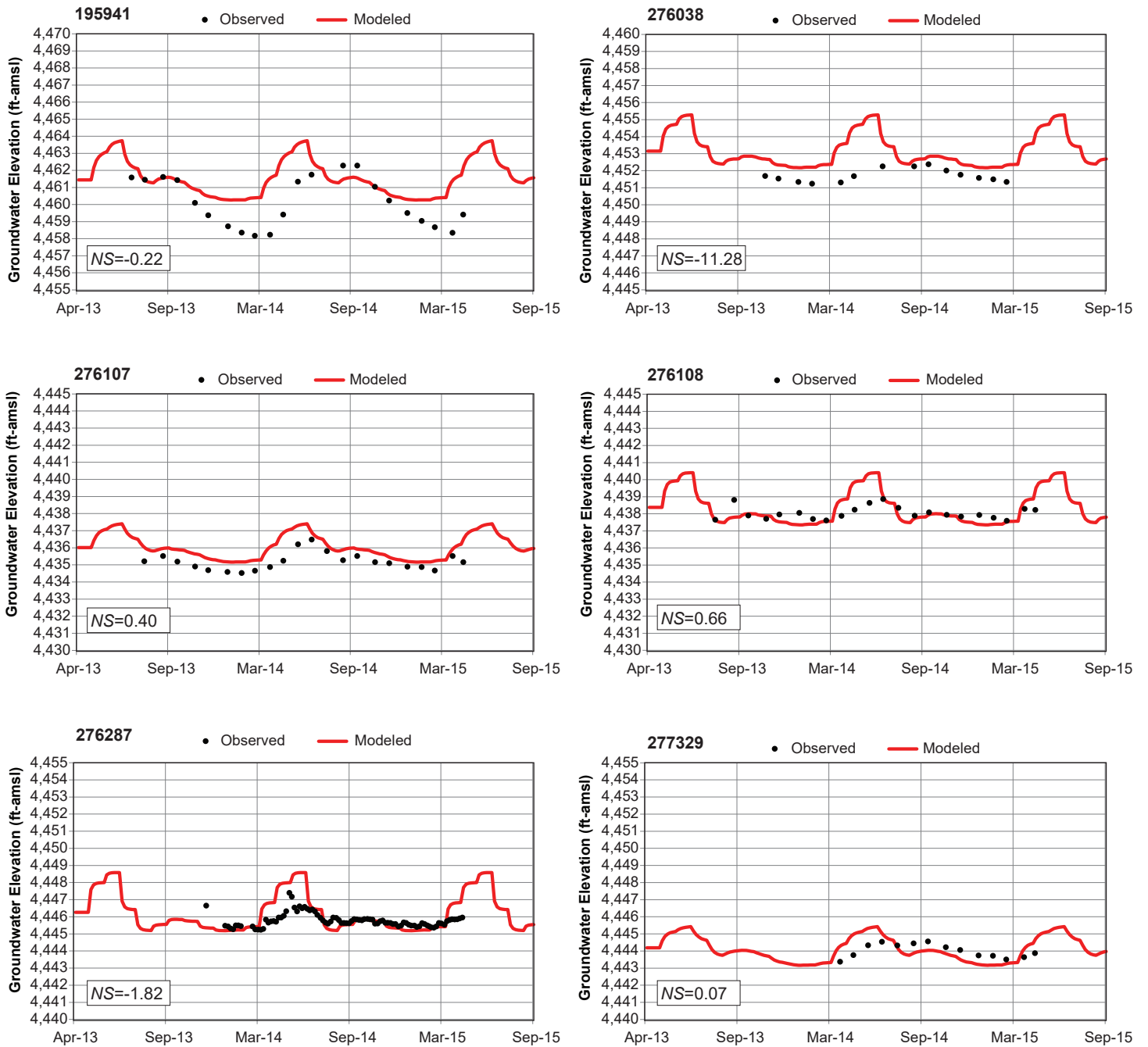


Figure 28. Transient model calibrated groundwater hydrographs (groundwater elevations) for six target wells (Group 4). Results show that the model captured seasonal head changes with a good fit in three of the wells (positive NS number), and three with negative NS number (poor fit). Simulated hydrographs from wells of this group show strong effect of simulated leakage from Jefferson River and irrigation recharge during the irrigation season.

and Willow Springs. In reality it feeds directly into the Jefferson and becomes part of the measured flow at Corbett station (exit point). In order to account for all flows at the river exit point, we added the simulated groundwater discharge to the drains (Parson's Slough and Willow Springs) to the flow at the end of the river (stream reach 3). This combined flow was compared to observed flows at Corbett station from May 2014 to November 2014. The transient simulation of the monthly average flows closely matched measured monthly average flows at Corbett station (fig. 29).

## MODEL VERIFICATION

A calibrated model applies a selected set of hydrogeological parameters, sources and sinks, and boundary conditions to match historical field data. Model verification includes testing the calibrated model by simulating other field data (targets) deliberately excluded during calibration. If successful, the model verification is a process that can increase confidence in the model, especially the use of the model to predict hydrological responses to future changes in applied stresses, such as the addition of wells or changes in irrigation recharge.

We verified the model performance using 11 target wells with water levels from the years 2004–2005. The model was run forward from 2003 to 2015. Simulated

groundwater hydrographs compared to observed heads show that in most target wells the model reasonably simulated head changes during the verification period, and captured seasonality (fig. 30). Several target wells showed a close match to historic observed water levels (e.g. wells 107080, 276103, 276108, 276287, and 277329). Therefore, in general, the transient model was considered to be verified. However, the model underpredicted heads at two wells (276285 and 276112). These wells are likely influenced by flood irrigation practices at adjacent fields, and by the management of the Parrot Canal (figs. 12, 13). For instance, the water-regulating structure for the Kurnow blowout immediately uphill from these wells (fig. 3) was upgraded to minimize leakage between 2006 and 2013. Thus, in the area near these wells, the calibration period of 2013 to 2015 was dissimilar to conditions during the verification period (2004–2005).

## SENSITIVITY ANALYSIS

A calibrated groundwater model contains the best estimates of the hydrogeologic parameters that produce results in good agreement with target values, or other calibration criteria. The objective of the sensitivity analysis is to “quantify the uncertainty of the calibrated model caused by uncertainty of aquifer parameters, stresses, and boundary conditions” (Anderson and others, 2015). Sensitivity analysis involves

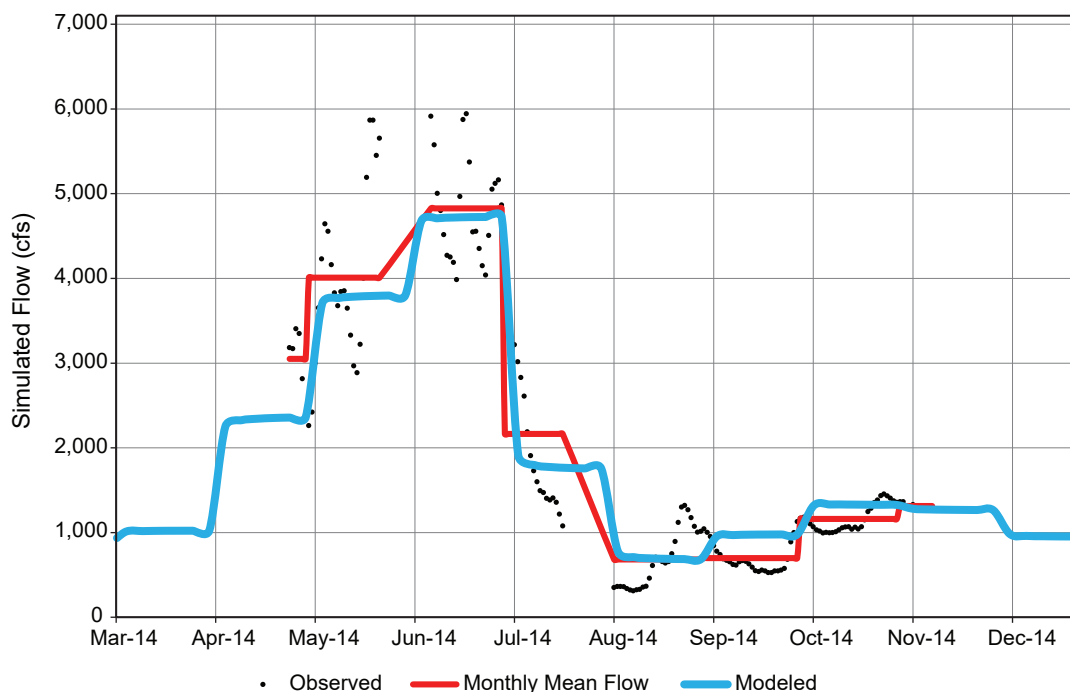


Figure 29. Transient model calibrated average monthly flows in the Jefferson River at Corbett's Station matched closely with the monthly average flows measured at the station.

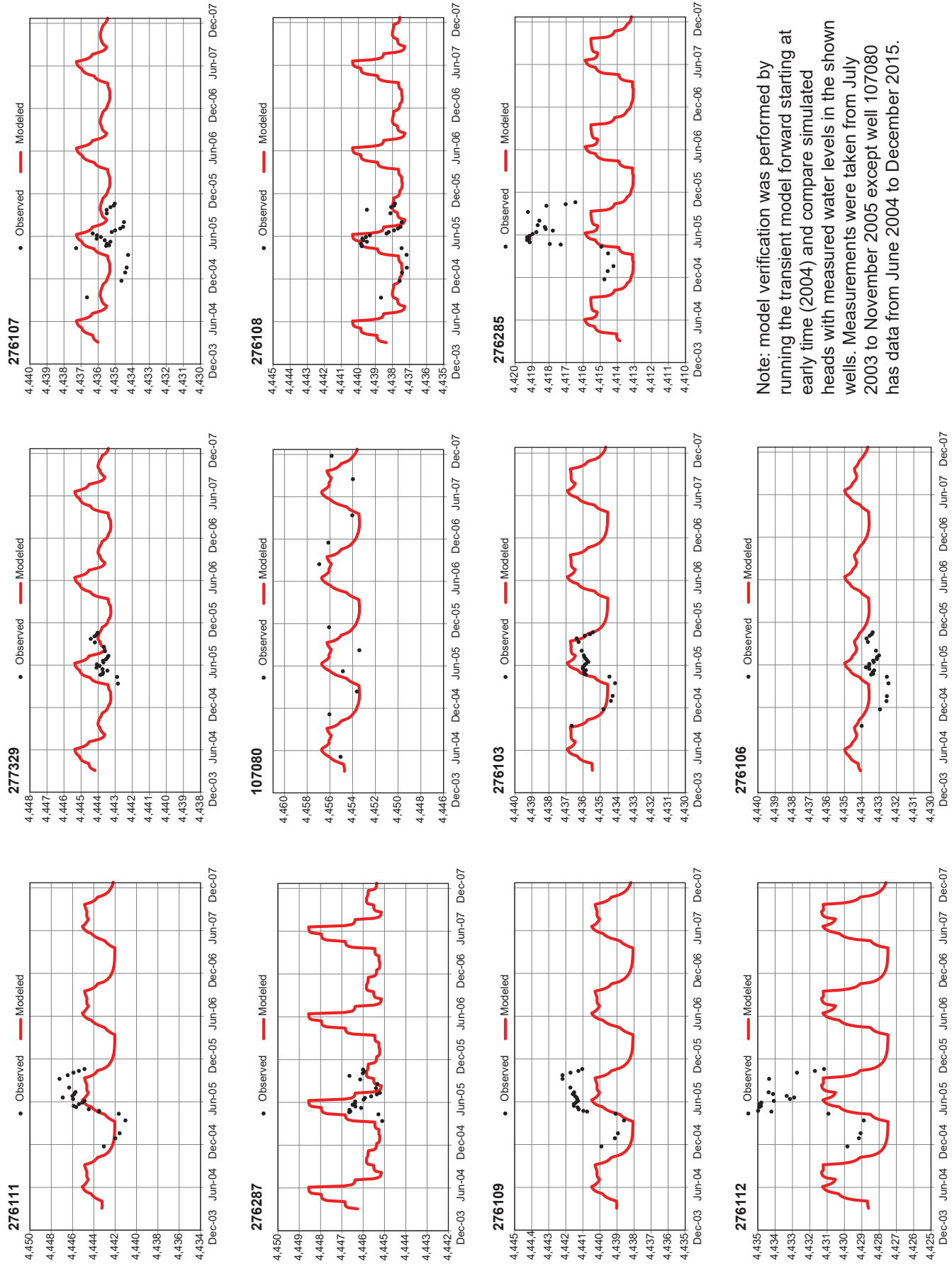


Figure 30. Transient model verification compared the modeled groundwater elevations in the 3 yr (2003–2005) with historic data collected in the same period.

running the calibrated model many times while varying model parameters or boundary stresses—one by one—over a reasonable range, and observing changes in model response (e.g., simulated heads) and/or calibration criteria (e.g. RMS error).

In the sensitivity analysis, 10 parameters were tested with the steady-state model. Parameters included horizontal hydraulic conductivity, Jefferson River stream conductance, Parson's Slough and Willow Springs drain conductance, aquifer thickness, irrigation recharge, canal leakage, lateral groundwater influx, evapotranspiration rates, alluvial groundwater inflow across model boundaries, and well pumping rates (table 8). The analysis was limited to the steady-state simulation in order to test model sensitivity under average long-term conditions. The process involved modifying the calibrated steady-state model (i.e., the

base run) using incremental changes to the various parameters (table 8). For each parameter value, a unique model was executed, for a total of 82 runs. For each model run, we documented groundwater discharge to Parson's Slough and Willow Springs, Jefferson River streamflow at Corbett station, and the calibration statistics RMS and RSS.

Sensitivity results (figs. 31–34) showed that the quantity of groundwater discharge to the groundwater-fed streams (drains) and river flow (streams) and calibration statistics RMS and RSS are all sensitive to (a) changes in horizontal hydraulic conductivity, (b) drain bed conductance, and (c) aquifer thickness.

Table 8. Sensitivity analysis setup and results.

Tested Parameters	Multipliers	Sensitivity Results					
		Drains Flow		River Flow	RMS	RSS	
		Zone 1 and	Zone 2	Zone 1	Zones 1, 2, and 3	Zone 1 and	Zone 2
Horizontal Hydraulic Conductivity	0.1, 0.5, 1, 2, 10						
Canal Leakage (Parrot)	0.75, 0.9, 1.0, 1.1, 1.25	NS		NS	NS		NS
Canal Leakage (Creeklyn)	0.75, 0.9, 1.0, 1.1, 1.25	"		"	"		"
Canal Leakage (Jefferson)	0.75, 0.9, 1.0, 1.1, 1.25	"		"	"		"
Lateral Groundwater Flux (Eastside)	0.75, 0.9, 1.0, 1.1, 1.25	"		"	"		"
Lateral Groundwater Flux (Westside)	0.75, 0.9, 1.0, 1.1, 1.25	"		"	"		"
GW Flux (South Boundary)	0.75, 0.9, 1.0, 1.1, 1.25	"		"	"		"
GW Flux (North Boundary)	0.75, 0.9, 1.0, 1.1, 1.25	"		"	"		"
Riverbed Conductance (reaches 1 & 3)	0.75, 0.9, 1.0, 1.1, 1.25	"		"	"		"
Drain Conductance (all reaches)	0.1, 0.5, 1.0, 2.0, 10	Multipliers (<1 & >1)		"	Multipliers (<1 & >1)		Multipliers (<1 & >1)
Evapotranspiration (ET rate)	0.75, 0.9, 1.0, 1.1, 1.25	NS		"	NS		NS
Evapotranspiration (ET depth)	0.75, 0.9, 1.0, 1.1, 1.25	"		"	"		"
Irrigation Recharge (Flood)	0.75, 0.9, 1.0, 1.1, 1.25	"		"	"		"
Irrigation Recharge (Sprinkle)	0.75, 0.9, 1.0, 1.1, 1.25	"		"	"		"
Irrigation Recharge (Pivot)	0.75, 0.9, 1.0, 1.1, 1.25	"		"	"		"
Aquifer Thickness	0.5, 0.8, 1.0, 1.2, 1.5	Multipliers (<1 & >1)		"	Multipliers (<1 & >1)		Multipliers (<1 & >1)
Pumping Wells (rate)	0.75, 0.9, 1.0, 1.1, 1.25	NS		"	NS		NS

Note. NS, Not sensitive.

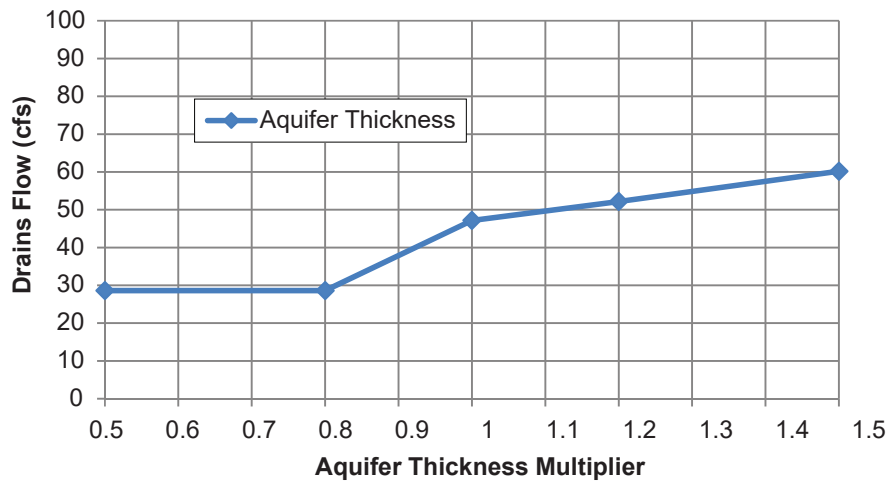
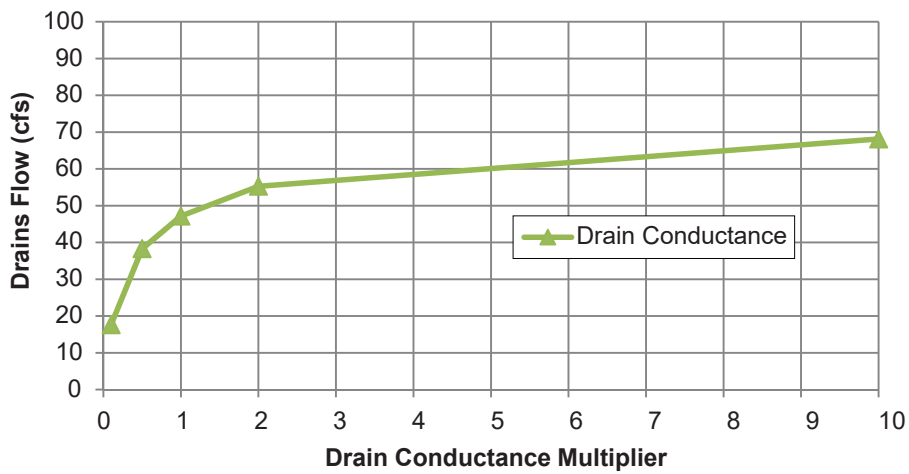
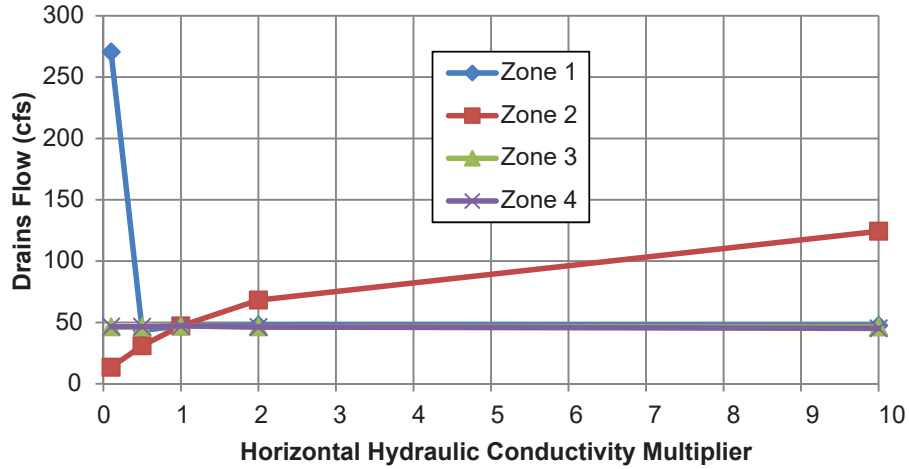


Figure 31. The sensitivity analysis done for the groundwater-fed streams (drains) indicates that the discharge is most sensitive to zone 2 hydraulic conductivity, drain bed conductance, and aquifer thickness.

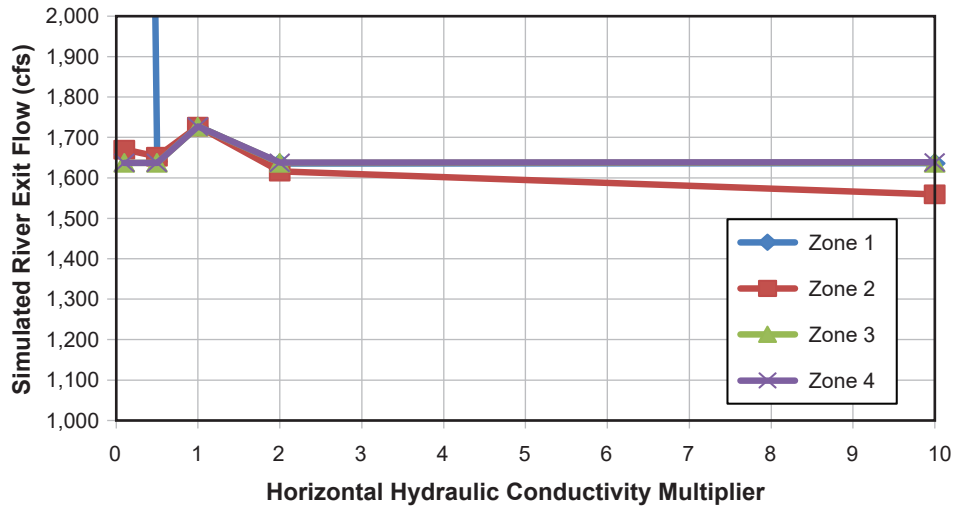


Figure 32. The Jefferson River flow at Corbett's station is sensitive to zone 1 hydraulic conductivity.

## MODEL PREDICTIONS (FUTURE SCENARIOS)

The objective of the Waterloo model was to evaluate how potential changes in irrigation practices would affect surface waters, with emphasis on late summer flows. For each surface-water feature, the effect of a scenario was measured as the difference between the simulated surface-water flows under the scenario conditions and the flows simulated by the *base-run model*. The base-run model is the calibrated transient model with an extended 20-yr simulation time, from January 2005 to December 2024.

It is important to note the limitations of these predictive scenarios. We did not set out to predict effects of specific proposals. Rather, the scenarios were intended to predict groundwater levels and streamflows under hypothetical conditions. This analysis assumes that all stresses and boundary conditions except for the hypothetical *canal lining and changing irrigation type* remain constant. In reality, future conditions will inevitably differ from the simulated base run due to changes in climate, land use, and other factors. The value of this analysis is to understand the types and relative magnitude of effects on surface water that would result from changes in irrigation practices. Although the model allows us to quantify these effects, future conditions will be affected by many variables. In spite of that, these simulations allow us to better understand the behavior of the system as opposed to precisely quantifying the effects of those changes.

Since Parson's Slough and Willow Springs discharge into the Jefferson River, the effects of each

scenario on the Jefferson River implicitly include effects on Parson's Slough and Willow Spring as well as effects on groundwater discharge (baseflow) to the Jefferson River. Particularly in late summer (August), these effects are important because they in turn affect pool connectivity and river temperature, which are both vital to fish and ecological health. We tested four combinations of changes in irrigation practices:

- Lining some or all of the Parrot and Creeklyn Canals. Simulated by setting canal leakage to zero.
- Converting some or all flood-irrigated areas to center pivot irrigation. Simulated by replacing the flood irrigation recharge rate with that of pivot irrigation (fig. 20).
- Combining canal lining (a) and conversion to pivot irrigation (b).
- Applying split season irrigation on flood-irrigated areas (fig. 20). In those areas, we used flood irrigation recharge rates in the first half of the irrigation season (April through June), then applied pivot recharge rates in the second half of the season (July through September). These scenarios test recharging the aquifer during the first half of the season to mitigate reduction in irrigation recharge by changing to pivot irrigation in the late summer (fig. 35).

Eighteen model runs were completed to understand the potential effects on late summer flows due to changing irrigation practices (tables 9, 10):

- Three scenarios represent extreme changes: lining all canals (scenario C1), converting all flood irrigation to pivot (scenario F1), and combining the two scenarios, lining all canals and converting all flood irrigation into pivot irrigation (scenario CF).

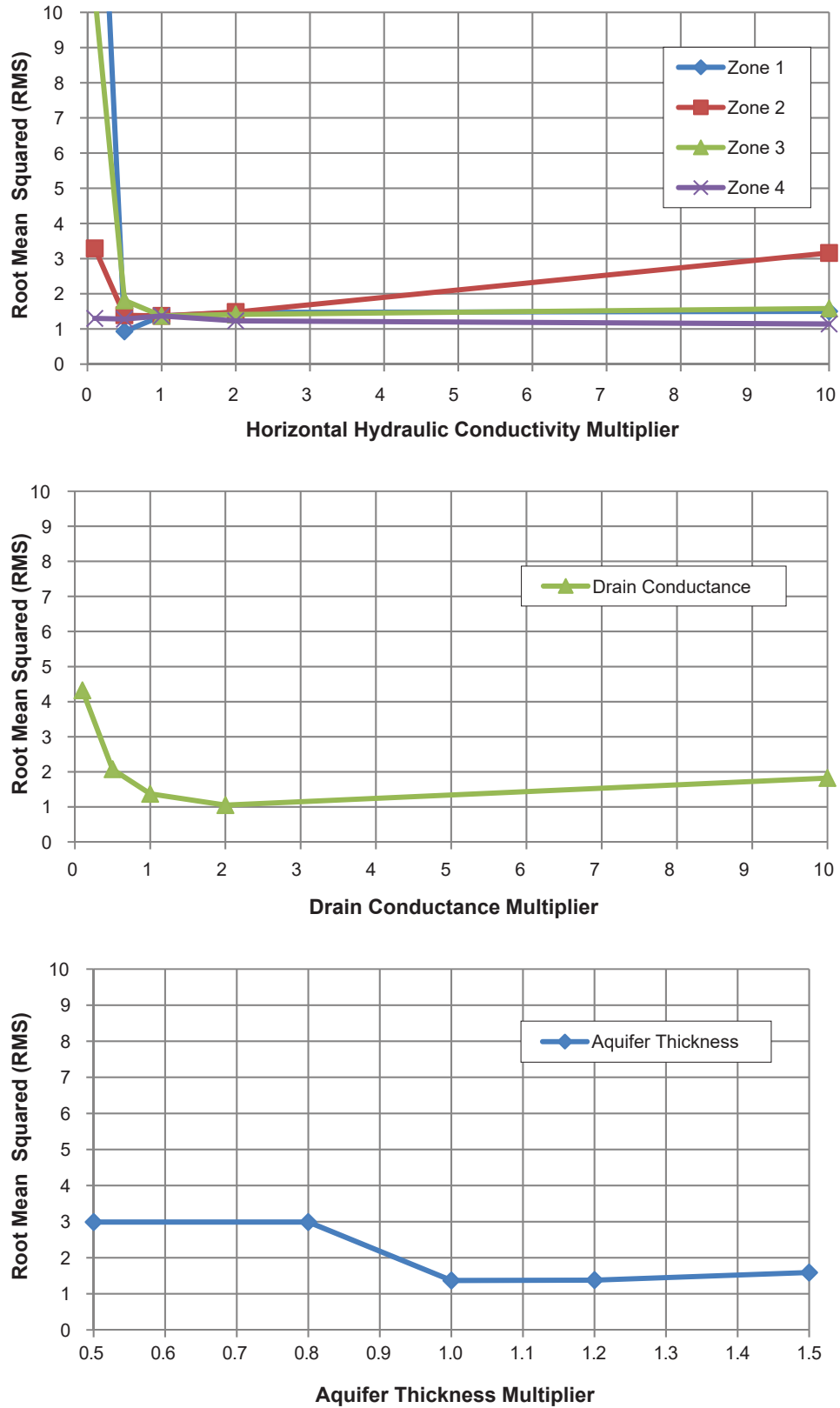


Figure 33. The model sensitivity analysis shows that the calibration statistic RMS is most sensitive to hydraulic conductivity in zones 1, 2, and 3, drain bed conductance for Parson’s Slough and Willow Spring, and aquifer thickness.

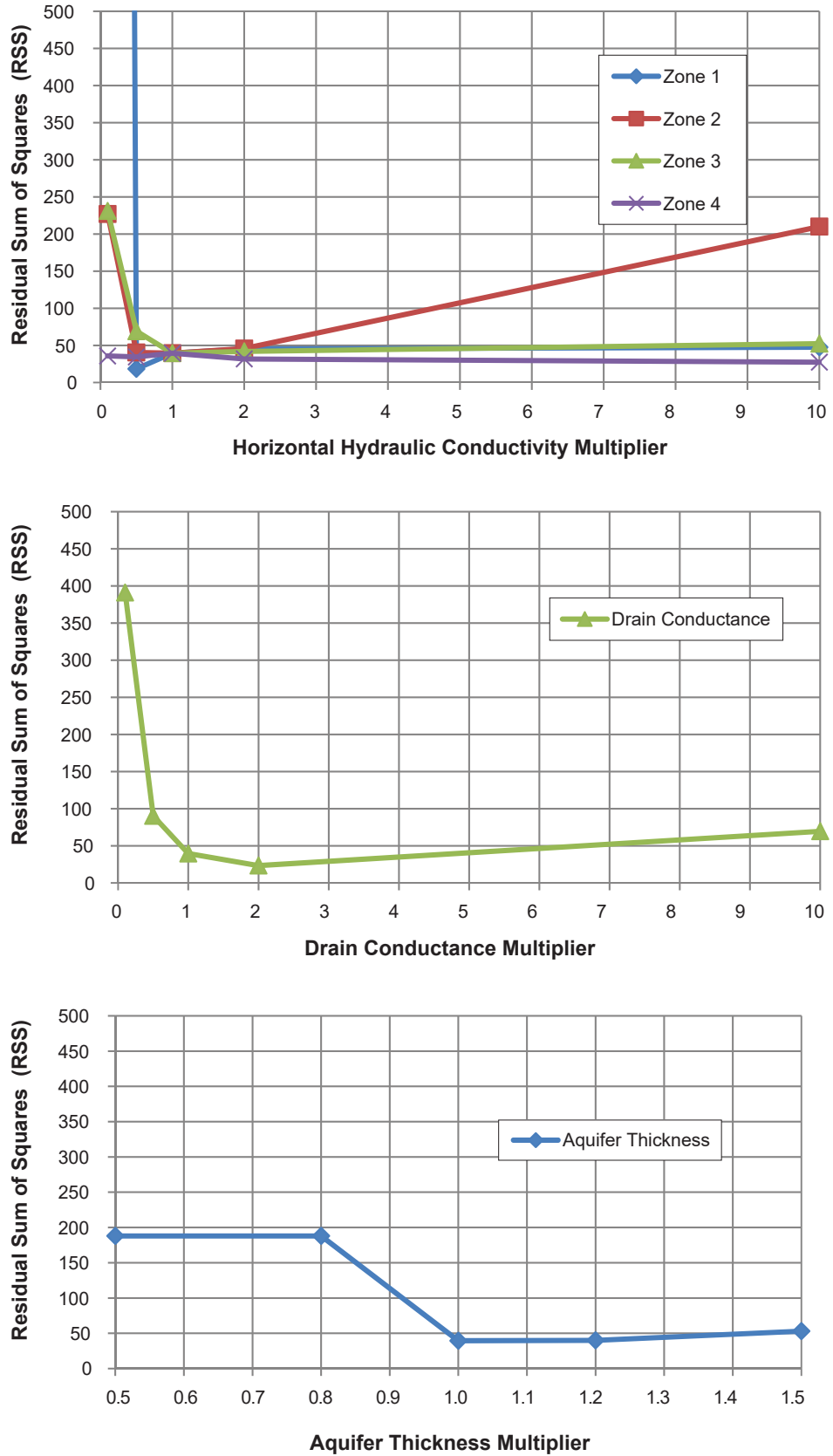


Figure 34. The model sensitivity analysis shows that calibration statistic RSS is most sensitive to hydraulic conductivity (zones 1, 2), drain bed conductance at Parson's Slough and Willow Springs, and aquifer thickness.

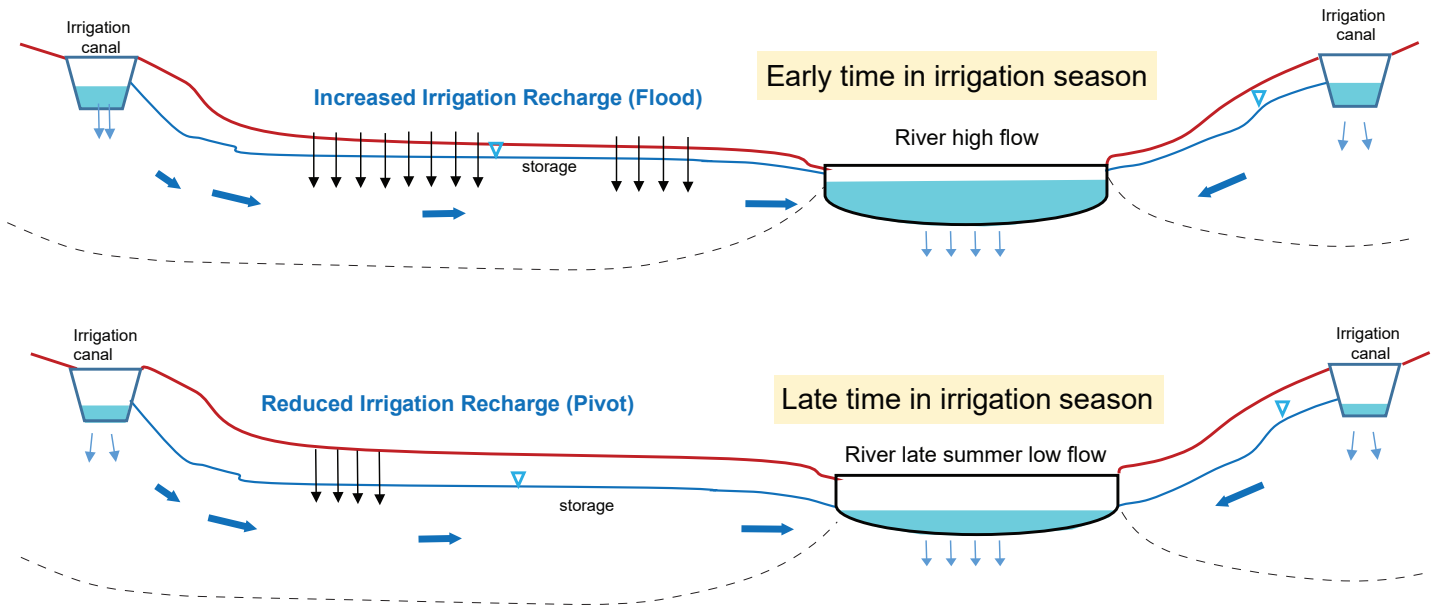


Figure 35. Schematic of groundwater and surface-water interactions in the Upper Jefferson River area during split-season irrigation. This includes flood irrigation during the first half of the season, and center pivot through the rest of the irrigation season.

Table 9. Summary of extreme predictive scenarios for July and August 2024.

Simulated Flow—July 2024							
Scenario	Parson's Slough (cfs)	Willow Springs (cfs)	Total (cfs)	Flow Reduction		Jefferson River Flow Reduction	
				cfs	%	cfs	%
Base run	24.6	40.8	65.5				
C1	23.7	38.4	62.1	3.4	6%	11.9	0.5%
F1	24.2	36.1	60.3	5.2	9%	10.2	0.5%
CF	23.2	33.7	57.0	8.5	15%	22.0	1.0%
SS1	24.5	36.7	61.2	4.3	7%	7.4	0.3%
SS2	25.5	37.7	63.2	2.3	4%	0.6	0.0%

Simulated Flow—August 2024							
Scenario	Parson's Slough (cfs)	Willow Springs (cfs)	Total (cfs)	Flow Reduction		Jefferson River Flow Reduction	
				cfs	%	cfs	%
Base run	18.85	38.69	57.53				
C1	17.24	34.54	51.78	5.8	10%	17.02	2.4%
F1	18.58	32.24	50.82	6.7	12%	12.80	1.8%
CF	16.98	28.29	45.27	12.3	21%	29.70	4.3%
SS1	18.61	32.39	51.00	6.5	11%	12.15	1.7%
SS2	18.76	32.59	51.35	6.2	11%	10.29	1.5%

Table 10. Summary of predictive scenarios for July and August 2024.

Scenario	Modeled Groundwater Discharge to Parson's Slough Flow				Modeled Groundwater Discharge to Willow Springs				Modeled Jefferson River Flow (Corbett Station)*				Corbett Station River Mean Annual Flow (without drain flow) (cfs)	Flow Reduction (Aug 2024)			
	Annual Volume (acre-ft) (Year 2024)	August Volume (acre-ft) (Aug 2024)	July Flow (cfs) (Jul. 2024)	August Flow (cfs) (Aug. 2024)	Annual Volume (acre-ft) (Year 2024)	August Volume (acre-ft) (Aug 2024)	July Flow (cfs) (Jul 2024)	August Flow (cfs) (Aug 2024)	Annual Volume (acre-ft) (Year 2024)	August Volume (acre-ft) (Aug 2024)	July Flow (cfs) (Jul 2024)	August Flow (cfs) (Aug 2024)		Mean Annual Flow (cfs) (Year 2024)	Parson's Slough	Willow Springs	Jefferson River
	1.42E+04	1.35E+03	24.65	18.8	2.42E+04	2.78E+03	40.85	38.7	1.24E+06	5.00E+04	2205.68	696.3	52.14	1638.1			
C1	1.35E+04	1.24E+03	23.68	17.2	2.24E+04	2.48E+03	38.42	34.5	1.23E+06	4.87E+04	2193.77	679.3	49.4	1632.6	8.5%	10.7%	
C2	1.40E+04	1.34E+03	24.59	18.7	2.39E+04	2.77E+03	40.82	38.6	1.23E+06	4.98E+04	2204.58	694.6	52.1	1637.1	0.6%	0.1%	
C3	1.39E+04	1.31E+03	24.28	18.2	2.38E+04	2.75E+03	40.63	38.3	1.23E+06	4.97E+04	2203.18	692.2	51.7	1636.4	3.3%	1.1%	
C4	1.39E+04	1.32E+03	24.41	18.4	2.37E+04	2.74E+03	40.63	38.2	1.23E+06	4.98E+04	2204.20	693.6	51.7	1636.8	2.3%	1.2%	
C5	1.39E+04	1.33E+03	24.43	18.5	2.34E+04	2.68E+03	40.16	37.4	1.23E+06	4.97E+04	2203.69	693.0	51.3	1636.8	1.8%	3.3%	
C6	1.39E+04	1.32E+03	24.35	18.4	2.28E+04	2.54E+03	38.87	35.4	1.23E+06	4.95E+04	2201.79	690.0	50.4	1636.2	2.3%	8.4%	
C7	1.39E+04	1.33E+03	24.43	18.5	2.34E+04	2.68E+03	40.15	37.4	1.23E+06	4.96E+04	2202.21	691.4	51.3	1636.1	1.9%	3.3%	
C8	1.39E+04	1.33E+03	24.43	18.5	2.34E+04	2.68E+03	40.15	37.4	1.23E+06	4.96E+04	2201.65	690.9	51.3	1636.0	1.8%	3.3%	
C9	1.39E+04	1.33E+03	24.43	18.5	2.34E+04	2.68E+03	40.15	37.4	1.23E+06	4.96E+04	2202.21	691.5	51.3	1635.9	1.8%	3.3%	
F1	1.39E+04	1.33E+03	24.21	18.6	2.19E+04	2.31E+03	36.08	32.2	1.23E+06	4.90E+04	2195.52	683.5	49.2	1634.6	1.4%	16.7%	
F2	1.39E+04	1.32E+03	24.37	18.4	2.34E+04	2.68E+03	40.14	37.4	1.23E+06	4.96E+04	2202.90	692.1	51.3	1636.2	2.1%	3.4%	
F3	1.39E+04	1.33E+03	24.37	18.5	2.34E+04	2.68E+03	40.15	37.4	1.23E+06	4.97E+04	2203.40	692.7	51.3	1636.7	2.0%	3.3%	
F4	1.39E+04	1.33E+03	24.39	18.5	2.34E+04	2.68E+03	40.02	37.3	1.23E+06	4.97E+04	2203.51	693.0	51.2	1637.1	1.9%	3.6%	
F5	1.41E+04	1.35E+03	24.58	18.8	2.21E+04	2.33E+03	36.40	32.5	1.23E+06	4.93E+04	2198.90	686.9	49.6	1636.7	0.4%	15.9%	
F6	1.39E+04	1.33E+03	24.43	18.5	2.34E+04	2.67E+03	40.01	37.3	1.23E+06	4.97E+04	2203.33	692.7	51.2	1636.7	1.8%	3.7%	
CF	1.33E+04	1.22E+03	23.24	17.0	2.05E+04	2.03E+03	33.72	28.3	1.22E+06	4.78E+04	2183.65	666.6	46.5	1629.0	9.9%	26.9%	
SS1	1.40E+04	1.34E+03	24.51	18.61	2.22E+04	3.04E+01	2323.23	36.74	1.23E+06	1.56E+05	2198.27	684.17	49.72	1635.81	1.2%	16.3%	
SS2	1.44E+04	1.35E+03	25.49	18.76	2.24E+04	3.08E+01	2337.84	37.68	1.23E+06	1.57E+05	2205.11	686.04	50.58	1638.00	0.4%	15.8%	

\*Modeled Jefferson River Flow at Corbett Station is the sum of simulated drains and streamflows.

Note. F1, Flood to Pivot—All Areas; F2, Change Flood to Pivot—Area 1; F3, Change Flood to Pivot—Area 2; F4, Change Flood to Pivot—Area 3; F5, Change Flood to Pivot—Area 4; F6, Change Flood to Pivot—Area 5; CF, No seepage—Flood to Pivot (All); SS1, Split Season—flood-irrigated areas (1-5); SS2, Split Season—flood-irrigated (all areas); C1, No seepage—All Canals; C2, No seepage—Parrot Reach 1; C3, No seepage—Parrot Reach 2; C4, No seepage—Parrot Reach 3; C5, No seepage—Parrot Reach 4; C6, No seepage—Parrot Reach 5; C7, No seepage—Creeklyn Reach 6; C8, No seepage—Creeklyn Reach 7; C9, No seepage—Creeklyn Reach 8.

- Thirteen scenarios test limited changes in irrigation practices, e.g., lining individual canal segments or converting a single flood-irrigated area to a pivot system.
- Two scenarios test the concept of split season irrigation. The first scenario (SS1) applies changes to five areas (same as scenario F1). Scenario SS2 converts all the flood-irrigated fields (fig. 20) to pivot irrigation from July through September.

We selected August as the most critical late summer month to evaluate the scenarios, because it is typically characterized by low surface-water flows, elevated stream temperatures, high evapotranspiration, and more water consumption. July was also considered when we tested the split season irrigation scenarios. All 18 simulations ran from January 2005 through December 2024 (20 yr), giving the model enough time to achieve stable groundwater–surface-water interactions. The simulations applied changes in irrigation practices starting in April 2015; we documented results for July and August in the years 2005 through 2024.

Before running the scenarios, a base run was executed in which the transient model simulation was extended to 20 yr (2005 to 2024) while keeping all stresses the same throughout the simulation (e.g.,

canal leakage rates, irrigation recharge rates, etc.). The base run average surface-water flows in August 2024 (most critical late summer month) became the reference flow to evaluate results from all scenarios.

### Canal Lining Scenarios

Scenario C1 stops canal leakage by lining both Parrot and Creeklyn Canals (fig. 20), which reduces recharge to the underlying aquifer. Lining was simulated by setting the leakage rate to zero along the canals. Results from this scenario show that it takes more than 1 yr (~16 mo) to develop the full effect on streams and the Jefferson River (figs. 36, 37). Relative to the base run, this resulted in about 6 cfs less groundwater discharge to Parson’s Slough and Willow Springs, which is a 10% reduction in late summer flow. Flow in the Jefferson River at Corbett station was reduced by about 17 cfs, a 2.4% reduction in late summer flow (tables 9, 10).

Other canal lining scenarios tested lining individual canal segments. The Parrot Canal was divided into five sections, segments 1 to 5, and the Creeklyn Canal was divided to three sections, segments 6 to 8 (fig. 11). As shown in table 10, Scenarios C2 to C6 simulated lining only one of the individual segments in the Parrot Canal (e.g., C2 lines segment 1; C3 lines segment

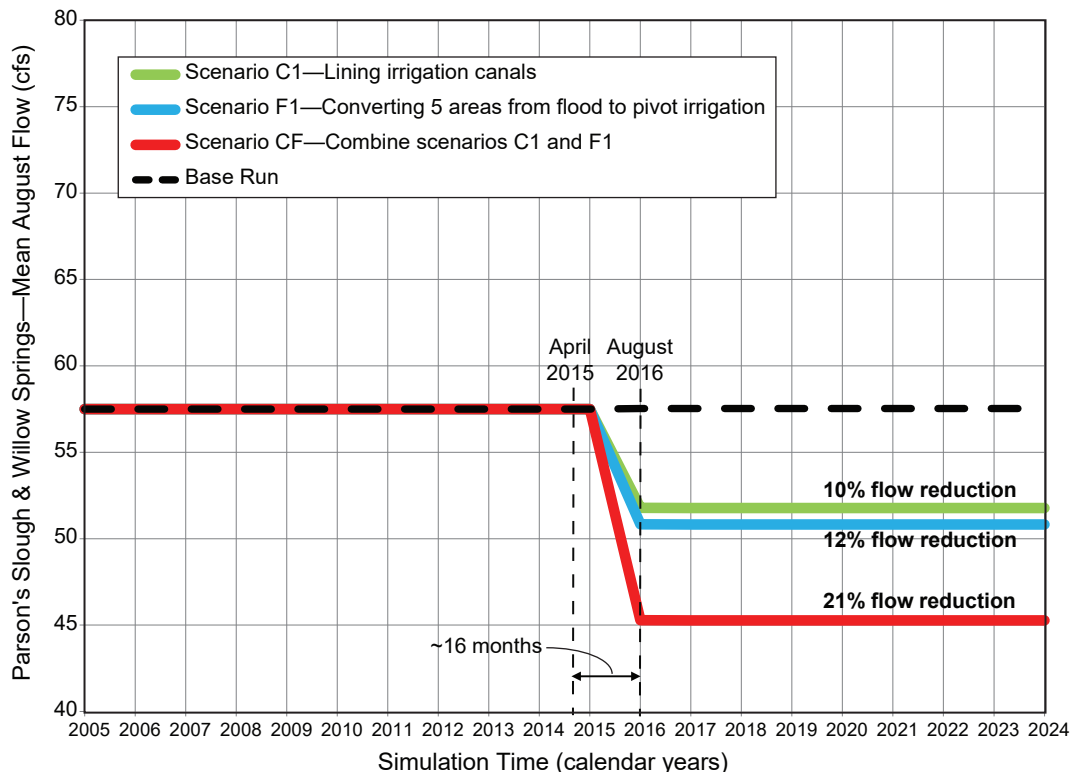


Figure 36. Predictive scenario results show that the greatest flow reduction in groundwater-fed streams discharge occurs with scenario CF. Scenario CF includes lining all irrigation canals (scenario C1) and converting five areas from flood to pivot irrigation (scenario F1).

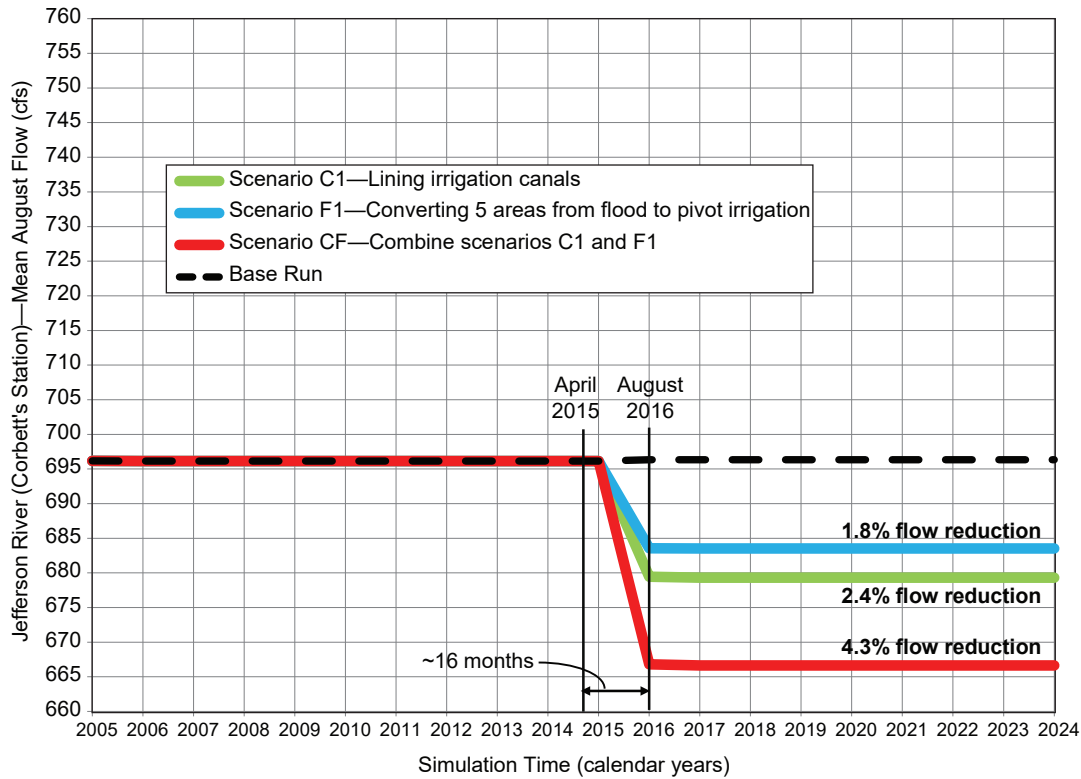


Figure 37. Predictive scenario results show the effect on Jefferson River flow at Corbett's station. The largest reduction in river flow occurs with scenario CF, with lining all irrigation canals and converting five flood-irrigated areas to pivot irrigation.

2). The Creeklyn Canal scenarios C7, C8, and C9 simulate the individual lining of canal segments 6, 7, and 8, respectively. Compared to lining all the canals, lining individual canal segments has a lesser effect on Jefferson River August flow, with flow reductions less than 1% in scenarios C2 to C8 compared to 10% in scenario C1 (table 10).

**Flood to Pivot Irrigation Scenarios**

Scenario F1 consisted of converting five major flood-irrigated areas (areas 1–5, fig. 20) to center pivot. This would reduce irrigation recharge to the underlying aquifer because center pivot systems are more efficient than flood irrigation. This is simulated by changing the recharge rate applied to the five zones to the lower rate used for pivot areas. The model response to this change occurs over more than 1 yr (~16 mo), the time needed for maximum flow reduction in groundwater-fed streams and rivers (figs. 36, 37). Relative to the base run, the conversion to pivot irrigation reduced the groundwater discharge to Parson's Slough and Willow Springs by 7 cfs in August 2024, a 13% reduction in late summer flow. The change to pivot irrigation also reduced flow in the Jefferson River at Corbett station by 13 cfs in August 2024, a 1.8% reduction in late summer flow (tables 9,

10). Parson's Slough and Willow Springs are relatively more sensitive to changes in irrigation recharge than to canal leakage, because irrigation recharge makes a larger portion of the water budget than canal leakage, and because of the proximity of the irrigated fields to the streams (fig. 20).

Five other scenarios (F2–F6) also tested converting individual flood irrigation areas to center pivot irrigation. In general, results from these scenarios showed less reduction in late summer flows to Parson's Slough, Willow Springs, and the Jefferson River compared to that of extreme scenario F1 (table 10); with the exception of scenarios F2, F3, F4, and F6, the reduction in Parson's Slough flow was more than that of F1 (table 10). Scenario F5 produced comparable flow reductions to that of scenario F1 for Willow Springs and the Jefferson River (table 10). Since the Willow Springs stream flows through the middle of irrigation area 4 (fig. 20), the proximity of the spring to the irrigated field results in a direct effect of changes in irrigation to the amount of groundwater discharge to Willow Springs, consequently affecting discharge to the Jefferson River.

## Canal Lining and Conversion to Pivot Scenario (CF)

Scenario CF combines scenarios C1 and F1 to produce an extreme change in irrigation practices. This simulation includes lining all of the Parrot and Creeklyn Canals and converting all major flood-irrigated areas (1 to 5, fig. 20) to center pivot irrigation, creating a pronounced reduction in recharge to the underlying aquifer. It takes about 16 mo to develop the full effect on groundwater-fed streams and river flows (figs. 36, 37). In comparison to the base run, the combined late summer flow in Parson's Slough and Willow Springs was reduced by 12 cfs, a 21% reduction. For the Jefferson River, the changes reduced flows at Corbett station by 30 cfs, a 4.3% reduction in late summer flow (tables 9, 10).

### Split Season Irrigation Scenarios

Split season irrigation scenario SS1 adopts the changes from scenario F1, converting five major flood-irrigated areas (1–5, fig. 20) to center pivot irrigation. Scenario SS1 limits center pivot rates to the second half of the irrigation season, July to September, and maintains flood irrigation recharge rates in the first half of the season, April to June. This scenario tested mitigating the reduction of flow in Parson's Slough, Willow Springs, and the Jefferson River caused by converting to pivot irrigation in scenario F1. As shown in table 10, during the summer of 2024, the SS1 scenario lowered the Jefferson River's flow by 7 cfs (0.34% reduction) in July relative to baseline, not much different than the effect of scenario F1 (10.2 cfs, 0.5% reduction). In August 2024, the reduction was about 12 cfs (1.7% reduction), which is also similar to that of scenario F1 (13 cfs, 1.8% reduction).

Split season irrigation scenario SS2 expands scenario SS1 to include all seven flood-irrigated areas in the model (fig. 20). As shown in table 10, for the Jefferson River, the SS2 scenario showed insignificant flow reduction in July 2024 (<1 cfs), a favorable result compared to that of scenario F1 (10.2 cfs, 0.5% reduction). In August 2024, the SS2 reduction was 10.3 cfs (1.5% reduction), similar to that of scenario F1 (13 cfs, 1.8% reduction).

In the split season scenarios, the July reduction in Jefferson River flow was less than in scenario F1; however, the August flow reduction was similar to that of scenario F1. Thus, the desired effect did not last long into the second half of the irrigation season.

Recharge to the alluvial aquifer and the increase in groundwater storage during the flood irrigation months was offset by relatively fast groundwater discharge to surface-water bodies, and therefore did not fully mitigate August low-flow conditions. We attribute this result to (a) the high transmissivity aquifer, and (b) the close proximity of the irrigated fields to Parson's Slough, Willow Springs, and the Jefferson River. As shown in figure 38, field data from Willow well 9 (GWIC276285), located about 1,630 ft from the Parrot Canal, indicates fast water table response to irrigation recharge.

### Model Prediction Results

The three extreme hypothetical irrigation scenarios, C1 (lining all irrigation canals), F1 (converting five areas from flood to pivot irrigation), and CF (lining all irrigation canals and converting five areas from flood to pivot irrigation) show that maximum flow reduction occurs during the critical low-flow, late summer month of August. The combined scenario CF produced the largest effect.

In August 2024, the reduction in flow on the combined flow coming from Parson's Slough and Willow Springs was 6 cfs (a 10% reduction) in scenario C1, 7 cfs (12% reduction) in scenario F1, and 12 cfs (21% reduction) in scenario CF (fig. 36).

The transient model base run produced about 700 cfs flow in the Jefferson River near Corbett's station in August 2024. For the same period, the effects were 17 cfs (2.4% reduction) in scenario C1, 13 cfs (1.8% reduction) in scenario F1, and 30 cfs (4.3% reduction) in scenario CF (fig. 37). The drought management plan includes a goal to maintain at least 50 cfs at the USGS station at Parson's Bridge (JRWC, 2013). The 50 cfs target is the minimum flow needed to maintain pool connectivity and buffer stream temperatures. Therefore, in drought years, these reductions (13 to 30 cfs) would approach the 50 cfs goal.

In general, Willow Springs is more sensitive to changes in irrigation recharge than Parson's Slough. Flow reduction in Willow Springs was 11%, 17%, and 27% in the three scenarios C1, F1, and CF, respectively. Flow reduction in Parson's Slough for these scenarios were 9%, 1%, and 10% (table 10).

Similarly, Willow Springs was more sensitive than Parson's Slough to conversion from flood irrigation

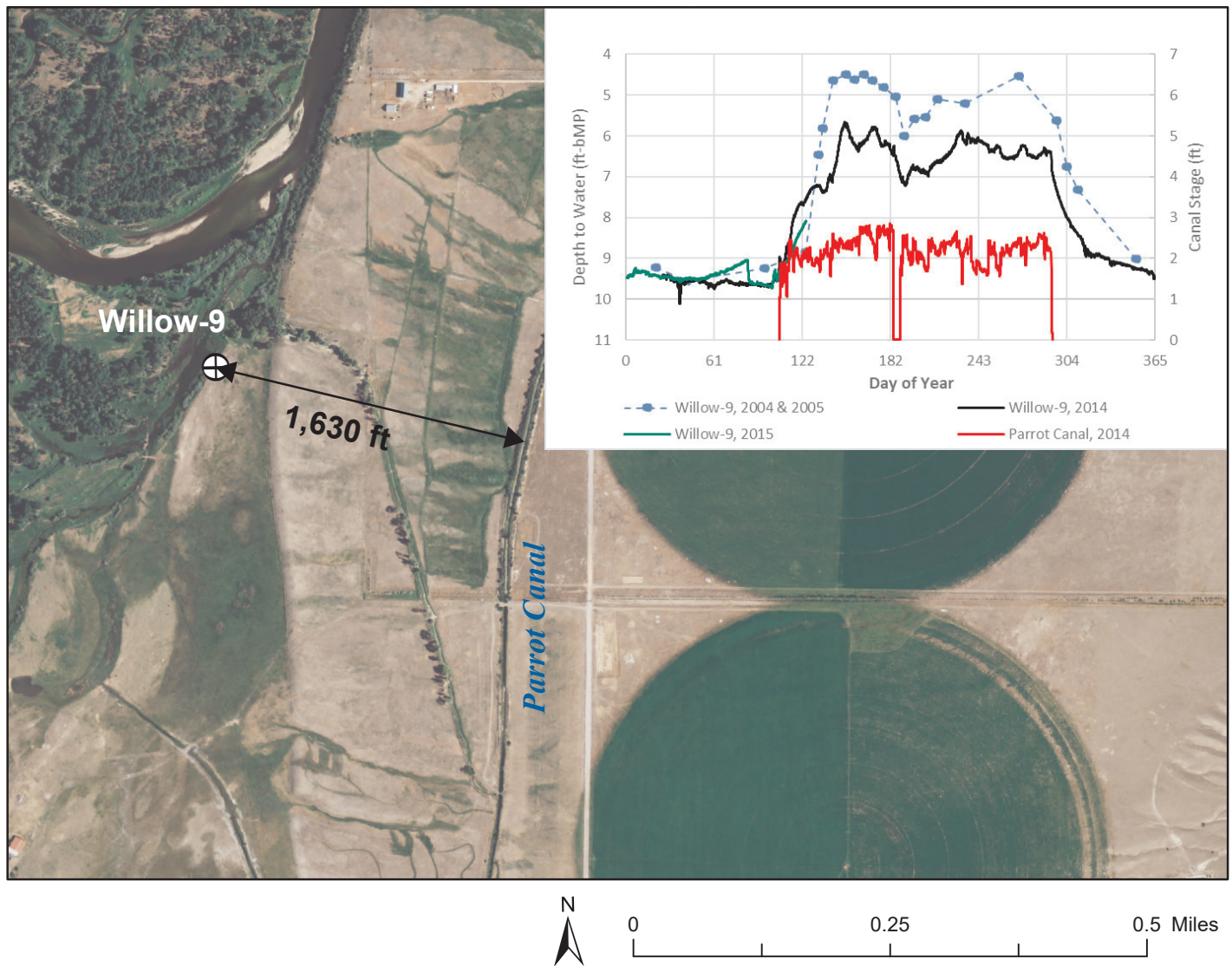


Figure 38. Field data from Willow well 9 (GWIC 276285), located about 1,630 ft from Parrot Canal, shows a fast response to canal stage changes, due to high transmissivity and close proximity to the recharge source. Note that the canal is turned off annually each 4th of July week (Julian day 182), corresponding to a rapid response in the water table elevation at Willow 9.

to center pivot systems (scenarios F1– F6, table 10). In the model, Willow Spring’s branches flow through flood-irrigated areas, while Parson’s Slough has less contact with flood-irrigated zones (fig. 20). Results from scenario F5 (converting flood area 4 to pivot) is a clear example of how the location and branching of drains (model cells that represent the spring) with respect to recharge zones can produce notable effects; there was a 16% reduction in Willow Springs flows compared to a 0.4% decrease in Parsons’s Slough (table 10).

Scenario results showed that lining Creeklyn Canal (scenarios C7 to C9) did not have a large effect on Parson’s Slough or Willow Springs (table 10), most likely due to the Jefferson River forming a hydrologic boundary between Creeklyn Canal and these streams.

In contrast, lining Creeklyn Canal had a noticeable effect on Jefferson River flows at Corbett station.

These simulations demonstrate that split season irrigation can provide a source of delayed discharge to surface water by supplementing aquifer storage early in the irrigation season. However, it is important to evaluate the rate at which the early season groundwater mound will dissipate. In the Waterloo area, the fields modeled with split season irrigation were too close to the surface-water features to allow for a sufficient time lag given the relatively high transmissivity of the alluvial aquifer.

### UNCERTAINTY ANALYSIS

For any model predictions, there are two broad sources of uncertainty: (1) uncertainty linked to the

model itself, and (2) uncertainty associated with accurate specifications of future conditions (Anderson and others, 2015).

The first type of uncertainty originates from the following:

- (a) Error in field measurements of certain parameters. Thus, uncertainty in predictions stemming from error in calibration of these parameters can be reduced but not eliminated.
- (b) Failure to capture the complexity of the natural setting relevant to the prediction. This error results from the conceptual model or from the spatial and temporal simplifications made during model construction and calibration.

The second source of uncertainty occurs when predictions require estimating future stresses and properties (e.g., recharge rates affected by changes in climate), and future non-hydrogeological conditions, such as political, economic, and societal actions that may affect hydrologic stresses (e.g., conversion from agricultural land use to residential development).

In this study, we focused on the first type—uncertainty caused by errors in field parameter estimation and the simplifications of spatial and temporal parameters during model construction and calibration. We employed a basic uncertainty analysis that is similar to the *scenario modeling method* presented by Anderson and others (2015). Model parameters selected for uncertainty analysis are based on the sensitivity analysis, and on the uncertainty associated with the method of estimating some model parameters (e.g., leakage rates from irrigation canals). We investigated six parameters that were the most likely to affect predictions:

1. aquifer thickness,
2. horizontal hydraulic conductivity ( $K_h$ ) in areas initially assigned as zones 1 and 2,
3. lateral groundwater influx ( $GW_{in-lat}$ ) in Parrot and Creeklyn boundaries,
4. canal leakage ( $CL$ ) in the three irrigation canals,
5. aquifer storage coefficients (4 zones), and
6. groundwater influx and outflux to the alluvial aquifer across the southern and northern model boundaries.

The uncertainty analysis involved completing the *base run* simulation and the three extreme scenario simulations (C1, F1, and CF) while changing one of the six parameters (e.g., aquifer thickness). Each parameter was varied by applying a low and a high multiplier, creating multiple versions of each model (table 11). The only exception was for changes to the zone 1 alluvium hydraulic conductivity, which was executed once with a low multiplier. A total of 100 models included 27 versions of the base run, 23 versions of scenario C1, 27 versions of scenario F1, and 23 versions of scenario CF (table 12). Each of the six parameters was considered to be independent, so that changing one parameter did not require changing any other parameters.

The uncertainty assessment focused on simulating August surface-water flows in Parson’s Slough, Willow Springs, and the Jefferson River. The error in model prediction is the difference between each scenario model’s August 2024 flows and that calculated by the base run, with changes to one parameter at a time. The assessment required running all 100 simulations (table 12) and calculating the “error” between the base run and the scenarios for August 2024 flows. This collection (or “ensemble”) of errors define an envelope of uncertainty limits around the prediction (Anderson and others, 2015).

Table 11. Uncertainty analysis parameters.

Uncertainty Parameter	Multipliers
Aquifer Thickness	0.5 & 1.5
Hydraulic Conductivity ( $K_x, K_y$ ) Zone 1	0.1
Hydraulic Conductivity ( $K_x, K_y$ ) Zone 2	0.1 & 2.0
Parrot Canal—Lateral Groundwater Flux	0.75 & 1.25
Parrot Canal—Leakage	0.75 & 1.25
Creeklyn Canal—Lateral Groundwater Flux	0.75 & 1.25
Creeklyn Canal—Leakage	0.75 & 1.25
Jefferson Canal—Leakage	0.75 & 1.25
South Boundary GW Flux	0.75 & 1.25
North Boundary GW Flux	0.75 & 1.25
Storage Coefficient Zone 1	0.1 & 10
Storage Coefficient Zone 2	0.1 & 10
Storage Coefficient Zone 3	0.1 & 10
Storage Coefficient Zone 4	0.1 & 10



The model uncertainty analysis indicated that the greatest uncertainty is associated with the extreme scenario CF (all canals lined and all flood irrigation converted to center pivot systems). This simulation had a maximum error in predicting August flow in Parson’s Slough and Willow Springs of about 40% (fig. 39), but remained at less than 10% for most tested parameters. Note that there are two groups of prediction errors that exceeded 10% error (fig. 39). These were due to sharp reductions in the transmissivity of the aquifer, consistent with the sensitivity analysis. For Jefferson River flows, the prediction error remained within 3% for the majority of scenarios using uncertainty parameters. The maximum error is less than 5% under conditions of low hydraulic conductivity (fig. 40).

### MODEL LIMITATIONS

The Waterloo groundwater flow model is a useful tool for refining the conceptual model and evaluating the effects of changes in water management practices on groundwater and surface-water flows. However, the model has limitations, mainly due to scale, parameter uncertainty, and lack of precision of the calibrated

river gains and losses. The modeling scale is limited to the Waterloo area and is not designed to account for flow calculations across the entire Jefferson River basin, beyond the model area. On the other hand, the model grid size (178 ft x 188 ft) may not be suitable to accurately simulate groundwater/surface-water interactions at a finer scale. The one-layer model grid cannot simulate vertical flow components in groundwater/surface-water interactions; this limits the model to simulate heat exchange or contaminant transport within the alluvial aquifer only, not between the alluvium and the lower Tertiary sediments (fig. 6).

Predictive sensitivity (uncertainty) analysis showed that parameter uncertainty is also a limitation on model results. In particular, the model predictions are sensitive to aquifer thickness, hydraulic conductivity, estimated inflow to the alluvial aquifer, and rates of canal leakage.

The lack of calibration targets (water levels in wells) in the west and northwest areas of the model limits modeling losses and gains in some reaches along the Jefferson River. The calibration focused on

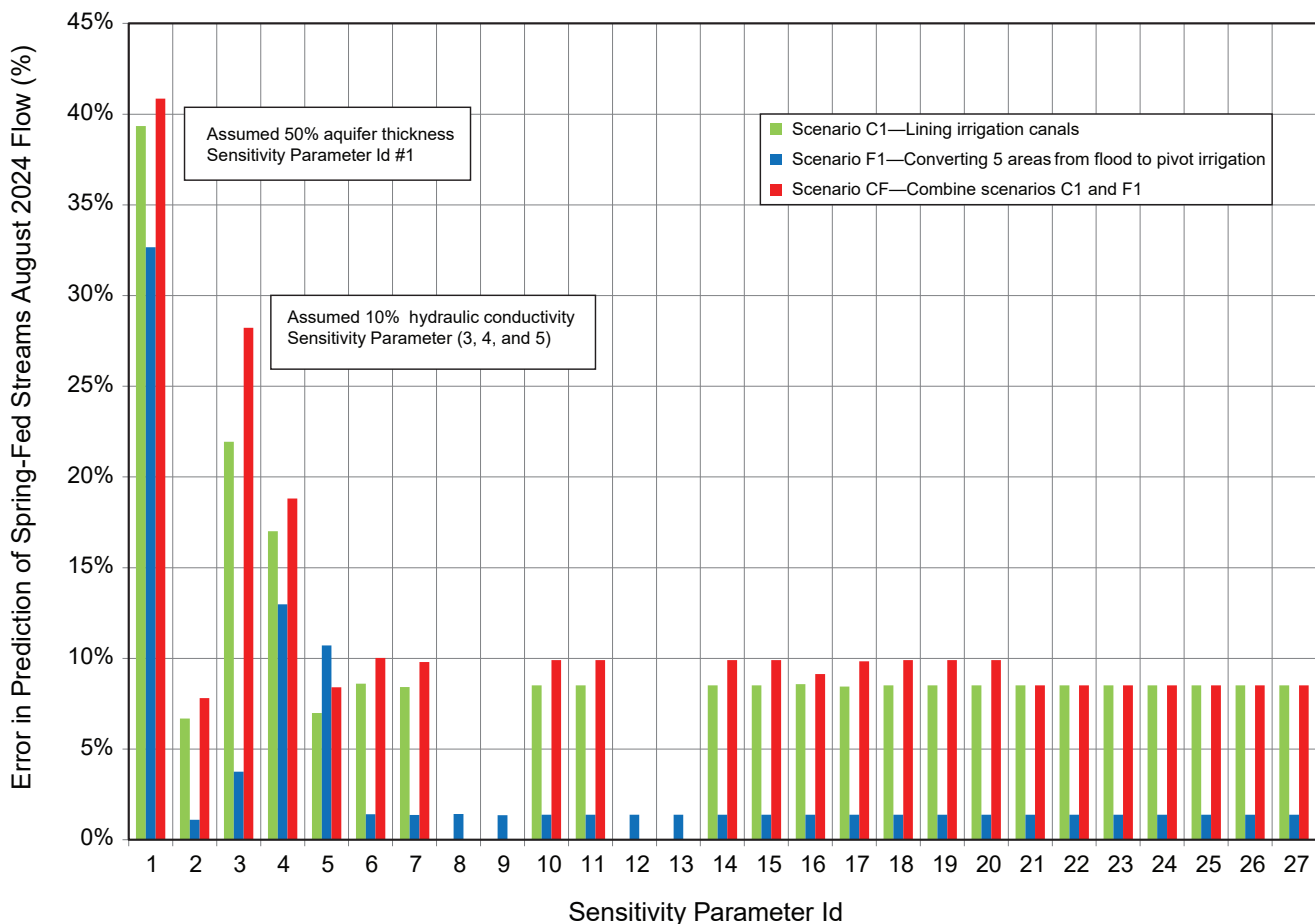


Figure 39. Model uncertainty analysis focused on the prediction error of the combined groundwater discharge to Parson’s Slough and Willow Springs. The figure shows the ensemble of prediction errors produced by the model.

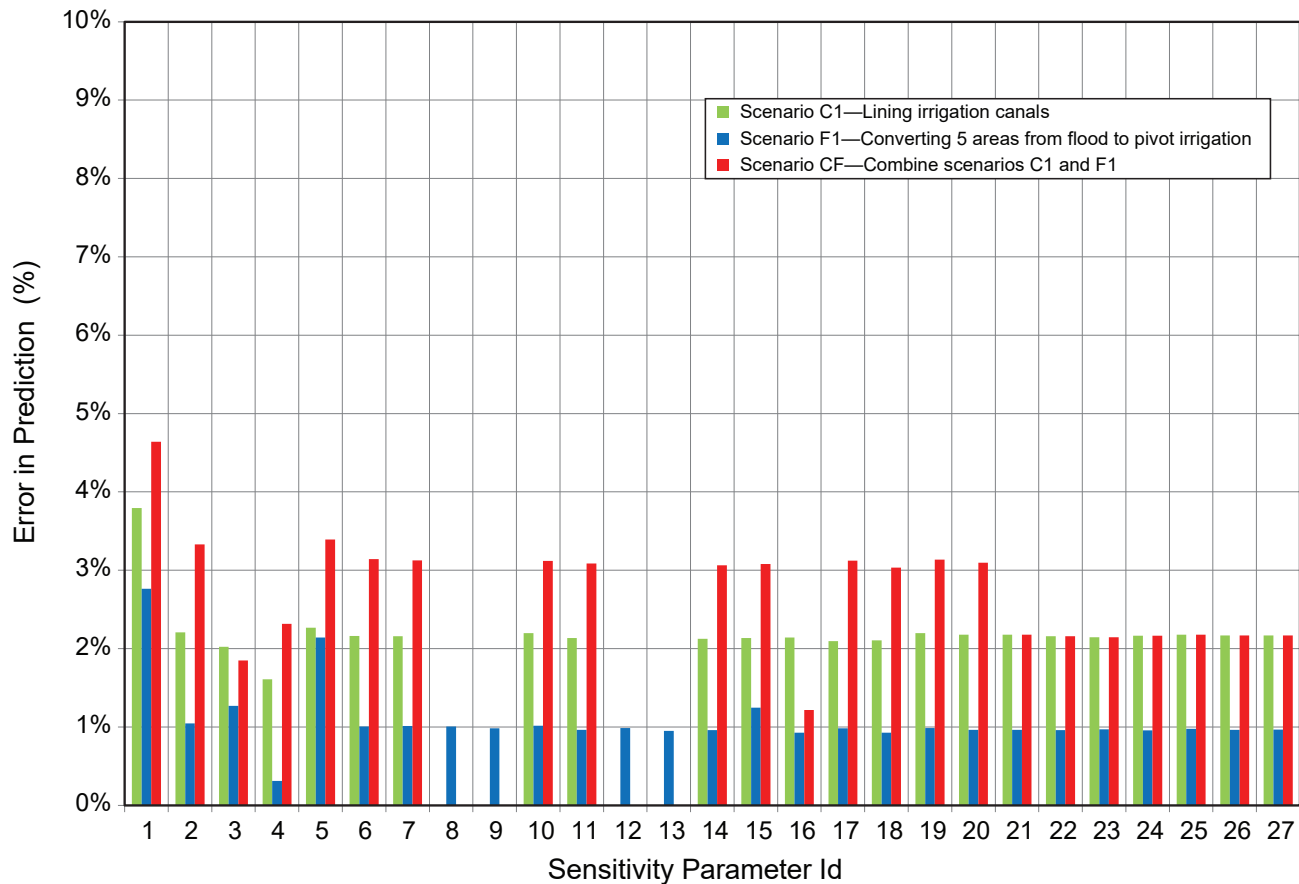


Figure 40. Model uncertainty analysis focused on the prediction error of Jefferson River flow at Corbett's station. The figure shows the ensemble of the prediction errors produced by the model.

simulating Jefferson River flow at the downstream point at Corbett's station and on estimating combined flows from Parson's Slough and Willow Springs.

Additional field information would improve the current model. For example, more groundwater-level measurements and longer monitoring periods from existing or new wells in the northwest region of the model would yield better estimates of river conductance and improve the model calibration and predictive power. Additional aquifer tests could improve the estimate of aquifer parameters, or confirm the calibrated ones. In addition, field measurements of Jefferson Canal leakage could provide a better leakage estimation.

More survey data and DEM information would help better develop the simulation of groundwater/surface-water interactions that are naturally sensitive to elevation differences. With respect to streambed elevations, LiDAR is recommended as the most cost-effective and efficient source of high-accuracy data. Also, additional lithological information can enhance the delineation of the alluvial aquifer thickness. This

would increase the accuracy of estimating groundwater flow into the aquifer and the water budget calculations.

The current model scenarios operate under the assumption that there is no reduction in diversions from the Jefferson River to the canals if the canals were lined or center pivot irrigation was used, i.e., the extra water is not accounted for. That requires more information to correlate leakage from irrigation canals to diversions, but this can be tested in a post audit study, where the decrease in diversions to the canals results in an increase in flows in the Jefferson River and groundwater, which would ultimately flow into the current model domain and offset the loss from the canal leakages.

## SUMMARY AND CONCLUSIONS

As development of land and water resources increase, it is apparent that use of either resource affects the quantity and quality of the other (Hirsch, 1999). The objectives of this modeling study were to: (a) simulate the interactions between groundwater and

surface-water components of the flow system in the Waterloo area of the Jefferson River Valley, and (b) forecast the changes in surface-water discharge in Parson's Slough, Willow Springs, and the Jefferson River due to changes in irrigation practices.

The steady-state calibrated model simulated—within specified error limits—the groundwater levels, the groundwater discharge to Parson's Slough and Willow Spring, and the Jefferson River flows at Corbett station. The model generated a balanced water budget that generally agreed with preliminary estimates of model area inflows and outflows. The transient model displayed a reasonable match to changes in heads, and captured the seasonality of water-level changes. The transient model also matched the Jefferson River monthly average flows measured at Corbett station. Eighteen future scenarios were tested to evaluate the effects of changing irrigation practices (lining canals and/or converting flood irrigation to center pivot) on surface-water flows during the August flow period. Results from the simulations indicated a reduction in groundwater discharge to Parson's Slough, Willow Spring, and the Jefferson River. The overall result suggests lower late summer stream flows, and possible warmer stream temperatures, a condition that may affect fish species in the area.

## REFERENCES

- Anderson, M.P., Woessner, W., and Hunt, R., 2015, Applied groundwater modeling: San Diego, Calif., Academic Press, 2nd ed., 564 p.
- ASTM, 1995 (reapproved 2006), ASTM Standard D5718-95—Documenting a ground-water flow model: West Conshohocken, Pa., ASTM International.
- Barnes, H.H., 1967, Roughness characteristics of natural channels: U.S. Geological Survey Water-Supply Paper 1849, 213 p.
- Bobst, A., Butler, J., and Carlson, L., 2016, Hydrogeologic investigation of the Boulder River Valley, Jefferson County, Montana: Interpretive report: Montana Bureau of Mines and Geology Open-File Report 682, 92 p.
- Bobst, A., and Gebril, A., 2020, Aquifer tests in the Upper Jefferson Valley: Montana Bureau of Mines and Geology Groundwater Open-File Report 727, 52 p.
- Bobst, A., and Gebril, A., 2021, Hydrogeologic investigation of the Upper Jefferson Valley, Montana—Interpretive report: Montana Bureau of Mines and Geology Report of Investigation 28, 130 p.
- Brancheau, Nicole, 2015, A hydrogeologic evaluation of the Waterloo area in the Upper Jefferson River Valley, Montana: Butte, Mont., Montana Tech of University of Montana, Master's thesis, 104 p.
- Daly, C., Halbleib, M., Smith, J.I., Gibson, W.P., Doggett, M.K., Taylor, G.H., Curtis, J., and Pasteris, P.P., 2008, Physiographically sensitive mapping of climatological temperature and precipitation across the conterminous United States: International Journal of Climatology, v. 28, no. 15, p. 2031–2064.
- Doherty, J.E., 2010, PEST model—Independent parameter estimation user manual: Brisbane, Australia, Watermark Numerical Computing, 5th ed., 336 p., <http://www.pesthomepage.org> [Accessed December 19, 2013].
- Doherty, J.E., 2013a, Addendum to the PEST manual: Brisbane, Australia, Watermark Numerical Computing, 266 p., <http://www.pesthomepage.org> [Accessed December 19, 2013].
- Doherty, J.E., 2013b, Getting the most out of PEST, August 2013, 12 p., <http://www.pesthomepage.org/> [Accessed October 2013].
- Environmental Simulations Incorporated, 2011, Guide to using Groundwater Vistas, version 6.77 Build9, 213 p.
- Fetter, C., 2001, Applied hydrogeology: Upper Saddle River, N.J., Prentice-Hall, Inc.
- Freeze, R.A., and J.A. Cherry, 1979, Groundwater, Prentice-Hall Inc., Englewood Cliffs, New Jersey
- Ground Water Information Center (GWIC), 2019, <http://datagwic.mtech.edu/v6/menus/menuMain.asp> [Accessed July 2021].
- Heath, C.R., 1983, Basic ground-water hydrology: U.S. Geological Survey, Water Supply Paper 2220.
- Hirsch, M.R., 1999, Groundwater and surface water: A single resource: U.S. Geological Survey, Circular 1139.
- Jefferson River Watershed Council (JRWC), 2013, Drought management plan, 11 p., available at <https://jeffersonriverwc.com/fish/up->

- loads/2016/06/JRWC\_Drought\_Mgt\_Plan\_2012.pdf [Accessed July 2021].
- Leenhouts, J.M., Stromber, J.C., and Scott, R.L., eds., 2006, Hydrologic requirements of and consumptive ground-water use by riparian vegetation along the San Pedro River, Arizona: USGS Scientific Investigations Report 2005-5163, 154 p.
- Montana Fish Wildlife and Parks Department (MFWP), 2012, Montana Statewide Fisheries Management Plan, 2013-2018, 478 p.
- NRCS, 2012, NRCS web soil survey, <http://websoilsurvey.nrcs.usda.gov/app/WebSoilSurvey.aspx> [Accessed November 2012].
- Oregon State University, 2013, PRISM Climate Group, Oregon State University, <http://prism.oregonstate.edu> [Accessed April 2013].
- Panday, S., Langevin, C.D., Niswonger, R.G., Ibaraki, M., and Hughes, J.D., 2013, MODFLOW-USG version 1: An unstructured grid version of MODFLOW for simulating groundwater flow and tightly coupled processes using a control volume finite-difference formulation: U.S. Geological Survey Techniques and Methods, book 6, chap. A45, 66 p.
- Scott, R.L., Edwards, E.A., Shuttleworth, W.J., Huxman, T.E., Watts, C., and Goodrich, D.C., 2004, Interannual and seasonal variation in fluxes of water and carbon dioxide from a riparian woodland ecosystem: *Agricultural and Forest Meteorology*, v. 122, p. 65–84.
- Shah, N., Nachabe, M., and Ross, M., 2007, Extinction depth and evapotranspiration from ground water under selected land covers: *Ground Water*, v. 45, no. 3, p. 329–338.
- U.S. Department of Agriculture and U.S. Department of Interior, 2014a, LANDFIRE, from existing vegetation type, <http://landfire.cr.usgs.gov/NationalProductDescriptions21.php> [Accessed July 23, 2014].
- U.S. Department of Agriculture, 2014b, Water management models, IWR Program, from Natural Resources Conservation Service, <http://www.nrcs.usda.gov/wps/portal/nrcs/detailfull/national/water/manage/irrigation/?&cid=stelprdb1044890> [Accessed September 2014].
- U.S. Geological Survey, 2004, A New streamflow-routing (SFR1) package to simulate stream-aquifer interaction with MODFLOW-2000: U.S. Geological Survey Open-File Report 2004-1042.
- U.S. Geological Survey, 2009, NED, ned19\_n37x50\_w122x25\_ca\_alamedaco\_2007 1/9 arc-second 2009 [Accessed July 2021].
- U.S. Geological Survey, 2010, LANDFIRE database, Wildland Fire Science, Earth Resources Observation and Science Center: U.S. Geological Survey, [http://www.landfire.gov/lf\\_mosaics.php](http://www.landfire.gov/lf_mosaics.php) [Accessed January 2013].
- Vuke, S.M., Coppinger, W.W., and Cox, B.E., 2004, Geologic map of Cenozoic deposits in the Upper Jefferson Valley, southwestern Montana: Montana Bureau of Mines and Geology Open-File Report 505, 35 p., 1 sheet, scale 1:50,000.
- Waren, K.B., Bobst, A.L., Swierc, J.E., and Madison, J.D., 2013, Hydrologic investigation of the North Hills Study area, Lewis and Clark County, Montana, Groundwater Modeling Report: Montana Bureau of Mines and Geology Open-File Report 628, 90 p.
- Water & Environmental Technologies (WET), 2006, Ground water study of the Waterloo area: Water & Environmental Technologies, <https://waterentech.com/projects/jefferson-river-ground-water-study-2>



**APPENDIX A**  
**WATERLOO AREA CONCEPTUAL**  
**WATER BUDGET**

## APPENDIX A— WATERLOO AREA CONCEPTUAL WATER BUDGET

A conceptual water budget was developed for the Waterloo area to aid in model construction and ensure that the amount of water entering and leaving the model through the boundaries was reasonable. This budget was largely based on the budget developed by Brancheau (2015) for the Waterloo area. The preliminary budget was modified during the model calibration process.

### 1. Alluvial Groundwater Inflow ( $GW_{in-ai}$ )

Groundwater flowed into the model area at the upstream end of the model domain (fig. A1). The inflow at this boundary was calculated using the Darcy Flux Equation:

$$Q = KAI,$$

where  $Q$  is groundwater inflow (ft<sup>3</sup>/d);  $K$  is hydraulic conductivity of the aquifer (ft/d);  $A$  is cross-sectional area of the saturated alluvial aquifer at the boundary (ft<sup>2</sup>); and  $I$  is hydraulic gradient across the boundary (ft/ft or unitless).

Brancheau (2015) estimated the aquifer thickness in this area to be 100 ft; however, further review of well logs showed that the deepest well was 159 ft, so we used a thickness of 200 ft. The alluvial width is estimated to be 10,600 ft based on geologic maps. The hydraulic conductivity was estimated to be 1,100 ft/d based on an aquifer test conducted in the alluvium near Waterloo, and lithologic descriptions from well logs. A gradient of 0.00235 was based on monitoring data.

Table A1. Flow into the model area through the alluvium was estimated using the Darcy Flux Equation.

	K(ft/d)			Width (ft)	Sat Tk (ft)	Area (ft <sup>2</sup> )	I (ft/ft)	BE Q (ft <sup>3</sup> /d)	Q (acre-ft/yr)		
	BE	MinE	MaxE						BE	MinE	MaxE
Jefferson River	1,100	825	1,375	10,600	200	2,120,000	0.00235	5,480,200	45,947	34,460	57,433

*Note.* K, range based on aquifer tests, sediment descriptions, and literature values (Heath, 1983; Fetter, 1994). The likely range was based on a range of K values, which is the most variable, and uncertain, component of the calculation. BE, best estimate; MinE, minimum estimate; MaxE, maximum estimate. Width-based geologic maps: Sat Tk, saturated thickness, based on well logs; Area, width x Sat Tk; I, calculated using observed water levels from April 2015.

Table A2. Monthly alluvial inflow (acre-ft).

	Jan	Feb	Mar	Apr	May	Jun	Jul	Aug	Sep	Oct	Nov	Dec	Total
BE	3,829	3,829	3,829	3,829	3,829	3,829	3,829	3,829	3,829	3,829	3,829	3,829	45,947
MinE	2,872	2,872	2,872	2,872	2,872	2,872	2,872	2,872	2,872	2,872	2,872	2,872	34,460
MaxE	4,786	4,786	4,786	4,786	4,786	4,786	4,786	4,786	4,786	4,786	4,786	4,786	57,433

*Note.* The estimates for total annual inflow (table A1) were divided by 12 to estimate inflow in each month.

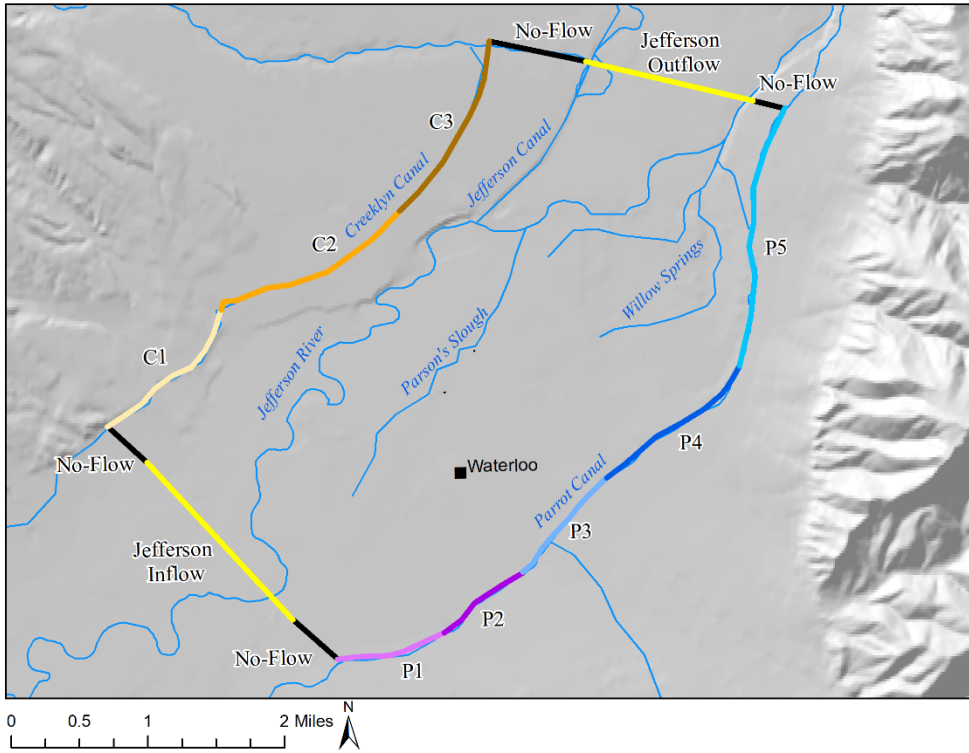


Figure A1. Groundwater inflow and outflow occur along the edges of the model domain. Alluvial inflow occurs along the yellow segment at the southern end. Alluvial outflow occurs along the yellow segment on the northern end. Lateral groundwater inflow occurs along the numbered segments (table A3).

## 2. Lateral Groundwater Inflow ( $GW_{in-lat}$ )

Groundwater inflow along the lateral edges of the model (fig. A1). The groundwater inflow was calculated by subtracting estimated evapotranspiration (based on plant types) from precipitation (PRISM 30-yr normal; PRISM, 2018) in the areas upgradient from each lateral edge, and assuming that half of the remaining water would run off and half would recharge the groundwater system.

Table A3. Estimated evapotranspiration—Highland Mountains.

Vegetation Group	Area (acres)	ET Rate (ft/yr)	ET (acre-ft/yr)
Upland Sagebrush	5,350	1.1	5,885
Douglas Fir	8,477	1.4	11,868
Shrub/Grass Lowlands	9,765	1.0	9,765
Mixed Evergreen	8,290	1.8	14,923
High Xeric Grasses	2,472	1.2	2,967
Ag Lands	309	2.1	650
Mesic Meadow	1,216	1.7	2,067
Whitebark Pine	2,838	2.2	6,244
Alpine Rangeland, Deciduous Shrubs	864	2.0	1,728
Developed	186	1.0	186
Riparian	170	2.3	392
<b>TOTAL</b>	<b>39,939</b>	<b>—</b>	<b>56,674</b>

Table A4. Estimated evapotranspiration—Tobacco Root Mountains.

Vegetation Group	Area (acres)	ET Rate (ft/yr)	ET (acre-ft/yr)
Upland Sagebrush	4,593	1.1	5,053
Douglas Fir	12,942	1.4	18,118
Shrub/Grass Lowlands	2,046	1.0	2,046
Mixed Evergreen	3,215	1.8	5,787
High Xeric Grasses	343	1.2	412
Ag Lands	1,995	2.1	4,190
Mesic Meadow	757	1.7	1,287
Whitebark Pine	1,492	2.2	3,283
Alpine Rangeland, Deciduous Shrubs	181	2.0	361
Developed	206	1.0	206
Riparian	422	2.3	971
<b>TOTAL</b>	<b>28,193</b>	<b>---</b>	<b>41,715</b>

Table A5. Lateral groundwater inflow calculated based on precipitation and vegetation types.

	Area (acres)	Average PCP (in/yr)	Annual PCP (acre-ft/yr)	Estimated ET (acre-ft/yr)			Excess Water (acre-ft/yr)			$GW_{lat}$ (acre-ft/yr) <sup>#</sup>		
				BE	MinE <sup>+</sup>	MaxE <sup>+</sup>	BE	MinE	MaxE	BE	MinE	MaxE
Highlands	39,939	18.36	61,116	56,674	53,840	59,508	4,442	1,608	7,276	2,221	804	3,638
Tobacco Root	28,193	19.02	44,676	41,715	39,629	43,801	2,961	875	5,047	1,480	438	2,523
TOTAL*										3,701	1,942	5,461

<sup>+</sup>ET values were considered to be the most uncertain element of the calculation, and their range was estimated based on 5% error.

<sup>#</sup> $GW_{lat}$  was estimated by assuming that half of the excess water infiltrates to groundwater.

\*Total range was based on root sum of squares error propagation.

Note. Lateral groundwater inflow was applied to the edges based on the side of the model (Highlands vs. Tobacco Root), and the length of each segment (fig. A1). Values were distributed by month by dividing the total by 12.

Table A6. Monthly lateral groundwater inflow (acre-ft).

	Jan	Feb	Mar	Apr	May	Jun	Jul	Aug	Sep	Oct	Nov	Dec	Total
BE	308	308	308	308	308	308	308	308	308	308	308	308	3,701
MinE	162	162	162	162	162	162	162	162	162	162	162	162	1,942
MaxE	455	455	455	455	455	455	455	455	455	455	455	455	5,461

### 3. Canal Leakage (CL)

The Parrot, Creeklyn, and Jefferson Canals leak water to the underlying aquifer from mid-April to mid-October (fig. A1). Monitoring data was used to estimate overall average leakage rates of 1.31 and 1.36 cfs/mi on the Parrot and Creeklyn Canals, respectively. The average of these rates (1.34 cfs/mi) was assigned to the Jefferson Canal. The total amount of leakage was based on multiplying canals were separated into the same segments used to calculate lateral groundwater inflow (fig. A1).

Table A7. Annual canal leakage amounts.

Canal	Leakage Rate (cfs/mi)			Miles	BE cfs	BE ft <sup>3</sup> /d	Days on per year	BE Leakage (ft <sup>3</sup> /yr)	Leakage (acre-ft/yr)		
	BE	MinE	MaxE						BE	MinE	MaxE
Parrot	1.31	1.18	1.44	5.70	7.46	644,973	183.5	118,352,520	2,717	2,445	2,989
Creeklyn	1.36	1.22	1.50	4.44	6.04	521,533	183.5	95,701,320	2,197	1,977	2,417
Jefferson	1.34	1.21	1.47	1.41	1.88	162,846	183.5	29,882,160	686	617	755
								TOTAL	5,600	5,244	5,956

Note. The likely range was based on a 10% error for the range of leakage rates, which is the most variable, and uncertain, component of the calculation.

Table A8. Monthly canal leakage amounts.

	Jan	Feb	Mar	Apr	May	Jun	Jul	Aug	Sep	Oct	Nov	Dec	Total
Days on	0	0	0	15	31	30	31	31	30	15.5	0	0	183.5
BE	0	0	0	458	946	916	946	946	916	473	0	0	5,600
MinE	0	0	0	429	886	857	886	886	857	443	0	0	5,244
MaxE	0	0	0	487	1006	974	1006	1006	974	503	0	0	5,956

Note. The estimates for total annual inflow (table A-7) were divided by the days the canal is on (183.5 d), and multiplied by the days on in each month.

#### 4. Irrigation Recharge (IR)

When more water is applied to fields than the crops can use, the excess may evaporate, run off, infiltrate and be stored within the root zone, or infiltrate through the root zone to create groundwater recharge (i.e., irrigation recharge). The Waterloo model area is affected by irrigation recharge within the model domain, and by irrigation recharge occurring immediately upgradient from the model boundaries. Irrigation recharge within the model domain was assigned as groundwater recharge. Upgradient irrigation recharge was applied at the segmented specified flux boundaries at the edges of the model domain (fig. A1).

The NRCS's Irrigation Water Requirements (IWR) program was used to calculate the amount of irrigation recharge (NRCS, 2003, 2019a; Brancheau, 2015; Butler and Bobst, 2017). This analysis considers soil types, crop type, irrigation method, and climate. Sandy loam is the predominant soil type within the study area (NRCS, 2019b). Field observations and landowner interviews indicated that in 2014 crop types included native grass, 50/50 alfalfa-grass mix, alfalfa, barley, peas, potatoes, corn, sod, and conifer trees. This was simplified into four classes of grass, 50/50 mix, alfalfa, and other. The "other" crops compose a small percentage of the crop land, and have similar irrigation requirements. The irrigated acres and irrigation types were based on the MT Department of Revenue's Final Land Units (FLU) Classification coverage (obtained from <http://geoinfo.msl.mt.gov/>), MDOR, 2013), with modifications based on aerial photographs and field observations. Irrigation efficiency was set at 25% for flood, 65% for sprinkler, and 80% for pivot (NRCS, 1993; Sterling and Neibling, 1994).

Table A9. Monthly IWR calculated irrigation recharge rates.

Irrigation & Vegetation Type	Area (acres)	Monthly IR (acre-ft/mo)											
		Jan	Feb	Mar	Apr	May	Jun	Jul	Aug	Sep	Oct	Nov	Dec
Pivot (Pasture Grass, Alfalfa Hay, 50/50, other)	1,498	0	0	0	0	0	124	171	144	6	0	0	0
Sprinkler (Pasture Grass, 50/50, other)	810	0	0	0	0	10	146	202	169	42	0	0	0
Sprinkler (Alfalfa Hay)	214	0	0	0	0	5	92	119	99	40	0	0	0
Flood (Pasture Grass, other)	1,333	0	0	0	0	398	1,450	1,993	1,690	693	0	0	0
Flood (50/50)	602	0	0	0	0	220	738	997	833	346	0	0	0
Flood (Alfalfa Hay)	64	0	0	0	0	28	87	116	96	40	0	0	0
TOTAL		0	0	0	0	660	2,638	3,599	3,031	1,168	0	0	0

Table A10. Annual IWR calculated irrigation recharge rates.

Irrigation & Vegetation Type	Area (acres)	Annual Totals (acre-ft/yr)		
		BE	MinE	MaxE
Pivot (Pasture Grass, Alfalfa Hay, 50/50, other)	1,498	446	401	491
Sprinkler (Pasture Grass, 50/50, other)	810	568	512	625
Sprinkler (Alfalfa Hay)	214	356	320	392
Flood (Pasture Grass, other)	1,333	6,223	5,601	6,845
Flood (50/50)	602	3,135	2,821	3,448
Flood (Alfalfa Hay)	64	368	331	405
TOTAL		11,096	10,394	11,798

Note. Ranges were based on 10% error.

## 5. Alluvial Groundwater Outflow ( $GW_{out-ai}$ )

Groundwater outflow occurs through the alluvium on the northern side of the model domain (fig. A1). The groundwater outflow was calculated using the Darcy Flux Equation (see Alluvial Groundwater Inflow section).

Table A11. Groundwater flow out of the model area through the Jefferson River alluvium was estimated using the Darcy Flux Equation.

	K (ft/d)			Width (ft)	Sat Tk (ft)	Area (ft <sup>2</sup> )	l (ft/ft)	BE Q (ft <sup>3</sup> /d)	Q (acre-ft/yr)		
	BE	MinE	MaxE						BE	MinE	MaxE
Jefferson River	1,100	825	1,375	6,400	200	1,280,000	0.0023	3,238,400	27,154	20,365	33,942

Note. K, range based on aquifer tests, sediment descriptions, and literature values (Heath, 1983; Fetter, 1994). The likely range was based on a range of K values, which is the most variable, and uncertain, component of the calculation. BE, best estimate; MinE, minimum estimate; MaxE, maximum estimate. Width-based geologic maps: Sat Tk, saturated thickness, based on well logs; Area, width x Sat Tk; l, calculated using observed water levels from April 2015.

Table A12. Monthly alluvial outflow (acre-ft).

	Jan	Feb	Mar	Apr	May	Jun	Jul	Aug	Sep	Oct	Nov	Dec	Total
BE	2,263	2,263	2,263	2,263	2,263	2,263	2,263	2,263	2,263	2,263	2,263	2,263	27,154
MinE	1,697	1,697	1,697	1,697	1,697	1,697	1,697	1,697	1,697	1,697	1,697	1,697	20,365
MaxE	2,829	2,829	2,829	2,829	2,829	2,829	2,829	2,829	2,829	2,829	2,829	2,829	33,942

Note. The estimates for total annual outflow (table A-9) were divided by 12 to get monthly values.

## 6. Riparian Evapotranspiration ( $ET_r$ )

Where groundwater is close to the ground surface, some plants, such as willow, cottonwood, and riparian grasses, can directly remove (transpire) groundwater from the saturated zone.

LANDFIRE data (USGS, 2010) showed that 547 acres have riparian plant coverage in the Waterloo area. Using a potential ET (PET) rate of 1.83 ft/yr (Hackett and others, 1960; Lautz, 2008), an upper bound estimate of 1,002 acre-ft/yr is calculated. Since the depth to groundwater in this area averages about 5 ft, and a 10 ft extinction depth is often used for riparian vegetation, the  $ET_r$  value for this area is likely about 50% of the upper bound. The range of values is based on 25% to 75% of the upper bound. The total values were distributed through the growing season (May–Sep) based on average monthly temperatures.

Table A13. Summary of annual actual riparian evapotranspiration.

	Jan	Feb	Mar	Apr	May	Jun	Jul	Aug	Sep	Oct	Nov	Dec	Total
BE	0	0	0	0	47	103	149	133	69	0	0	0	501
MinE	0	0	0	0	24	51	74	67	35	0	0	0	251
MaxE	0	0	0	0	71	154	223	200	104	0	0	0	752

Note. BE is based on 50% of PET. MinE and MaxE are based on 25% and 75% of PET.

## 7. Well Pumping (WEL)

Well pumping amounts are based on the number and type of pumping wells (GWIC, 2016; DNRC, 2016):

Table A14. Summary of types of wells.

Livestock	15
Irrigation	3
Domestic	61

### *Livestock Wells*

Water used by livestock is assumed to be 100% consumed. The total amount of water used for livestock was based on the acreage of the Waterloo area relative to the area of Madison County, and the estimated water use for livestock in Madison County (770,000 gpd; Cannon and Johnson, 2004). This resulted in a usage of 2,646 gpd from the 15 wells, or 176 gpd per well. This is equivalent to pumping each of the wells for 35 min per day at 5 gpm. The calculated consumptive use was 2.97 acre-ft/yr. The distribution of livestock water use was split among months using a time-weighted distribution.

Table A15. Livestock water use (acre-ft).

	Jan	Feb	Mar	Apr	May	Jun	Jul	Aug	Sep	Oct	Nov	Dec	Total
Days	31	28.25	31	30	31	30	31	31	30	31	30	31	365.25
BE	0.25	0.23	0.25	0.24	0.25	0.24	0.25	0.25	0.24	0.25	0.24	0.25	2.97
MinE	0.23	0.21	0.23	0.22	0.23	0.22	0.23	0.23	0.22	0.23	0.22	0.23	2.67
MaxE	0.28	0.25	0.28	0.27	0.28	0.27	0.28	0.28	0.27	0.28	0.27	0.28	3.27

Note. The range of likely values was based on an estimated uncertainty of  $\pm 10\%$ .

### *Irrigation Wells*

The use of water by the three irrigation wells was based on water rights, air photos, and calculations using DNRCs IWR program.

Table A16. Summary of irrigation well annual total pumping.

GWIC ID or Water Right	Acres Irrigated <sup>1</sup>	Annual Use <sup>2</sup> (acre-ft)		
		BE	MinE	MaxE
107066	18	48	43	53
107064	12	27	25	30
130437	17	26	23	28
TOTAL	47	101	91	111

<sup>1</sup>Acres irrigated based on DNRC water rights information and NAIP areal imagery.

<sup>2</sup>Annual rates based on DNRC's Water Use Standards (ARM 36.12.115; 2.5 ft/yr for hay) and water right information.

<sup>3</sup>The range of likely values was based on an estimated uncertainty of  $\pm 10\%$ .

Table A17. Monthly distribution of BE irrigation well pumping (acre-ft).

GWIC ID	Jan	Feb	Mar	Apr	May	June	July	Aug	Sept	Oct	Nov	Dec	Total
107066	0.0	0.0	0.0	0.0	3.6	10.7	15.0	13.5	5.0	0.2	0.0	0.0	48
107064	0.0	0.0	0.0	0.0	0.0	6.6	9.3	8.4	3.1	0.0	0.0	0.0	27
130437	0.0	0.0	0.0	0.0	1.9	5.7	8.0	7.2	2.6	0.1	0.0	0.0	26

<sup>1</sup>Monthly values are annual rates distributed based on monthly crop requirements from NRCS's IWR program, and water rights dates.

<sup>2</sup>The range of likely values was based on an estimated uncertainty of  $\pm 10\%$ .

Domestic Wells

The consumptive use for the 61 domestic wells was based on a previous GWIP study (Waren and others, 2012) which used 15 yr of subdivision water-use records near Helena, MT, to calculate an average annual usage rate of 0.49 acre-ft/yr per home.

Table A18. Domestic well pumping rates (61 wells; acre-ft).

	Jan	Feb	Mar	Apr	May	June	July	Aug	Sept	Oct	Nov	Dec	Total
BE	0.09	0.09	0.12	0.18	3.03	5.41	7.79	7.85	4.22	0.71	0.15	0.06	29.7
MinE	0.08	0.08	0.11	0.16	2.73	4.87	7.01	7.07	3.80	0.64	0.13	0.05	26.7
MaxE	0.10	0.10	0.13	0.20	3.34	5.95	8.57	8.64	4.65	0.79	0.16	0.07	32.7

Note. Total annual rate and distribution by month based on Waren and others, 2012. The range of likely values was based on an estimated uncertainty of  $\pm 10\%$ .

Total Well Pumping

Table A19. Summary of well pumping rates by month (acre-ft).

	Jan	Feb	Mar	Apr	May	June	July	Aug	Sept	Oct	Nov	Dec	BE	MinE	MaxE
Livestock	0.25	0.23	0.25	0.24	0.25	0.24	0.25	0.25	0.24	0.25	0.24	0.25	3.0	2.7	3.3
Irrigation	0.00	0.00	0.00	0.03	5.57	23.03	32.28	29.04	10.70	0.26	0.00	0.00	100.9	91.0	111.0
Domestic	0.09	0.09	0.12	0.18	3.03	5.41	7.79	7.85	4.22	0.71	0.15	0.06	29.7	26.7	32.7
TOTAL	0.34	0.32	0.37	0.45	8.85	28.68	40.32	37.14	15.16	1.22	0.39	0.31	133.6	120.4	147.0

**8. Net Outflow from Groundwater to Surface-Water ( $SW_{net}$ )**

The net discharge from groundwater to surface waters was based on the difference between the calculated inflows and outflows (table A21). Monthly values were estimated based on monitoring data from groundwater-fed streams (Parson's Slough and Willow Springs). Note that these gains occur along Parson's Slough, Willow Springs, and the mainstem of the Jefferson River.

Using best estimate (BE) values, calculated inflows totaled 66,345 acre-ft/yr (table A22), and calculated outflows other than surface water totaled 27,789 acre-ft/yr. Therefore, it is estimated that the average net groundwater discharge to surface waters is about 38,556 acre-ft/yr (53 cfs, on average). Using the likely range of inflow and outflow values based on root sum of squares error propagation (MinE and MaxE), the likely range of net surface water gain was estimated to be from 25,073 to 52,040 acre-ft/yr (35–72 cfs). The best estimate value also correlates well with the monitoring-based estimate of surface-water gains in this area developed by Brancheau (2015) of 39,974 acre-ft/yr (55 cfs).

Table A20. Estimated net flow from groundwater to surface waters (acre-ft).

	Jan	Feb	Mar	Apr	May	Jun	Jul	Aug	Sep	Oct	Nov	Dec	Total
BE	3,071	2,537	2,497	2,418	3,090	3,248	3,624	4,361	3,677	3,403	3,272	3,359	38,556
MinE	1,997	1,650	1,623	1,572	2,009	2,112	2,356	2,836	2,391	2,213	2,128	2,184	25,073
MaxE	4,145	3,424	3,370	3,264	4,170	4,384	4,891	5,887	4,963	4,593	4,416	4,533	52,040

**9. Overall Budget**

Table A21. Waterloo preliminary groundwater budget (acre-ft).

Inflows	Jan	Feb	Mar	Apr	May	Jun	Jul	Aug	Sep	Oct	Nov	Dec	Annual		
													BE	MinE	MaxE
$GW_{in-ai}$	3,829	3,829	3,829	3,829	3,829	3,829	3,829	3,829	3,829	3,829	3,829	3,829	45,947	34,460	57,433
$GW_{in-lat}$	309	309	309	309	309	309	309	309	309	309	309	309	3,702	1,942	5,461
CL	0	0	0	458	946	916	946	946	916	473	0	0	5,600	5,244	5,956
IR	0	0	0	0	660	2,638	3,599	3,031	1,168	0	0	0	11,096	10,394	11,798
Total Inflow	4,137	4,137	4,137	4,595	5,744	7,691	8,682	8,114	6,221	4,610	4,137	4,137	66,345	54,697	77,992
<b>Outflows</b>															
$GW_{out-ai}$	2,263	2,263	2,263	2,263	2,263	2,263	2,263	2,263	2,263	2,263	2,263	2,263	27,154	20,365	33,942
$ET_r$	0	0	0	0	47	103	149	133	69	0	0	0	501	251	752
WEL	0.3	0.3	0.4	0.4	8.9	28.7	40.3	37.1	15.2	1.2	0.4	0.3	134	120	147
$SW_{net}^*$	3,071	2,537	2,497	2,418	3,090	3,248	3,624	4,361	3,677	3,403	3,272	3,359	38,556	25,073	52,040
Total Outflow	5,334	4,880	4,760	4,681	5,409	5,643	6,075	6,794	6,024	5,667	5,535	5,622	66,345	51,247	81,443
$\Delta S$	-1,179	-663	-622	-86	335	2,048	2,607	1,320	197	-1,057	-1,398	-1,484	0	0	0

Note. Change in storage ( $\Delta S$ ) is calculated as the difference between monthly inflows and outflows.  $GW_{in-ai}$ , alluvial groundwater inflow;  $GW_{in-lat}$ , lateral groundwater inflow; CL, canal leakage; IR, irrigation recharge;  $GW_{out-ai}$ , alluvial groundwater outflow;  $ET_r$ , riparian evapotranspiration; WEL, well pumping;  $SW_{net}$ , net outflow from groundwater to surface waters.

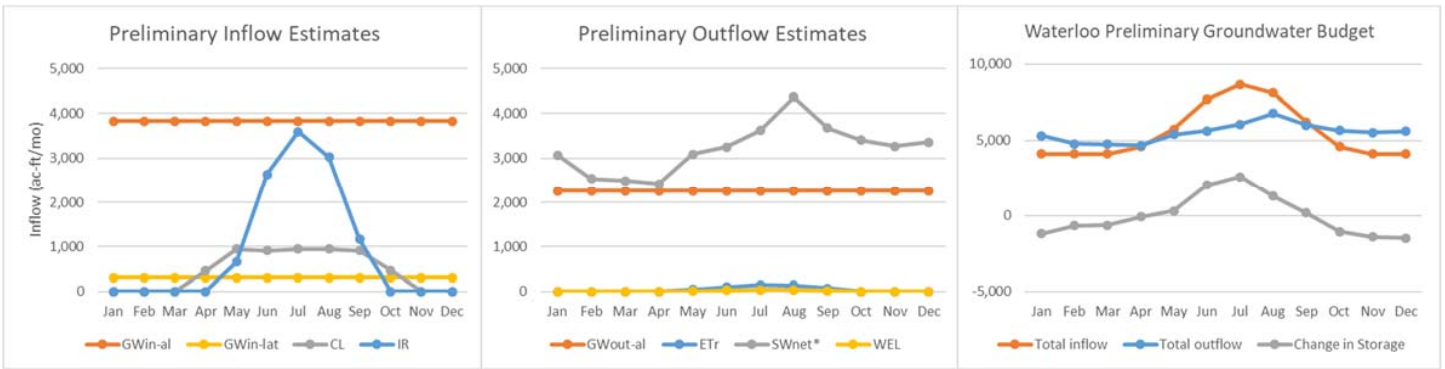


Table A22: Groundwater budget developed by Brancheau (2015).

GW <sub>in</sub>	Initial Estimate (acre-ft/yr)	Uncertainty (%)	Range (are-ft/yr)		Adjusted Estimate (acre-ft/yr)
			low	high	
Darcy Influx	22,364	10%	20,128	24,601	23,371
Lateral Groundwater Influx	3,702	10%	3,332	4,072	3,869
Canal Leakage	12,829	5%	12,187	13,470	13,406
Irrigation Recharge	11,096	5%	10,541	11,651	11,595
<i>TOTAL IN</i>	49,991				52,241
<b>GW<sub>out</sub></b>					
Darcy Flux <sub>out</sub>	13,503	10%	12,153	14,853	12,963
Spring-fed Streams	16,365	5%	15,547	17,183	15,670
Evapotranspiration	1,002	10%	902	1,102	957
Jefferson River Recharge	23,609	10%	21,248	25,970	22,653
<i>TOTAL OUT</i>	54,479				52,243

**REFERENCES**

- Brancheau, N.L., 2015, A hydrogeologic evaluation of the Waterloo area in the Upper Jefferson River Valley, Montana: Butte, Mont., Montana Tech, M.S. thesis, 104 p.
- Butler, J., and Bobst, A., 2017, Hydrogeologic investigation of the Boulder Valley, Jefferson County, Montana: Groundwater modeling report: Montana Bureau of Mines and Geology Open-File Report 688, 131 p.
- Cannon, M.R., and Johnson, D.R., 2004, Estimated water use in Montana in 2000: USGS Scientific Investigations Report 2004-5223, 61 p.
- Fetter, C.W., 1994, Applied hydrogeology, 3rd ed: New York, MacMillan, 691 p.
- Hackett, O.M., Visser, F.N., McMurtrey, R.G., and Steinhilber, W.L., 1960, Geology and ground water resources of the Gallatin Valley, Gallatin County, Montana: USGS Water-Supply Paper 1482, 282 p.
- Heath, R., 1983, Basic ground-water hydrology: USGS Water Supply Paper 2220, 86 p.
- Lautz, L.K., 2008. Estimating groundwater evapotranspiration rates using diurnal water-table fluctuations in a semi-arid riparian zone: *Hydrogeology Journal*, v. 16, p. 483-497.
- Montana Department of Revenue (MDOR), 2013, Revenue final land unit classification, [https://mslservices.mt.gov/Geographic\\_Information/Data/DataList/datalist\\_Details.aspx?did={09a1da08-972c-46d9-afd3-14da6df385aa}](https://mslservices.mt.gov/Geographic_Information/Data/DataList/datalist_Details.aspx?did={09a1da08-972c-46d9-afd3-14da6df385aa}) [Accessed April 2019].
- NRCS, 1993, NRCS National engineering handbook (NEH), part 623, chap. 2: Irrigation water requirements: USDA.
- NRCS, 2003, IWR Program User Manual Version 1.0; [https://www.nrcs.usda.gov/Internet/FSE\\_DOCUMENTS/nrcs144p2\\_013838.pdf](https://www.nrcs.usda.gov/Internet/FSE_DOCUMENTS/nrcs144p2_013838.pdf) [Accessed January 2019].
- NRCS, 2019a, IWR Program, <https://www.nrcs.usda.gov/wps/portal/nrcs/detailfull/national/ndcsmc/?cid=stelprdb1042198> [Accessed January 2019].
- NRCS, 2019b, NRCS Web Soil Survey, <http://websoilsurvey.nrcs.usda.gov/app/WebSoilSurvey.aspx> [Accessed January 2019].
- PRISM, 2018, PRISM Climate Data, <http://www.prism.oregonstate.edu/> [Accessed November 7, 2018].
- Sterling, R., and Neibling, W.H., 1994, Final report of the Water Conservation Task Force: Boise, Ida., Idaho Department of Water Resources.
- U.S. Geological Survey (USGS), 2010, LANDFIRE database, <http://www.landfire.gov/> [Accessed April 2019].
- Waren, K.B., Bobst, A.L., Swierc, J.E., and Madison, J.D., 2012, Hydrogeologic investigation of the North Hills study area, Lewis and Clark County, Montana, Interpretive Report: Montana Bureau of Mines and Geology Open-File Report 610, 99 p.

**APPENDIX B**  
**JEFFERSON RIVER SLOPE**  
**CALCULATIONS**

From Survey data:

Elevation of 0.00 on Staff Gage at Corbett's (downstream end) = 4405.081 ft-amsl

Elevation of Rebar at Funston's = 4469.951 ft-amsl (~3 ft above 0.00 on gage) ~ 4466.951

Elevation of Rebar at Silver Star = 4516.52 ft-amsl (per our survey 0.00 is 5.28 ft lower) = 4511.24

From Google:

River miles from Silver Star to Corbett's = 12.9 miles – Overall Slope =  $106/68,112 = 0.001556$  ft/ft

River miles from Silver Star to Funston's = 6.12 miles – Slope =  $44/32,314 = 0.001362$

River miles from Funston's to Corbett's = 6.78 miles – Slope =  $62/35,798 = 0.001732$

Source:

Andrew L Bobst

Hydrogeologist/Project Manager

Groundwater Investigations Program

Montana Bureau of Mines and Geology

1300 W. Park

Butte, MT 59701

abobst@mtech.edu

406-496-4409

**APPENDIX C**  
**HUNT AQUIFER TEST RESULTS**

### APPENDIX C Hunt Aquifer Test Results (Hunt, 2015)

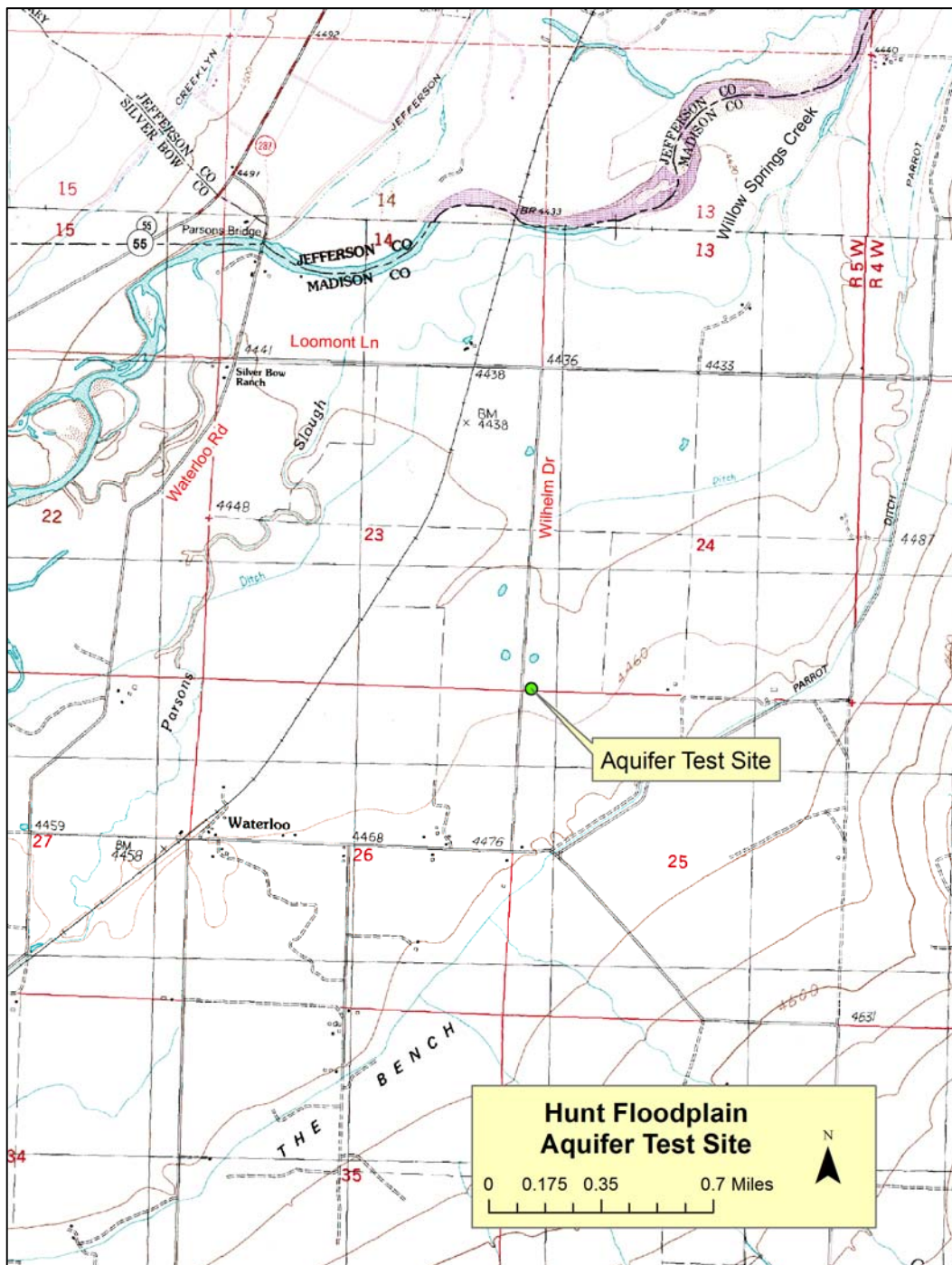
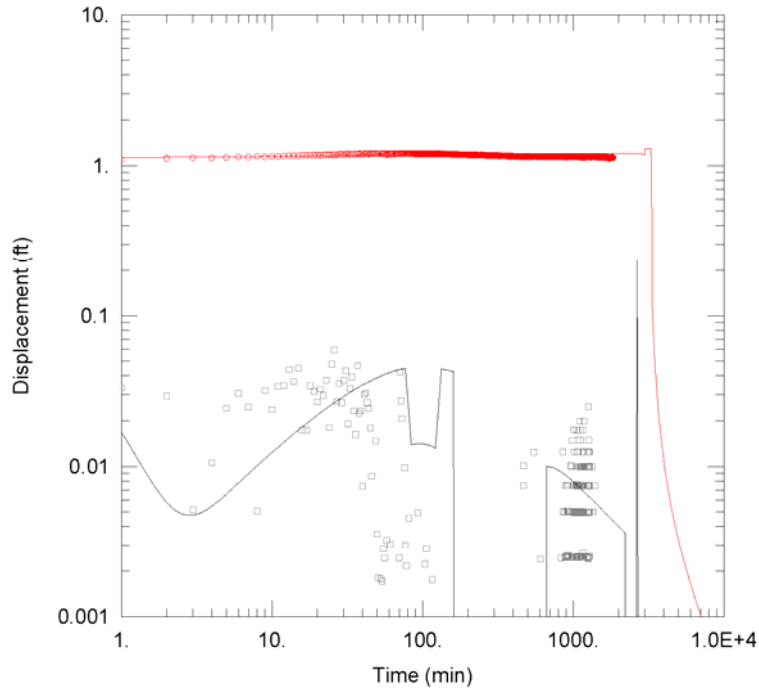
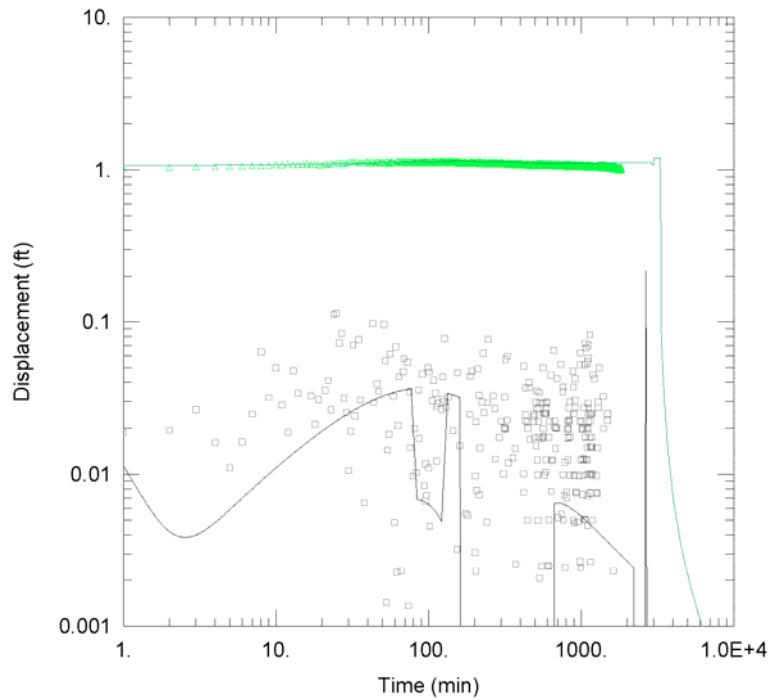


Figure C1. Location of Hunt aquifer test



<u>HUNTA AQUIFER TEST</u>					
Data Set: <u>M:\...\HuntA_CR_OW1_UC_CHB.aqt</u>			Time: <u>09:11:05</u>		
Date: <u>11/19/19</u>					
<u>PROJECT INFORMATION</u>					
Company: <u>MBMG</u>					
Client: <u>HuntA</u>					
Project: <u>BWIPUJ</u>					
Location: <u>Upper Jefferson</u>					
Test Well: <u>PW</u>					
Test Date: <u>2/24/15</u>					
<u>AQUIFER DATA</u>					
Saturated Thickness: <u>100. ft</u>					
<u>WELL DATA</u>					
<u>Pumping Wells</u>			<u>Observation Wells</u>		
Well Name	X (ft)	Y (ft)	Well Name	X (ft)	Y (ft)
PW	0	0	○ OW1	-1.112	22.767
<u>SOLUTION</u>					
Aquifer Model: <u>Unconfined</u>			Solution Method: <u>Neuman</u>		
T	= <u>4.1E+4 ft<sup>2</sup>/day</u>		S	= <u>0.0013</u>	
Sy	= <u>0.14</u>		Kz/Kr	= <u>0.2</u>	

Figure C2. Observation well (OW1) analysis (Neuman method)



HUNTA AQUIFER TEST					
Data Set: M:\...\HuntA_CR_OW2_UC_CHB.aqt			Time: 09:11:16		
Date: 11/19/19					
PROJECT INFORMATION					
Company: MBMG					
Client: HuntA					
Project: BWIPUJ					
Location: Upper Jefferson					
Test Well: PW					
Test Date: 2/24/15					
AQUIFER DATA					
Saturated Thickness: 100. ft					
WELL DATA					
Pumping Wells			Observation Wells		
Well Name	X (ft)	Y (ft)	Well Name	X (ft)	Y (ft)
PW	0	0	△ OW2	-21.792	2.695
SOLUTION					
Aquifer Model: Unconfined			Solution Method: Neuman		
T	= 4.45E+4 ft <sup>2</sup> /day		S	= 0.0013	
Sy	= 0.14		Kz/Kr	= 0.2	

Figure C3. Observation well (OW2) analysis (Neuman method)

**APPENDIX D**  
**MODEL CONSTRUCTION**

Table D1. Summary of model grid construction.

Grid construction item	Value
Rows	150
Columns	150
Layers	1
Total area	27.13 sq mi
Active area	12.31 sq mi
Row spacing	178.18 ft
Column spacing	188.66 ft
Number of active cells	10,212
No. Inactive/no-flow cells	12,288
Vertical datum	NAVD 88
Spatial units	feet
Temporal units	days
Max thickness	215 ft
Min thickness	199 ft
Max saturated thickness*	208 ft
Min saturated thickness*	109 ft
No. STR cells <sup>a</sup>	795
No. DRN cells <sup>b</sup>	285
No. WELL cells <sup>c</sup>	578
Coordinate system	State Plane MT FIPS 2500, International Ft

\*Steady-state simulation results

<sup>a</sup>MODFLOW STR Package cells represent Jefferson River

<sup>b</sup>MODFLOW DRN Package cells represent Parson's Slough and Willow Spring

<sup>c</sup>MODFLOW WELL Package cells represent pumping wells, canal leakage, alluvial Darcy flow, and lateral groundwater

Table D2. Stress periods and time steps applied to the Waterloo model.

Start Date	Stress Period #	Stress period length (days)	No. of time steps	Time step length (days)	Simulation Type	Remarks
Mar-04	1	1	1	1	Steady-State	
Apr-04	2	30	6	5.0	Transient	Skipped during calibration
May-04	3	31	6	5.2	Transient	""
Jun-04	4	30	6	5.0	Transient	""
Jul-04	5	31	6	5.2	Transient	""
Aug-04	6	31	6	5.2	Transient	""
Sep-04	7	30	6	5.0	Transient	""
Oct-04	8	31	6	5.2	Transient	""
Nov-04	9	30	6	5.0	Transient	""
Dec-04	10	31	6	5.2	Transient	""
<b>Jan-05</b>	11	31	6	5.2	Transient	""
<b>Feb-05</b>	12	28	6	4.7	Transient	""
<b>Mar-05</b>	13	31	6	5.2	Transient	""
<b>Apr-05</b>	14	30	6	5.0	Transient	""
<b>May-05</b>	15	31	6	5.2	Transient	""
<b>Jun-05</b>	16	30	6	5.0	Transient	""
<b>Jul-05</b>	17	31	6	5.2	Transient	""
<b>Aug-05</b>	18	31	6	5.2	Transient	""
<b>Sep-05</b>	19	30	6	5.0	Transient	""
<b>Oct-05</b>	20	31	6	5.2	Transient	""
<b>Nov-05</b>	21	30	6	5.0	Transient	""
<b>Dec-05</b>	22	31	6	5.2	Transient	""
Jan-06	23	31	6	5.2	Transient	""
Feb-06	24	28	6	4.7	Transient	""
Mar-06	25	31	6	5.2	Transient	""
Apr-06	26	30	6	5.0	Transient	""
May-06	27	31	6	5.2	Transient	""
Jun-06	28	30	6	5.0	Transient	""
Jul-06	29	31	6	5.2	Transient	""
Aug-06	30	31	6	5.2	Transient	""
Sep-06	31	30	6	5.0	Transient	""
Oct-06	32	31	6	5.2	Transient	""
Nov-06	33	30	6	5.0	Transient	""
Dec-06	34	31	6	5.2	Transient	""
Jan-07	35	31	6	5.2	Transient	""
Feb-07	36	28	6	4.7	Transient	""
Mar-07	37	31	6	5.2	Transient	""
Apr-07	38	30	6	5.0	Transient	""
May-07	39	31	6	5.2	Transient	""
Jun-07	40	30	6	5.0	Transient	""
Jul-07	41	31	6	5.2	Transient	""

Table D2 (Continued). Stress periods and time steps applied to the Waterloo model.						
Start Date	Stress Period #	Stress period length (days)	No. of time steps	Time step length (days)	Simulation Type	Remarks
Aug-07	42	31	6	5.2	Transient	Skipped during calibration
Sep-07	43	30	6	5.0	Transient	""
Oct-07	44	31	6	5.2	Transient	""
Nov-07	45	30	6	5.0	Transient	""
Dec-07	46	31	6	5.2	Transient	""
Jan-08	47	31	6	5.2	Transient	""
Feb-08	48	29	6	4.8	Transient	""
Mar-08	49	31	6	5.2	Transient	""
Apr-08	50	30	6	5.0	Transient	""
May-08	51	31	6	5.2	Transient	""
Jun-08	52	30	6	5.0	Transient	""
Jul-08	53	31	6	5.2	Transient	""
Aug-08	54	31	6	5.2	Transient	""
Sep-08	55	30	6	5.0	Transient	""
Oct-08	56	31	6	5.2	Transient	""
Nov-08	57	30	6	5.0	Transient	""
Dec-08	58	31	6	5.2	Transient	""
Jan-09	59	31	6	5.2	Transient	""
Feb-09	60	28	6	4.7	Transient	""
Mar-09	61	31	6	5.2	Transient	""
Apr-09	62	30	6	5.0	Transient	""
May-09	63	31	6	5.2	Transient	""
Jun-09	64	30	6	5.0	Transient	""
Jul-09	65	31	6	5.2	Transient	""
Aug-09	66	31	6	5.2	Transient	""
Sep-09	67	30	6	5.0	Transient	""
Oct-09	68	31	6	5.2	Transient	""
Nov-09	69	30	6	5.0	Transient	""
Dec-09	70	31	6	5.2	Transient	""
Jan-10	71	31	6	5.2	Transient	""
Feb-10	72	28	6	4.7	Transient	""
Mar-10	73	31	6	5.2	Transient	""
Apr-10	74	30	6	5.0	Transient	""
May-10	75	31	6	5.2	Transient	""
Jun-10	76	30	6	5.0	Transient	""
Jul-10	77	31	6	5.2	Transient	""
Aug-10	78	31	6	5.2	Transient	""
Sep-10	79	30	6	5.0	Transient	""
Oct-10	80	31	6	5.2	Transient	""
Nov-10	81	30	6	5.0	Transient	""
Dec-10	82	31	6	5.2	Transient	""

Start Date	Stress Period #	Stress period length (days)	No. of time steps	Time step length (days)	Simulation Type	Remarks
Jan-11	83	31	6	5.2	Transient	Skipped during calibration
Feb-11	84	28	6	4.7	Transient	""
Mar-11	85	31	6	5.2	Transient	""
Apr-11	86	30	6	5.0	Transient	""
May-11	87	31	6	5.2	Transient	""
Jun-11	88	30	6	5.0	Transient	""
Jul-11	89	31	6	5.2	Transient	""
Aug-11	90	31	6	5.2	Transient	""
Sep-11	91	30	6	5.0	Transient	""
Oct-11	92	31	6	5.2	Transient	""
Nov-11	93	30	6	5.0	Transient	""
Dec-11	94	31	6	5.2	Transient	""
Jan-12	95	31	6	5.2	Transient	""
Feb-12	96	29	6	4.8	Transient	""
Mar-12	97	31	6	5.2	Transient	""
Apr-12	98	30	6	5.0	Transient	""
May-12	99	31	6	5.2	Transient	""
Jun-12	100	30	6	5.0	Transient	""
Jul-12	101	31	6	5.2	Transient	""
Aug-12	102	31	6	5.2	Transient	""
Sep-12	103	30	6	5.0	Transient	""
Oct-12	104	31	6	5.2	Transient	""
Nov-12	105	30	6	5.0	Transient	""
Dec-12	106	31	6	5.2	Transient	""
Jan-13	107	31	6	5.2	Transient	""
Feb-13	108	28	6	4.7	Transient	""
Mar-13	109	31	6	5.2	Transient	""
Apr-13	110	30	6	5.0	Transient	Start calibration simulation
May-13	111	31	6	5.2	Transient	Calibration simulation
Jun-13	112	30	6	5.0	Transient	""
Jul-13	113	31	6	5.2	Transient	""
Aug-13	114	31	6	5.2	Transient	""
Sep-13	115	30	6	5.0	Transient	""
Oct-13	116	31	6	5.2	Transient	""
Nov-13	117	30	6	5.0	Transient	""
Dec-13	118	31	6	5.2	Transient	""
Jan-14	119	31	6	5.2	Transient	""
Feb-14	120	28	6	4.7	Transient	""
Mar-14	121	31	6	5.2	Transient	""
Apr-14	122	30	6	5.0	Transient	""
May-14	123	31	6	5.2	Transient	""

Table D2 (Continued). Stress periods and time steps applied to the Waterloo model.

Start Date	Stress Period #	Stress period length (days)	No. of time steps	Time step length (days)	Simulation Type	Remarks
Jun-14	124	30	6	5.0	Transient	Calibration simulation
Jul-14	125	31	6	5.2	Transient	""
Aug-14	126	31	6	5.2	Transient	""
Sep-14	127	30	6	5.0	Transient	""
Oct-14	128	31	6	5.2	Transient	""
Nov-14	129	30	6	5.0	Transient	""
Dec-14	130	31	6	5.2	Transient	""
Jan-15	131	31	6	5.2	Transient	""
Feb-15	132	28	6	4.7	Transient	""
Mar-15	133	31	6	5.2	Transient	""
Apr-15	134	30	6	5.0	Transient	""
May-15	135	31	6	5.2	Transient	""
Jun-15	136	30	6	5.0	Transient	""
Jul-15	137	31	6	5.2	Transient	""
Aug-15	138	31	6	5.2	Transient	""
Sep-15	139	30	6	5.0	Transient	""
Oct-15	140	31	6	5.2	Transient	""

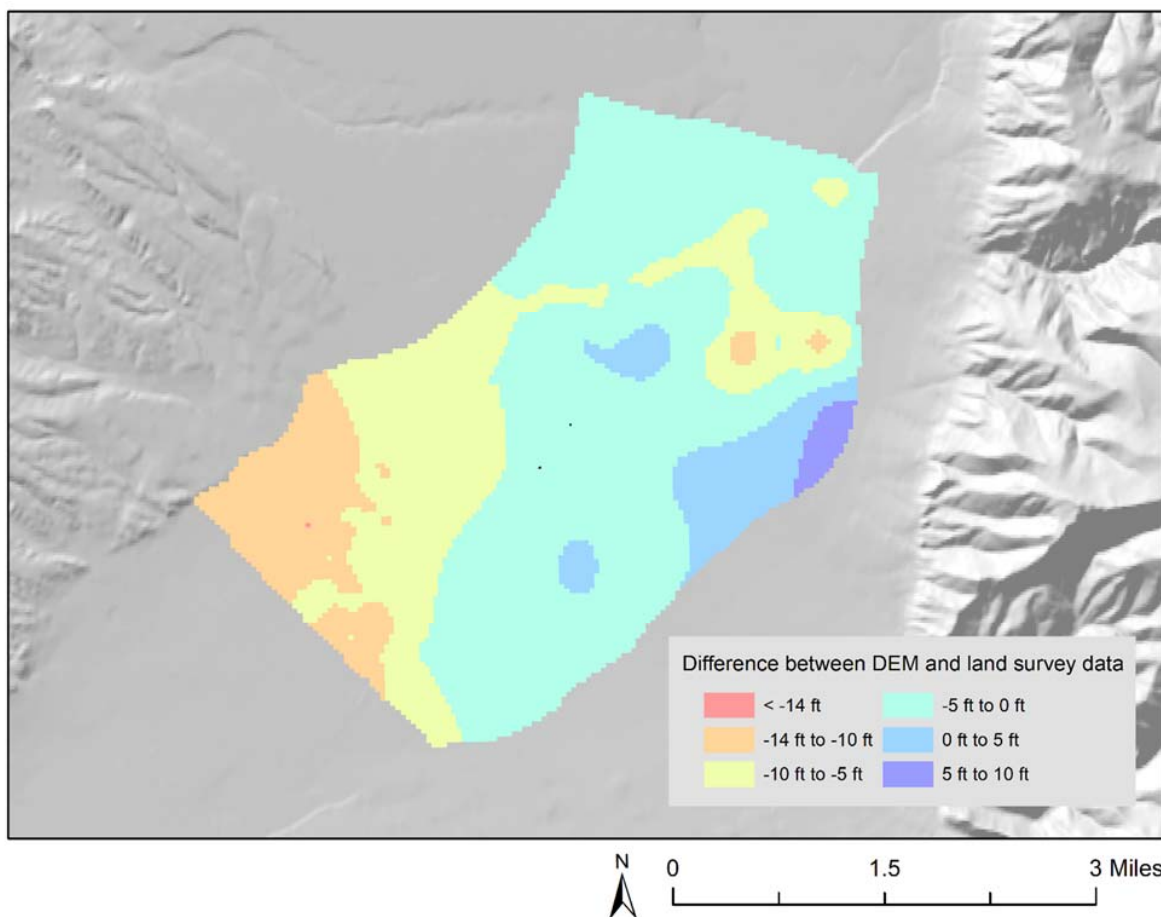


Figure D1. The distribution of the difference between DEM and land surveyed points (Sept 2016).

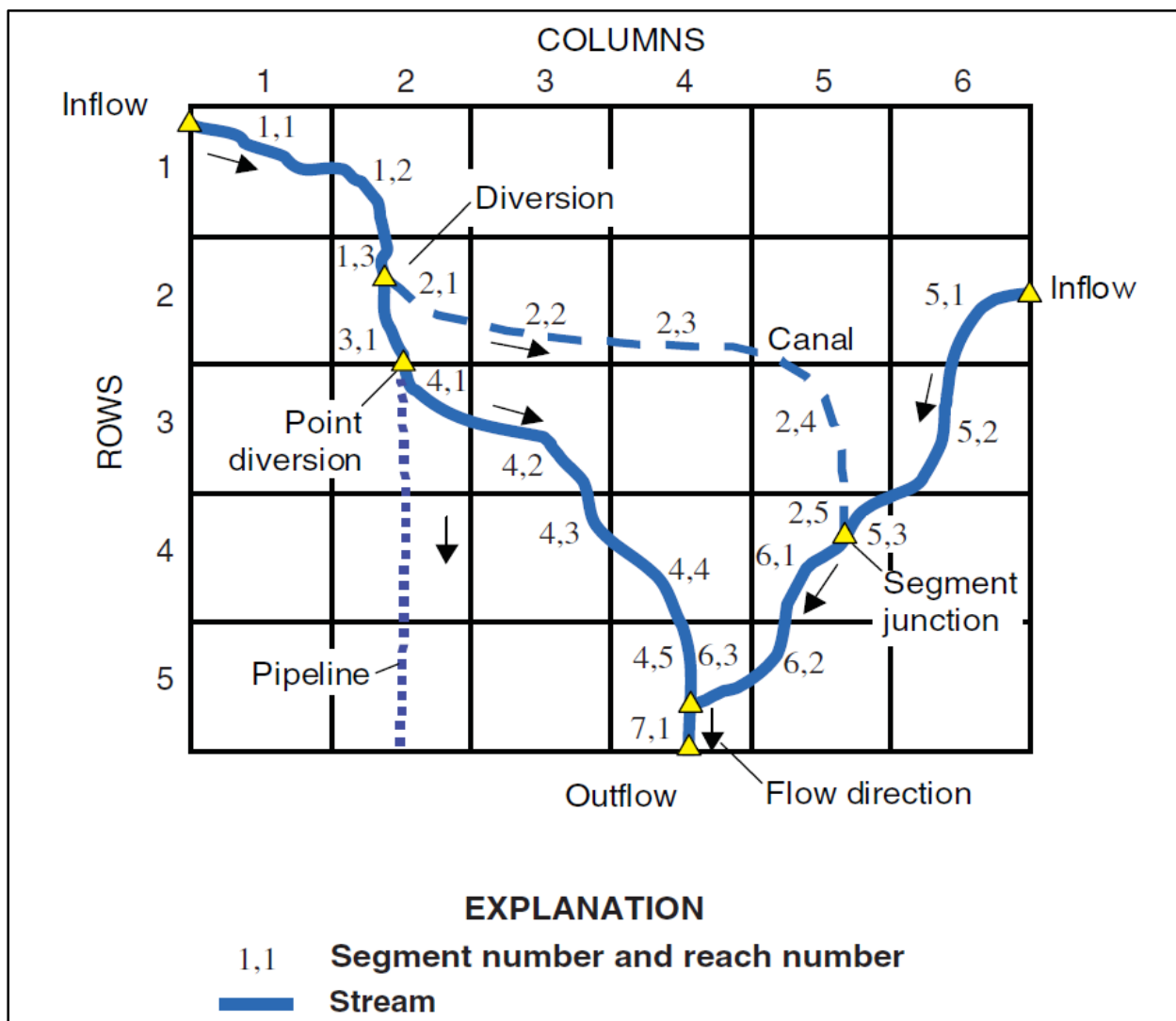


Figure D2. Schematic of the stream package (STR) shows the network of segments and reaches (from Prudic and others, 2004). The stream is divided into segments (arches between yellow triangles) in a sequential order indicated by the first number. A stream segment can extend over multiple model grid cells. Within each grid cell, the segment is defined by a reach number (second number), only one reach number per cell. The number of reaches represent the number of cells a segment passes through (e.g., the first segment passes through three cells, it has three reaches designated as 1.1, 1.2, and 1.3). Diversions and junctions can also be incorporated into the network.

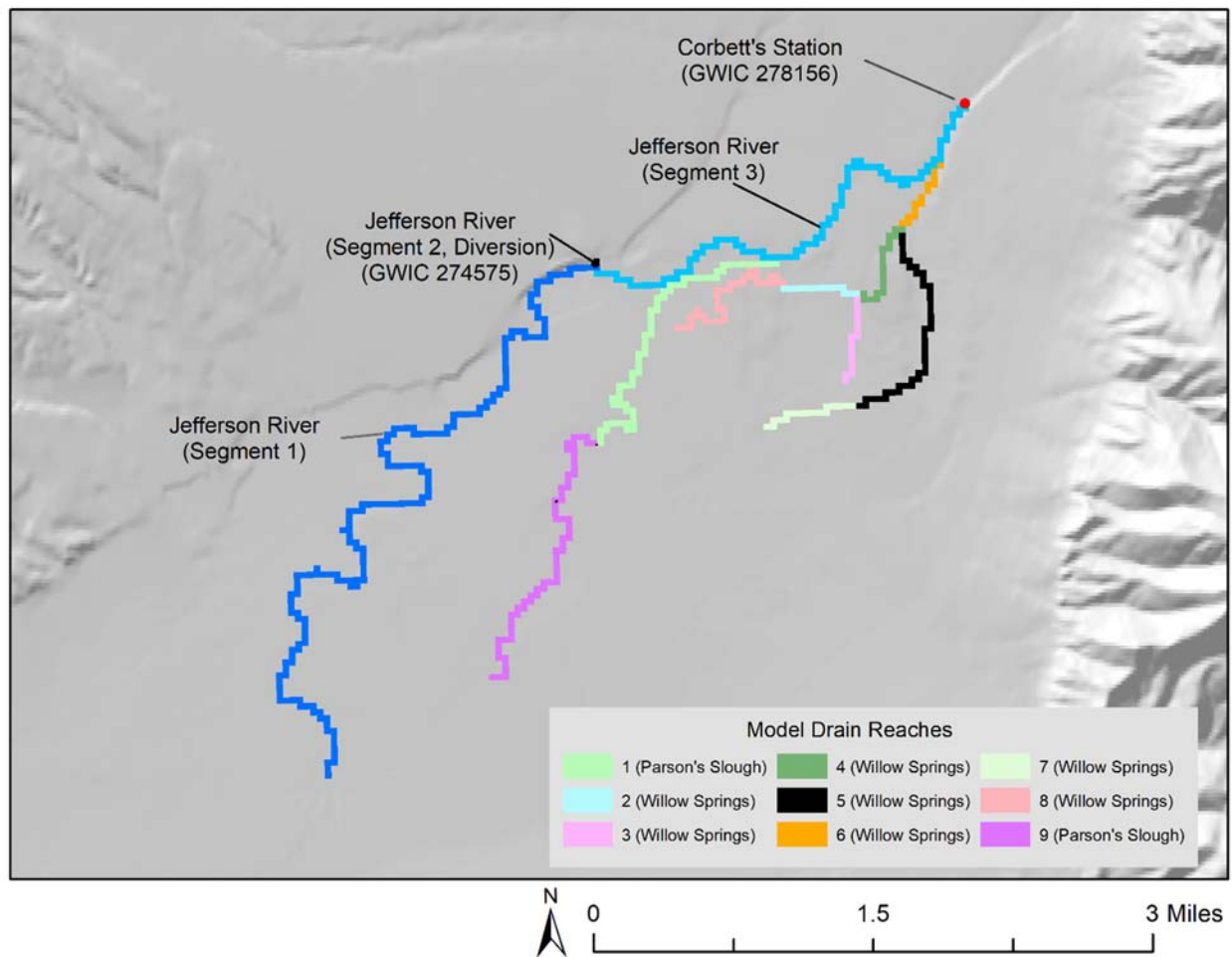


Figure D3. Three segments of the stream package (STR) represent the Jefferson River within the model area[GM1]. Stream segment 2 consists of one cell to simulate water diverted from the river. The diverted water flows through the Jefferson Canal and part of the flow returns to the simulated aquifer as canal leakage.

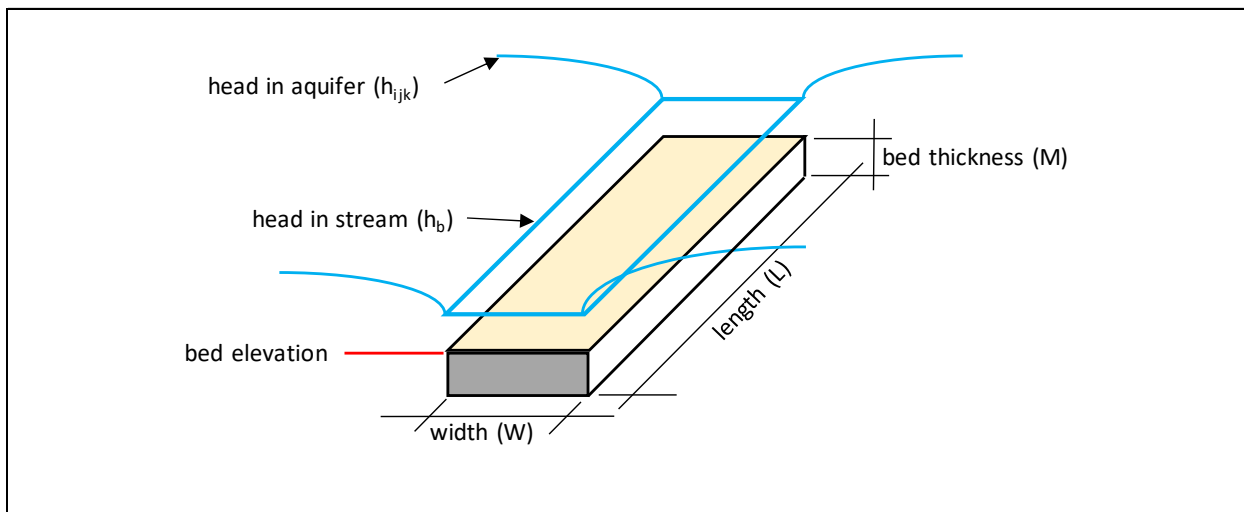


Figure D4. A schematic of the stream package (STR) shows that when the head in the aquifer exceeds the stream’s head (e.g., Jefferson River stage), water discharges from the aquifer to the stream (gaining stream). But when head in the stream exceeds the head in the aquifer, water infiltrates from the stream to the aquifer (losing stream). The rate of exchange is also controlled by the streambed conductance, a function of streambed vertical hydraulic conductivity and streambed geometry ( $W$ ,  $L$ , and  $M$ ).

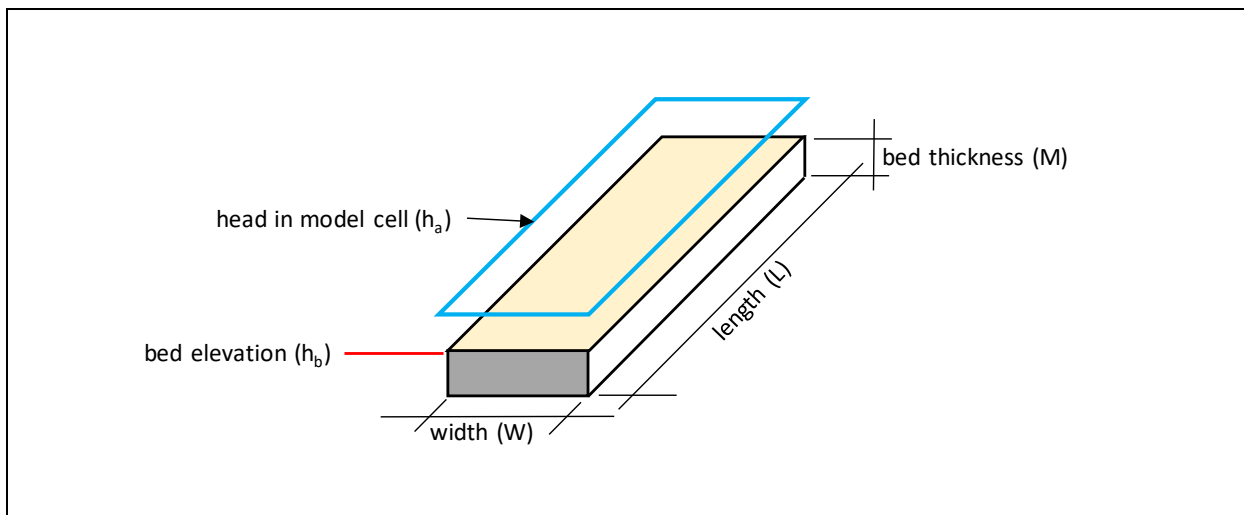


Figure D5. Schematic of the drain package (DRN) shows that when the head in the aquifer exceeds the drain’s bed elevation (e.g., Willow Springs bed elevation), groundwater discharges from the aquifer to the drain, and the drain collects water. When the head in the aquifer is equal to or less than the drain’s bed elevation, there is no exchange of groundwater between the aquifer and the drain. The drain boundary condition only allows groundwater to flow in one direction, from the aquifer to the drain. The flow rate is also controlled by the drain’s bed conductance, a function of drain bed vertical hydraulic conductivity and drain bed geometry ( $W$ ,  $L$ , and  $M$ ).



**APPENDIX E**  
**MODEL RESULTS**

Table E1. Steady-state calibration results comparing observed and modeled groundwater elevations.

GWIC Id	Observed Average (GWE ft-amsl)	Modeled (ft-amsl)	GWE*	Residual (ft) (observed - modeled)
107080	4453.35	4454.32		-0.97
195941	4458.34	4461.31		-2.97
209718	4439.01	4439.06		-0.05
259547	4461.78	4463.03		-1.25
261912	4464.04	4466.72		-2.68
276038	4451.55	4453.14		-1.59
276041	4455.34	4456.37		-1.03
276103	4434.22	4435.14		-0.92
276106	4432.59	4433.98		-1.39
276107	4435.52	4436.02		-0.50
276108	4438.29	4438.40		-0.11
276109	4437.99	4438.66		-0.67
276111	4441.15	4442.80		-1.65
276112	4427.96	4428.13		-0.17
276285	4414.40	4413.54		0.86
276287	4445.83	4446.28		-0.45
277329	4443.63	4444.15		-0.52
277868	4426.41	4428.32		-1.91
279258	4449.30	4450.97		-1.67
279259	4449.37	4450.99		-1.62
279260	4449.89	4451.00		-1.11

\*GWE, Groundwater elevation

**Nash efficiency coefficient analysis (Targets group 1)**

Well (259547)					276111				
Date	Obs head (ft)	$F_o = \sum[\text{obs} - (\text{avg. obs})]^2$	Sim head (ft)	$F = \sum(\text{obs-sim})^2$	Date	Obs head (ft)	$F_o = \sum[\text{obs} - (\text{avg. obs})]^2$	Sim head (ft)	$F = \sum(\text{obs-sim})^2$
7/19/2013	4467.63	6.16	4468.591	0.92	9/19/2013	4447.25	16.56	4444.757	6.22
8/14/2013	4467.33	4.76	4468.953	2.63	10/17/2013	4445.1	3.69	4443.934	1.36
9/19/2013	4467.04	3.58	4468.831	3.21	11/21/2013	4443.29	0.01	4442.595	0.48
10/17/2013	4466.92	3.14	4466.063	0.73	12/17/2013	4442.44	0.55	4442.192	0.06
11/21/2013	4464.83	0.10	4462.514	5.36	1/25/2014	4441.69	2.22	4441.972	0.08
12/17/2013	4463.11	4.15	4462.031	1.16	2/21/2014	4441.3	3.53	4441.928	0.39
1/25/2014	4462.14	9.05	4461.680	0.21	3/19/2014	4441.2	3.92	4441.901	0.49
2/21/2014	4461.53	13.09	4461.429	0.01	5/14/2014	4442.32	0.74	4443.602	1.64
3/19/2014	4461.22	15.43	4461.358	0.02	6/12/2014	4443.4	0.05	4444.755	1.84
4/18/2014	4461.45	13.67	4463.363	3.66	7/9/2014	4443.99	0.66	4444.946	0.91
5/14/2014	4464.25	0.81	4466.580	5.43	8/8/2014	4446.31	9.80	4444.622	2.85
6/12/2014	4467.89	7.52	4467.781	0.01	10/7/2014	4445.45	5.15	4444.420	1.06
7/9/2014	4468.3	9.94	4468.859	0.31	11/11/2014	4444.01	0.69	4442.939	1.15
8/8/2014	4468.64	12.20	4468.887	0.06	12/9/2014	4443.16	0.00	4442.316	0.71
9/9/2014	4468.57	11.71	4468.705	0.02	1/14/2015	4442.32	0.74	4442.015	0.09
10/7/2014	4468.19	9.26	4466.988	1.44	2/11/2015	4442	1.39	4441.934	0.00
11/11/2014	4466.35	1.45	4463.002	11.21	3/9/2015	4441.65	2.34	4441.908	0.07
12/9/2014	4464.31	0.70	4462.228	4.33	4/13/2015	4441.15	4.12	4442.390	1.54
1/14/2015	4463.3	3.41	4461.747	2.41	5/4/2015	4442.39	0.62	4442.926	0.29
2/11/2015	4462.76	5.70	4461.450	1.72					
3/9/2015	4462.34	7.88	4461.345	0.99					
4/13/2015	4461.78	11.34	4463.000	1.49					
5/4/2015	4463.79	1.84	4463.875	0.01					
Average =	4465.1	156.89		47.36	Average =	4443.2	56.79		21.24
NS = 1 - (F/F <sub>o</sub> ) =	0.70				NS = 1 - (F/F <sub>o</sub> ) =	0.63			

209718					
Date	Obs head (ft)	$F_o = \sum[\text{obs} - (\text{avg. obs})]^2$	Sim head (ft)	$F = \sum(\text{obs-sim})^2$	
7/19/2013	4443.0		11.67	4444.809	3.13
7/25/2013	4442.6		8.62	4444.775	4.91
9/19/2013	4443.0		11.67	4442.520	0.27
10/17/2013	4440.1		0.26	4440.738	0.37
11/21/2013	4437.8		3.36	4439.061	1.62
12/17/2013	4437.0		6.73	4438.116	1.18
1/25/2014	4436.9		7.26	4437.583	0.43
1/29/2014	4436.9		7.42	4437.526	0.39
2/3/2014	4436.9		7.53	4437.466	0.34
2/8/2014	4436.9		7.70	4437.479	0.40
2/13/2014	4436.8		7.75	4437.479	0.41
2/18/2014	4436.8		7.81	4437.467	0.41
2/21/2014	4436.9		7.70	4437.448	0.36
3/19/2014	4437.0		6.89	4437.292	0.09
4/18/2014	4437.9		2.87	4438.236	0.09
5/14/2014	4442.3		7.16	4440.366	3.74
6/12/2014	4444.6		24.56	4442.958	2.63
7/9/2014	4444.6		24.26	4444.187	0.13
8/8/2014	4444.2		20.48	4443.709	0.19
9/9/2014	4443.1		12.29	4442.360	0.59
11/11/2014	4439.7		0.00	4439.151	0.28
12/9/2014	4438.7		0.95	4438.238	0.17
1/14/2015	4439.1		0.31	4437.456	2.60
2/11/2015	4438.9		0.47	4437.310	2.66
3/9/2015	4438.9		0.55	4437.210	2.79
4/13/2015	4439.0		0.38	4437.834	1.38
5/4/2015	4440.3		0.47	4438.741	2.46
Average =	4439.6		197.11		34.01
NS = 1 - (F/F <sub>o</sub> ) =	0.83				

### Nash efficiency coefficient analysis (Targets group 2)

276103					276106				
Date	Obs head (ft)	$F_o = \sum[\text{obs} - (\text{avg. obs})]^2$	Sim head (ft)	$F = \sum(\text{obs} - \text{sim})^2$	Date	Obs head (ft)	$F_o = \sum[\text{obs} - (\text{avg. obs})]^2$	Sim head (ft)	$F = \sum(\text{obs} - \text{sim})^2$
10/8/2004	4436.66	1.07			10/8/2004	4434.01	0.58		
12/17/2004	4434.8	0.68			12/17/2004	4432.95	0.09		
1/21/2005	4434.36	1.60			1/21/2005	4432.57	0.46		
2/11/2005	4434.26	1.87			2/11/2005	4432.55	0.49		
4/6/2005	4434.12	2.27			4/6/2005	4432.46	0.62		
5/4/2005	4434.45	1.38			5/4/2005	4432.55	0.49		
5/13/2005	4435.84	0.05			5/13/2005	4433.46	0.04		
5/16/2005	4435.91	0.08			5/16/2005	4433.34	0.01		
5/23/2005	4435.94	0.10			5/23/2005	4433.38	0.02		
5/31/2005	4435.83	0.04			5/31/2005	4433.29	0.00		
6/6/2005	4436.01	0.15			6/6/2005	4433.57	0.10		
6/13/2005	4436.01	0.15			6/13/2005	4433.76	0.26		
6/20/2005	4435.92	0.09			6/20/2005	4433.58	0.11		
6/27/2005	4435.83	0.04			6/27/2005	4433.57	0.10		
7/5/2005	4435.69	0.00			7/5/2005	4433.31	0.00		
7/11/2005	4435.76	0.02			7/11/2005	4433.34	0.01		
7/18/2005	4435.83	0.04			7/18/2005	4433.13	0.01		
7/26/2005	4435.92	0.09			7/26/2005	4433.12	0.02		
8/2/2005	4435.95	0.10			8/2/2005	4433.01	0.06		
8/22/2005	4436.07	0.20			8/22/2005	4433.18	0.00		
9/28/2005	4436.26	0.40			9/28/2005	4433.65	0.16		
10/13/2005	4436.37	0.55			10/13/2005	4433.73	0.23		
10/24/2005	4435.9	0.07			10/24/2005	4433.55	0.09		
10/31/2005	4435.59	0.00			10/31/2005	4433.43	0.03		
11/8/2005	4435.42	0.04			11/8/2005	4433.37	0.01		
8/13/2013	4435.92	0.09	4436.272	0.12	8/13/2013	4433.17	0.01		
9/19/2013	4436.63	1.01	4436.293	0.11	9/19/2013	4433.53	0.08	4434.395	0.75
10/17/2013	4435.83	0.04	4435.765	0.00	10/17/2013	4433.49	0.06	4434.222	0.54
11/21/2013	4435.05	0.33	4434.937	0.01	11/21/2013	4433.04	0.04	4433.837	0.64
12/17/2013	4434.63	0.99	4434.631	0.00	12/17/2013	4432.69	0.31	4433.625	0.87
1/25/2014	4434.38	1.55	4434.472	0.01	1/25/2014	4432.57	0.46	4433.496	0.86
2/21/2014	4434.23	1.95	4434.442	0.04	2/21/2014	4432.47	0.61	4433.476	1.01
3/19/2014	4434.24	1.92	4434.425	0.03	3/19/2014	4432.61	0.41	4433.496	0.78
4/18/2014	4434.13	2.24	4434.986	0.73	4/18/2014	4432.58	0.45	4433.863	1.65
5/14/2014	4434.77	0.73	4435.744	0.95	5/14/2014	4432.86	0.15	4434.426	2.45
6/12/2014	4435.51	0.01	4436.459	0.90	6/12/2014	4433.37	0.01	4434.885	2.30
7/9/2014	4435.32	0.09	4436.539	1.49	7/9/2014	4433.38	0.02	4434.899	2.31
8/8/2014	4435.85	0.05	4436.254	0.16	8/8/2014	4433.58	0.11	4434.496	0.84
9/9/2014	4436.35	0.52	4436.262	0.01	9/9/2014	4433.5	0.06	4434.350	0.72
10/7/2014	4435.88	0.06	4436.063	0.03	10/7/2014	4433.56	0.10	4434.349	0.62
11/11/2014	4435.3	0.11	4435.174	0.02	11/11/2014	4433.24	0.00	4433.964	0.52
12/9/2014	4435.01	0.38	4434.727	0.08	12/9/2014	4433.13	0.01	4433.707	0.33
1/14/2015	4434.63	0.99	4434.503	0.02	1/14/2015	4432.82	0.19	4433.522	0.49
2/11/2015	4434.53	1.20	4434.446	0.01	2/11/2015	4432.8	0.20	4433.476	0.46
3/9/2015	4434.36	1.60	4434.431	0.01	3/9/2015	4432.6	0.42	4433.481	0.78
4/13/2015	4434.22	1.98	4434.837	0.38	4/13/2015	4432.59	0.44	4433.749	1.34
5/4/2015	4434.86	0.59	4435.230	0.14	5/4/2015	4432.78	0.22	4434.063	1.65
Average =	4435.6	29.55		5.26	Average =	4433.3	8.38		21.91
NS = 1 - (F/Fo) =	0.82				NS = 1 - (F/Fo) =	-1.62			

276109					276112				
Date	Obs head (ft)	$F_o = \sum [\text{obs} - (\text{avg. obs})]^2$	Sim head (ft)	$F = \sum (\text{obs} - \text{sim})^2$	Date	Obs head (ft)	$F_o = \sum [\text{obs} - (\text{avg. obs})]^2$	Sim head (ft)	$F = \sum (\text{obs} - \text{sim})^2$
12/17/2004	4439.9	0.09			38338	4429.82	2.40		
1/21/2005	4439.1	1.17			38373	4429.16	4.87		
2/11/2005	4438.9	1.59			38394	4429.06	5.33		
4/6/2005	4438.6	2.60			38448	4428.88	6.19		
5/4/2005	4439.1	1.26			38476	4430.92	0.20		
5/13/2005	4440.8	0.30			38485	4434.21	8.08		
5/16/2005	4441.0	0.59			38488	4434.98	13.05		
5/23/2005	4441.2	1.08			38495	4435.2	14.69		
5/31/2005	4441.3	1.21			38504	4434.89	12.41		
6/6/2005	4441.5	1.74			38509	4434.81	11.85		
6/13/2005	4441.5	1.76			38516	4434.88	12.34		
6/20/2005	4441.4	1.46			38523	4434.79	11.71		
6/27/2005	4441.3	1.16			38530	4434.07	7.30		
7/5/2005	4441.3	1.27			38538	4433.14	3.14		
7/11/2005	4441.4	1.36			38544	4432.89	2.32		
7/18/2005	4441.5	1.58			38551	4433.33	3.85		
7/26/2005	4441.6	1.93			38559	4434.12	7.57		
8/2/2005	4441.5	1.71			38566	4434.37	9.01		
8/22/2005	4441.7	2.33			38623	4434.34	8.83		
9/28/2005	4442.2	3.95			38649	4432.73	1.86		
10/13/2005	4442.2	3.95			38656	4431.7	0.11		
10/24/2005	4441.7	2.30			38664	4431.17	0.04		
10/31/2005	4441.3	1.12			41536	4433.81	5.96	4429.663	17.20
11/8/2005	4441.0	0.69			41564	4431.17	0.04	4428.853	5.37
9/19/2013	4441.3	1.18	4440.067	1.50	41599	4429.23	4.57	4427.870	1.85
10/17/2013	4440.7	0.20	4439.483	1.36	41625	4428.65	7.39	4427.557	1.19
11/21/2013	4439.5	0.55	4438.502	0.92	41664	4428.33	9.23	4427.397	0.87
12/17/2013	4438.8	1.91	4438.180	0.41	41691	4428.05	11.01	4427.368	0.47
1/25/2014	4438.3	3.47	4438.008	0.11	41717	4428.03	11.14	4427.354	0.46
2/21/2014	4438.1	4.50	4437.974	0.01	41747	4427.94	11.75	4428.012	0.01
3/19/2014	4438.1	4.63	4437.951	0.01	41773	4429.83	2.37	4429.010	0.67
4/18/2014	4437.8	5.63	4438.487	0.43	41802	4431.82	0.20	4429.948	3.50
5/14/2014	4438.8	1.97	4439.283	0.23	41829	4430.43	0.88	4430.039	0.15
6/12/2014	4439.9	0.09	4440.149	0.06	41859	4430.91	0.21	4429.627	1.65
7/9/2014	4439.9	0.10	4440.264	0.14	41891	4432.28	0.83	4429.642	6.96
8/8/2014	4441.0	0.69	4439.989	1.08	41919	4430.92	0.20	4429.245	2.81
9/9/2014	4441.4	1.48	4440.013	1.98	41954	4429.5	3.49	4428.122	1.90
10/7/2014	4440.8	0.39	4439.839	0.98	42018	4428.45	8.51	4427.426	1.05
11/11/2014	4439.9	0.12	4438.772	1.18	42046	4428.39	8.87	4427.371	1.04
12/9/2014	4439.4	0.69	4438.279	1.19	42072	4428.19	10.10	4427.359	0.69
1/14/2015	4438.8	2.02	4438.041	0.55	42107	4427.96	11.61	4427.851	0.01
2/11/2015	4438.6	2.73	4437.978	0.33	42128	4430.1	1.61	4428.265	3.37
3/9/2015	4438.3	3.66	4437.958	0.11					
4/13/2015	4438.0	4.89	4438.342	0.12					
5/4/2015	4438.8	1.86	4438.773	0.00					
Average =	4440.2	80.96		12.71	Average =	4431.4	257.10		51.20
NS = 1 - (F/Fo) =	0.84				NS = 1 - (F/Fo) =	0.80			

276285					276285 (continued)					
Date	Obs head (ft)	$F_o = \sum[\text{obs} - (\text{avg. obs})]^2$	Sim head (ft)	$F = \sum(\text{obs} - \text{sim})^2$	Date	Obs head (ft)	$\sum[\text{obs} - (\text{avg. obs} - \text{Sim head (ft)})$	$F = \sum(\text{obs} - \text{sim})^2$		
12/17/2004	4414.76		1.41		5/18/2014	4416.54	0.35	4414.40	4.57	
1/21/2005	4414.56		1.93		5/23/2014	4416.90	0.90	4414.46	5.95	
2/11/2005	4414.23		2.96		5/29/2014	4417.81	3.46	4414.50	10.94	
4/6/2005	4414.54		1.99		6/3/2014	4417.84	3.58	4414.54	10.92	
5/4/2005	4414.94		1.02		6/8/2014	4417.53	2.50	4414.74	7.79	
5/13/2005	4417.32		1.88		6/13/2014	4417.64	2.86	4414.83	7.89	
5/16/2005	4417.96		4.04		6/18/2014	4417.90	3.81	4414.89	9.07	
5/23/2005	4419.14		10.18		6/23/2014	4417.76	3.28	4414.93	8.00	
6/1/2005	4419.29		11.16		6/28/2014	4417.58	2.66	4414.97	6.83	
6/7/2005	4419.17		10.37		7/3/2014	4417.37	2.02	4415.00	5.64	
6/13/2005	4419.29		11.16		7/8/2014	4416.85	0.81	4414.53	5.39	
6/19/2005	4419.14		10.18		7/13/2014	4416.74	0.63	4414.37	5.61	
6/27/2005	4418.97		9.13		7/18/2014	4416.99	1.08	4414.31	7.17	
7/5/2005	4418.75		7.84		7/23/2014	4416.92	0.94	4414.28	6.95	
7/11/2005	4417.78		3.35		7/29/2014	4416.97	1.04	4414.27	7.31	
7/18/2005	4418.2		5.07		8/3/2014	4417.15	1.44	4414.25	8.39	
7/26/2005	4418.25		5.29		8/8/2014	4417.26	1.72	4414.13	9.77	
8/3/2005	4418.67		7.40		8/13/2014	4417.47	2.31	4414.08	11.51	
8/22/2005	4418.57		6.87		8/18/2014	4417.81	3.46	4414.06	14.03	
9/28/2005	4419.24		10.83		8/23/2014	4417.69	3.03	4414.06	13.17	
10/24/2005	4418.16		4.89		8/29/2014	4417.67	2.96	4414.06	13.02	
10/31/2005	4417.03		1.17		9/3/2014	4417.62	2.79	4414.07	12.64	
11/8/2005	4416.46		0.26		9/8/2014	4417.45	2.25	4414.12	11.08	
12/17/2013	4414.87		1.16	4413.173	2.88	9/13/2014	4417.47	2.31	4414.15	11.05
1/23/2014	4414.38		2.46	4413.026	1.83	9/18/2014	4417.26	1.72	4414.16	9.64
1/29/2014	4414.32		2.65	4413.016	1.70	9/23/2014	4417.26	1.72	4414.16	9.62
2/3/2014	4414.22		2.99	4413.009	1.47	9/28/2014	4417.41	2.13	4414.16	10.54
2/8/2014	4414.12		3.35	4413.013	1.23	10/3/2014	4417.42	2.16	4414.17	10.60
2/13/2014	4414.23		2.96	4413.011	1.49	10/8/2014	4417.26	1.72	4413.99	10.73
2/18/2014	4414.24		2.92	4413.008	1.52	10/13/2014	4417.35	1.96	4413.91	11.86
2/23/2014	4414.19		3.09	4413.004	1.41	10/18/2014	4417.36	1.99	4413.85	12.33
2/27/2014	4414.13		3.31	4413.000	1.28	10/23/2014	4416.57	0.39	4413.81	7.64
3/3/2014	4414.12		3.35	4412.997	1.26	10/29/2014	4415.98	0.00	4413.77	4.88
3/8/2014	4414.22		2.99	4413.035	1.40	11/3/2014	4415.59	0.13	4413.74	3.41
3/13/2014	4414.19		3.09	4413.044	1.31	11/8/2014	4415.34	0.37	4413.61	3.00
3/18/2014	4414.16		3.20	4413.045	1.24	11/13/2014	4415.00	0.90	4413.53	2.15
3/23/2014	4414.15		3.24	4413.043	1.23	11/18/2014	4414.86	1.19	4413.48	1.91
3/29/2014	4414.15		3.24	4413.040	1.23	11/23/2014	4414.84	1.23	4413.43	1.98
4/3/2014	4414.12		3.35	4413.037	1.17	11/28/2014	4414.75	1.44	4413.40	1.83
4/8/2014	4414.12		3.35	4413.406	0.51	12/3/2014	4414.67	1.64	4413.37	1.70
4/13/2014	4414.28		2.79	4413.555	0.53	12/8/2014	4414.64	1.71	4413.25	1.92
4/18/2014	4414.71		1.54	4413.625	1.18	12/13/2014	4414.59	1.85	4413.20	1.93
4/23/2014	4415.33		0.38	4413.669	2.76	12/18/2014	4414.53	2.01	4413.17	1.85
4/28/2014	4415.99		0.00	4413.700	5.24	12/23/2014	4414.49	2.13	4413.15	1.80
5/3/2014	4416.19		0.06	4413.724	6.08	12/29/2014	4414.39	2.43	4413.13	1.59
5/8/2014	4416.48		0.28	4414.153	5.41	1/3/2015	4414.36	2.53	4413.12	1.55
5/13/2014	4416.52		0.33	4414.318	4.85	1/8/2015	4414.46	2.22	4413.07	1.93

276285 (continued)					277868				
Date	Obs head (ft)	$\Sigma[\text{obs}-(\text{avg. obs})]$	Sim head (ft)	$F = \Sigma(\text{obs-sim})^2$	Date	Obs head (ft)	$F_o = \Sigma[\text{obs}-(\text{avg. obs})]^2$	Sim head (ft)	$F = \Sigma(\text{obs-sim})^2$
1/13/2015	4414.44	2.28	4413.05	1.94	5/14/2014	4426.66	0.03	4429.178	6.34
1/18/2015	4414.37	2.49	4413.03	1.78	6/12/2014	4426.98	0.02	4429.793	7.91
1/23/2015	4414.33	2.62	4413.02	1.71	7/9/2014	4426.97	0.02	4429.680	7.34
1/29/2015	4414.32	2.65	4413.02	1.70	8/8/2014	4427.18	0.12	4429.056	3.52
2/3/2015	4414.28	2.79	4413.01	1.62	8/19/2014	4427.27	0.20	4428.929	2.75
2/8/2015	4414.26	2.85	4413.01	1.56	9/9/2014	4427.27	0.20	4428.935	2.77
2/13/2015	4414.28	2.79	4413.01	1.61	10/7/2014	4427.31	0.23	4428.776	2.15
2/18/2015	4414.27	2.82	4413.01	1.60	11/11/2014	4427.05	0.05	4428.150	1.21
2/23/2015	4414.29	2.75	4413.00	1.66	11/18/2014	4426.91	0.01	4428.060	1.32
2/27/2015	4414.35	2.56	4413.00	1.83	12/9/2014	4426.84	0.00	4427.822	0.96
3/3/2015	4414.39	2.43	4413.00	1.94	1/14/2015	4426.59	0.06	4427.607	1.03
3/8/2015	4414.46	2.22	4413.03	2.04	1/30/2015	4426.58	0.06	4427.573	0.99
3/13/2015	4414.53	2.01	4413.04	2.21	2/11/2015	4426.57	0.07	4427.569	1.00
3/18/2015	4414.62	1.77	4413.04	2.48	3/9/2015	4426.45	0.14	4427.587	1.29
3/23/2015	4414.67	1.64	4413.04	2.65	3/30/2015	4426.44	0.15	4427.610	1.37
3/29/2015	4414.17	3.17	4413.04	1.28	4/13/2015	4426.41	0.17	4428.120	2.92
4/3/2015	4414.15	3.24	4413.04	1.24	5/4/2015	4426.6	0.05	4428.454	3.44
4/8/2015	4414.10	3.42	4413.41	0.48	Average =	4426.8	1.58		48.33
4/13/2015	4414.33	2.62	4413.55	0.60	NS =1-(F/Fo) =	-29.60			
4/18/2015	4414.56	1.93	4413.62	0.88					
4/23/2015	4414.85	1.21	4413.67	1.40					
42122.00	4415.29	0.43	4413.70	2.53					
42127.00	4415.58	0.14	4413.72	3.44					
Average =	4415.95	327.04		421.45					
NS =1-(F/Fo) =	-0.29								

**Nash efficiency coefficient analysis (Targets group 3)**

107080					107080 (continue..)				
Date	Obs head (ft)	$F_o = \sum[\text{obs} - (\text{avg. obs})]^2$	Sim head (ft)	$F = \sum(\text{obs} - \text{sim})^2$					
6/2/2004	4455.06	0.07			3/3/2011	4455.05	0.07		
11/30/2004	4456.04	0.52			4/6/2011	4454.93	0.15		
3/7/2005	4453.63	2.85			5/6/2011	4454.94	0.14		
6/1/2005	4454.86	0.21			6/6/2011	4455.52	0.04		
8/29/2005	4453.4	3.68			9/7/2011	4458.05	7.46		
12/5/2005	4456.07	0.57			12/20/2011	4456.44	1.26		
8/30/2006	4456.94	2.63			3/12/2012	4454.90	0.17		
11/30/2006	4456.13	0.66			9/27/2012	4458.20	8.31		
3/26/2007	4454.02	1.69			12/6/2012	4455.75	0.19		
8/27/2007	4453.97	1.82			3/13/2013	4453.76	2.43		
12/4/2007	4455.85	0.28			6/18/2013	4453.88	2.07	4456.60	7.38
3/4/2008	4454.02	1.69			7/15/2013	4454.18	1.30	4456.63	6.00
5/8/2008	4453.91	1.98			8/14/2013	4456.39	1.15	4456.16	0.05
6/5/2008	4456.45	1.28			9/19/2013	4456.43	1.24	4456.24	0.04
9/4/2008	4457.84	6.36			10/17/2013	4456.39	1.15	4455.35	1.08
10/23/2008	4457.76	5.96			11/21/2013	4455.05	0.07	4454.11	0.88
11/3/2008	4457.17	3.43			12/17/2013	4454.26	1.12	4453.66	0.36
12/3/2008	4456.06	0.55			1/25/2014	4453.60	2.95	4453.38	0.05
1/7/2009	4455.16	0.02			2/21/2014	4453.21	4.44	4453.33	0.01
2/12/2009	4454.64	0.46			3/19/2014	4453.07	5.05	4453.35	0.08
3/8/2009	4454.37	0.90			4/18/2014	4452.36	8.75	4454.09	2.99
4/7/2009	4454.33	0.98			5/14/2014	4451.77	12.59	4455.27	12.22
5/7/2009	4454.7	0.38			7/9/2014	4455.32	0.00	4456.79	2.16
6/7/2009	4456.16	0.71			8/8/2014	4455.03	0.08	4456.20	1.37
8/6/2009	4458.01	7.25			9/9/2014	4457.37	4.21	4456.08	1.66
9/3/2009	4456.48	1.35			10/7/2014	4457.31	3.97	4455.86	2.11
10/8/2009	4458.56	10.51			11/11/2014	4456.13	0.66	4454.44	2.85
11/3/2009	4457.49	4.72			12/9/2014	4450.31	25.08	4453.82	12.34
12/3/2009	4456.46	1.30			1/14/2015	4454.49	0.69	4453.44	1.11
1/7/2010	4455.44	0.01			2/11/2015	4454.08	1.53	4453.33	0.56
2/2/2010	4455.07	0.06			3/9/2015	4453.76	2.43	4453.33	0.19
3/2/2010	4454.68	0.41			4/13/2015	4453.35	3.87	4453.87	0.27
4/2/2010	4454.36	0.92			5/4/2015	4453.95	1.87	4454.51	0.32
5/5/2010	4454.53	0.62			6/30/2015	4455.18	0.02	4456.78	2.56
10/7/2010	4458.43	9.68			12/23/2015	4454.72	0.36	4455.02	0.09
11/4/2010	4457.89	6.61							
12/7/2010	4456.84	2.32							
1/6/2011	4456.04	0.52							
Average =					4455.32	192.90	58.72		
NS = 1 - (F/Fo) =					0.70				

261912					276041					279258					
Date	Obs head (ft)	$F_o = \sum[\text{obs} - (\text{avg. obs})]^2$	Sim head (ft)	$F = \sum(\text{obs} - \text{sim})^2$	Date	Obs head (ft)	$F_o = \sum[\text{obs} - (\text{avg. obs})]^2$	Sim head (ft)	$F = \sum(\text{obs} - \text{sim})^2$	Date	Obs head (ft)	$F_o = \sum[\text{obs} - (\text{avg. obs})]^2$	Sim head (ft)	$F = \sum(\text{obs} - \text{sim})^2$	
7/23/2013	4468.36	4.84	4467.417	0.89	10/25/2013	4457.53	1.00	4457.056	0.22	9/9/2014	4452.89	4452.883	7.07	0.00	
9/19/2013	4467.83	2.79	4466.563	1.61	11/21/2013	4456.63	0.01	4456.116	0.26	10/7/2014	4452.79	4452.634	6.55	0.02	
10/17/2013	4467.32	1.34	4466.638	0.47	12/17/2013	4455.88	0.43	4455.687	0.04	11/11/2014	4451.74	4451.162	2.28	0.33	
11/21/2013	4465.75	0.17	4466.223	0.22	1/25/2014	4455.26	1.62	4455.428	0.03	12/9/2014	4451.08	4450.502	0.72	0.33	
12/17/2013	4465.13	1.06	4465.810	0.46	3/19/2014	4454.74	3.21	4455.423	0.47	1/14/2015	4450.3	4450.126	0.00	0.03	
1/25/2014	4464.44	2.96	4465.598	1.34	4/18/2014	4454.75	3.18	4456.225	2.18	2/13/2015	4449.94	4450.020	0.08	0.01	
2/21/2014	4464.15	4.04	4465.606	2.12	5/14/2014	4455.43	1.21	4457.377	3.79	2/18/2015	4449.903	4450.016	0.11	0.01	
3/19/2014	4463.91	5.07	4465.748	3.38	7/9/2014	4457.63	1.21	4458.663	1.07	2/23/2015	4449.863	4450.013	0.14	0.02	
4/18/2014	4464.05	4.46	4466.989	8.64	8/8/2014	4458.29	3.09	4457.937	0.12	2/27/2015	4449.757	4450.011	0.23	0.06	
5/14/2014	4466.12	0.00	4468.203	4.34	9/9/2014	4459.03	6.24	4457.754	1.63	3/3/2015	4449.71	4450.009	0.27	0.09	
6/12/2014	4468.75	6.70	4469.082	0.11	10/7/2014	4459.02	6.19	4457.599	2.02	3/8/2015	4449.627	4450.006	0.37	0.14	
7/9/2014	4468.65	6.20	4468.174	0.23	11/11/2014	4457.89	1.84	4456.402	2.21	3/13/2015	4449.58	4450.010	0.42	0.18	
8/8/2014	4468.14	3.92	4466.730	1.99	12/9/2014	4457.13	1.99	4455.851	1.64	3/18/2015	4449.542	4450.017	0.47	0.23	
9/9/2014	4468.31	4.62	4466.441	3.49	1/14/2015	4456.36	0.03	4455.480	0.77	3/23/2015	4449.508	4450.025	0.52	0.27	
10/7/2014	4468.18	4.08	4466.700	2.19	2/11/2015	4455.64	0.80	4455.388	0.06	3/29/2015	4449.443	4450.032	0.62	0.35	
11/11/2014	4466.71	0.30	4466.344	0.13	3/9/2015	4455.34	1.42	4455.393	0.00	4/3/2015	4449.386	4450.038	0.71	0.42	
12/9/2014	4465.85	0.10	4465.957	0.01	4/13/2015	4455.34	1.42	4456.006	0.44	4/8/2015	4449.337	4450.233	0.80	0.80	
1/14/2015	4465.27	0.79	4465.631	0.13	5/4/2015	4455.69	0.71	4456.608	0.84	4/13/2015	4449.305	4450.453	0.86	1.32	
2/11/2015	4464.73	2.05	4465.604	0.76						4/18/2015	4449.345	4450.660	0.79	1.73	
3/9/2015	4464.21	3.81	4465.694	2.20						4/23/2015	4449.459	4450.836	0.60	1.90	
4/13/2015	4464.04	4.50	4466.812	7.68						4/28/2015	4449.684	4450.979	0.30	1.68	
5/4/2015	4465.64	0.27	4467.205	2.45						5/3/2015	4449.804	4451.092	0.18	1.66	
Average =					4456.2	64.05	44.85	Average =			4450.2	33.69	11.74		
NS = 1 - (F/Fo) =					0.30	NS = 1 - (F/Fo) =					0.48	NS = 1 - (F/Fo) =			0.65

**Nash efficiency coefficient analysis (Targets group 4)**

195941					276038				
Date	Obs head (ft)	$\sum[\text{obs}-(\text{avg. obs})]$	Sim head (ft)	$F = \sum(\text{obs-sim})^2$	Date	Obs head (ft)	$F_o = \sum[\text{obs}-(\text{avg. obs})]^2$	Sim head (ft)	$F = \sum(\text{obs-sim})^2$
6/16/2011	4462.78	6.55			11/21/2013	4451.69	0.00	4452.684	0.99
7/19/2013	4461.58	1.85	4462.328	0.56	12/17/2013	4451.53	0.03	4452.343	0.66
8/14/2013	4461.45	1.51	4461.481	0.00	1/25/2014	4451.34	0.13	4452.182	0.71
9/19/2013	4461.61	1.93	4461.539	0.01	2/21/2014	4451.23	0.22	4452.208	0.96
10/17/2013	4461.43	1.46	4461.432	0.00	4/18/2014	4451.31	0.15	4453.497	4.78
11/21/2013	4460.1	0.01	4460.896	0.63	5/14/2014	4451.68	0.00	4454.505	7.98
12/17/2013	4459.37	0.72	4460.496	1.27	7/9/2014	4452.25	0.30	4454.183	3.74
1/25/2014	4458.72	2.25	4460.281	2.44	9/9/2014	4452.25	0.30	4452.551	0.09
2/21/2014	4458.35	3.50	4460.278	3.72	10/7/2014	4452.37	0.45	4452.814	0.20
3/19/2014	4458.17	4.21	4460.392	4.94	11/11/2014	4452	0.09	4452.730	0.53
4/18/2014	4458.23	3.96	4461.477	10.54	12/9/2014	4451.76	0.00	4452.472	0.51
5/14/2014	4459.41	0.66	4462.618	10.29	1/14/2015	4451.57	0.02	4452.204	0.40
6/12/2014	4461.34	1.25	4463.519	4.75	2/11/2015	4451.49	0.04	4452.203	0.51
7/9/2014	4461.75	2.34	4462.948	1.44	3/9/2015	4451.34	0.13	4452.297	0.92
9/9/2014	4462.28	4.24	4461.405	0.77					
10/7/2014	4462.28	4.24	4461.568	0.51					
11/11/2014	4461.04	0.67	4461.048	0.00					
12/9/2014	4460.23	0.00	4460.649	0.18					
1/14/2015	4459.5	0.52	4460.318	0.67					
2/11/2015	4459.04	1.39	4460.277	1.53					
3/9/2015	4458.67	2.41	4460.341	2.79					
4/13/2015	4458.34	3.54	4461.291	8.71					
5/4/2015	4459.41	0.66	4461.721	5.34					
Average =	4460.2	49.87		61.06	Average =	4451.7	1.87		22.97
NS =1-(F/F <sub>o</sub> ) =	-0.22				NS =1-(F/F <sub>o</sub> ) =	-11.28			

276107					276108				
Date	Obs head (ft)	$F_o = \sum[\text{obs}-(\text{avg. obs})]^2$	Sim head (ft)	$F = \sum(\text{obs-sim})^2$	Date	Obs head (ft)	$F_o = \sum[\text{obs}-(\text{avg. obs})]^2$	Sim head (ft)	$F = \sum(\text{obs-sim})^2$
10/8/2004	4436.65	1.92			10/8/2004	4438.67	0.17		
12/17/2004	4434.63	0.40			12/17/2004	4437.57	0.47		
1/21/2005	4434.41	0.73			1/21/2005	4437.44	0.67		
2/11/2005	4434.33	0.87			2/11/2005	4437.15	1.23		
4/5/2005	4434.24	1.05			4/6/2005	4437.17	1.18		
5/4/2005	4437.29	4.11			5/4/2005	4437.46	0.64		
5/13/2005	4435.53	0.07			5/13/2005	4439.8	2.38		
5/16/2005	4435.36	0.01			5/16/2005	4439.8	2.38		
5/23/2005	4435.48	0.05			5/23/2005	4439.85	2.53		
5/31/2005	4435.28	0.00			5/31/2005	4439.49	1.52		
6/6/2005	4435.61	0.12			6/6/2005	4439.7	2.08		
6/13/2005	4436.08	0.67			6/13/2005	4439.76	2.26		
6/20/2005	4435.84	0.33			6/20/2005	4439.55	1.67		
6/27/2005	4436.07	0.65			6/27/2005	4439.32	1.13		
7/5/2005	4436.32	1.12			7/5/2005	4438.34	0.01		
7/11/2005	4435.2	0.00			7/11/2005	4438.21	0.00		
7/18/2005	4435	0.07			7/18/2005	4437.9	0.13		
7/26/2005	4434.7	0.32			7/26/2005	4437.67	0.35		
8/2/2005	4434.53	0.54			8/2/2005	4437.52	0.54		
8/22/2005	4434.48	0.61			8/22/2005	4437.45	0.65		
9/28/2005	4435.49	0.05			9/28/2005	4438.11	0.02		
10/13/2005	4435.5	0.06			10/13/2005	4439.49	1.52		
10/24/2005	4435.27	0.00			10/24/2005	4438.07	0.04		
10/31/2005	4435.08	0.03			10/31/2005	4437.89	0.14		
11/8/2005	4435.02	0.06			11/8/2005	4437.85	0.17		
8/13/2013	4435.21	0.00	4436.091	0.78	8/13/2013	4437.65	0.37	4437.697	0.00
9/19/2013	4435.51	0.06	4435.935	0.18	9/19/2013	4438.81	0.30	4437.782	1.06
10/17/2013	4435.19	0.01	4435.897	0.50	10/17/2013	4437.9	0.13	4438.000	0.01
11/21/2013	4434.9	0.13	4435.648	0.56	11/21/2013	4437.7	0.31	4437.876	0.03
12/17/2013	4434.69	0.33	4435.375	0.47	12/17/2013	4437.96	0.09	4437.532	0.18
1/24/2014	4434.58	0.47	4435.179	0.36	1/25/2014	4438.05	0.04	4437.358	0.48
2/21/2014	4434.52	0.55	4435.171	0.42	2/21/2014	4437.69	0.32	4437.389	0.09
3/19/2014	4434.65	0.38	4435.261	0.37	3/19/2014	4437.61	0.42	4437.551	0.00
4/18/2014	4434.87	0.15	4435.985	1.24	4/18/2014	4437.88	0.14	4438.772	0.80
5/14/2014	4435.24	0.00	4436.777	2.36	5/14/2014	4438.24	0.00	4439.787	2.39
6/12/2014	4436.2	0.88	4437.278	1.16	6/12/2014	4438.64	0.15	4440.345	2.91
7/9/2014	4436.48	1.48	4437.107	0.39	7/9/2014	4438.86	0.36	4439.334	0.22
8/8/2014	4435.8	0.29	4436.282	0.23	8/8/2014	4438.35	0.01	4437.999	0.12
9/9/2014	4435.27	0.00	4435.848	0.33	9/9/2014	4437.89	0.14	4437.657	0.05
10/7/2014	4435.52	0.07	4435.930	0.17	10/7/2014	4438.08	0.03	4437.922	0.02
11/11/2014	4435.16	0.01	4435.725	0.32	11/11/2014	4437.94	0.10	4437.904	0.00
12/9/2014	4435.1	0.03	4435.509	0.17	12/9/2014	4437.84	0.17	4437.670	0.03
1/14/2015	4434.89	0.14	4435.219	0.11	1/14/2015	4437.93	0.11	4437.383	0.30
2/11/2015	4434.87	0.15	4435.167	0.09	2/11/2015	4437.77	0.24	4437.382	0.15
3/9/2015	4434.67	0.35	4435.207	0.29	3/9/2015	4437.59	0.45	4437.484	0.01
4/13/2015	4435.52	0.07	4435.820	0.09	4/13/2015	4438.29	0.00	4438.634	0.12
5/4/2015	4435.16	0.01	4436.210	1.10	5/4/2015	4438.23	0.00	4438.871	0.41
Average =	4435.3	19.39		11.70	Average =	4438.3	27.74		9.40
NS =1-(F/F <sub>o</sub> ) =	0.40				NS =1-(F/F <sub>o</sub> ) =	0.66			

276287					276287 (continued)				
Date	Obs head (ft)	$F_o = \sum [\text{obs} - (\text{avg. obs})]^2$	Sim head (ft)	$F = \sum (\text{obs} - \text{sim})^2$	Date	Obs head (ft)	$F_o = \sum [\text{obs} - (\text{avg. obs})]^2$	Sim head (ft)	$F = \sum (\text{obs} - \text{sim})^2$
4/6/2005	4445.1	0.51			8/3/2014	4445.78	0.00	4446.42	0.41
5/4/2005	4445.28	0.29			8/8/2014	4445.65	0.03	4445.54	0.01
5/13/2005	4446.65	0.69			8/13/2014	4445.59	0.05	4445.32	0.07
5/16/2005	4446.6	0.61			8/18/2014	4445.71	0.01	4445.25	0.22
5/23/2005	4446.64	0.68			8/23/2014	4445.95	0.02	4445.22	0.53
5/31/2005	4446.09	0.07			8/29/2014	4445.93	0.01	4445.21	0.53
6/6/2005	4446.36	0.30			9/3/2014	4445.80	0.00	4445.20	0.36
6/13/2005	4446.49	0.45			9/8/2014	4445.63	0.03	4445.45	0.03
6/20/2005	4446.38	0.32			9/13/2014	4445.63	0.04	4445.51	0.01
6/27/2005	4446.37	0.31			9/18/2014	4445.62	0.04	4445.54	0.01
7/5/2005	4445.97	0.02			9/23/2014	4445.61	0.04	4445.55	0.00
7/12/2005	4445.91	0.01			9/28/2014	4445.75	0.00	4445.55	0.04
7/19/2005	4445.62	0.04			10/3/2014	4445.85	0.00	4445.55	0.09
7/27/2005	4445.35	0.22			10/8/2014	4445.83	0.00	4445.79	0.00
8/2/2005	4445.21	0.37			10/13/2014	4445.81	0.00	4445.84	0.00
8/22/2005	4445.39	0.18			10/18/2014	4445.79	0.00	4445.85	0.00
9/9/2005	4445.33	0.24			10/23/2014	4445.85	0.00	4445.85	0.00
9/28/2005	4446.13	0.10			10/29/2014	4445.87	0.00	4445.84	0.00
10/13/2005	4446.64	0.68			11/3/2014	4445.85	0.00	4445.84	0.00
10/24/2005	4446.01	0.04			11/8/2014	4445.82	0.00	4445.78	0.00
10/31/2005	4445.95	0.02			11/13/2014	4445.59	0.05	4445.76	0.03
11/8/2005	4446	0.03			11/18/2014	4445.60	0.05	4445.75	0.02
12/17/2013	4446.64	0.68	4445.357	1.65	11/23/2014	4445.74	0.01	4445.74	0.00
1/23/2014	4445.471667	0.12	4445.190	0.08	11/28/2014	4445.77	0.00	4445.74	0.00
1/29/2014	4445.423056	0.16	4445.188	0.06	12/3/2014	4445.64	0.03	4445.73	0.01
2/3/2014	4445.300333	0.27	4445.187	0.01	12/8/2014	4445.64	0.03	4445.45	0.03
2/8/2014	4445.26	0.31	4445.219	0.00	12/13/2014	4445.63	0.03	4445.38	0.06
2/13/2014	4445.485167	0.11	4445.227	0.07	12/18/2014	4445.57	0.06	4445.36	0.05
2/18/2014	4445.486917	0.11	4445.229	0.07	12/23/2014	4445.56	0.06	4445.35	0.05
2/23/2014	4445.450714	0.13	4445.230	0.05	12/29/2014	4445.43	0.15	4445.34	0.01
3/18/2014	4445.424286	0.15	4445.413	0.00	1/3/2015	4445.48	0.11	4445.34	0.02
3/23/2014	4445.253417	0.32	4445.417	0.03	1/8/2015	4445.66	0.02	4445.23	0.19
3/29/2014	4445.244931	0.33	4445.420	0.03	1/13/2015	4445.63	0.03	4445.21	0.18
4/3/2014	4445.228333	0.35	4445.421	0.04	1/18/2015	4445.53	0.08	4445.20	0.11
4/8/2014	4445.2815	0.29	4446.455	1.38	1/23/2015	4445.48	0.12	4445.19	0.08
4/13/2014	4445.828333	0.00	4446.699	0.76	1/29/2015	4445.48	0.11	4445.19	0.09
4/18/2014	4445.650917	0.03	4446.778	1.27	2/3/2015	4445.40	0.17	4445.19	0.05
4/23/2014	4445.7185	0.01	4446.811	1.19	2/8/2015	4445.44	0.14	4445.22	0.05
4/28/2014	4445.74025	0.01	4446.827	1.18	2/13/2015	4445.62	0.04	4445.23	0.15
5/3/2014	4445.699583	0.01	4446.836	1.29	2/18/2015	4445.57	0.06	4445.23	0.11
5/8/2014	4445.952333	0.02	4447.717	3.11	2/23/2015	4445.49	0.11	4445.23	0.07
5/13/2014	4445.951	0.02	4447.903	3.81	2/27/2015	4445.43	0.15	4445.23	0.04
5/18/2014	4446.046167	0.05	4447.958	3.66	3/3/2015	4445.37	0.20	4445.23	0.02
5/23/2014	4446.320667	0.25	4447.979	2.75	3/8/2015	4445.35	0.22	4445.37	0.00
5/29/2014	4447.387153	2.47	4447.989	0.36	3/13/2015	4445.43	0.15	4445.40	0.00
6/3/2014	4447.165417	1.82	4447.995	0.69	3/18/2015	4445.63	0.04	4445.41	0.05
6/8/2014	4446.527	0.50	4448.451	3.70	3/23/2015	4445.60	0.05	4445.42	0.03
6/13/2014	4446.301333	0.23	4448.543	5.03	3/29/2015	4445.53	0.08	4445.42	0.01
6/18/2014	4446.6	0.61	4448.570	3.88	4/3/2015	4445.73	0.01	4445.42	0.10
6/23/2014	4446.489583	0.45	4448.580	4.37	4/8/2015	4445.80	0.00	4446.46	0.43
6/28/2014	4446.57275	0.57	4448.585	4.05	4/13/2015	4445.85	0.00	4446.70	0.72
7/3/2014	4446.461417	0.42	4448.587	4.52	4/18/2015	4445.84	0.00	4446.78	0.88
7/8/2014	4446.37125	0.31	4446.919	0.30	4/23/2015	4445.85	0.00	4446.81	0.92
7/13/2014	4446.415167	0.36	4446.576	0.03	4/28/2015	4445.90	0.01	4446.83	0.86
7/18/2014	4446.303917	0.24	4446.478	0.03	5/3/2015	4445.95	0.02	4446.84	0.78
7/23/2014	4446.103417	0.08	4446.442	0.11	Average =	4445.82	20.65		58.32
7/29/2014	4445.93125	0.01	4446.426	0.24	NS = 1 - (F/Fo) =	-1.82			

277329				
Date	Obs head (ft)	$F_o = \sum [\text{obs} - (\text{avg. obs})]^2$	Sim head (ft)	$F = \sum (\text{obs} - \text{sim})^2$
4/6/2005	4442.84		1.00	
5/4/2005	4442.89		0.90	
5/13/2005	4443.86		0.00	
5/16/2005	4443.74		0.01	
5/23/2005	4443.71		0.02	
5/31/2005	4443.46		0.15	
6/6/2005	4443.74		0.01	
6/13/2005	4444.1		0.07	
6/20/2005	4443.91		0.00	
6/27/2005	4444.07		0.05	
7/5/2005	4443.69		0.02	
7/12/2005	4443.71		0.02	
7/18/2005	4443.54		0.09	
7/26/2005	4443.45		0.15	
8/2/2005	4443.39		0.20	
8/22/2005	4443.6		0.06	
9/9/2005	4443.66		0.03	
9/28/2005	4444.19		0.12	
10/13/2005	4444.43		0.35	
10/24/2005	4444.21		0.14	
10/31/2005	4444.08		0.06	
11/8/2005	4444.03		0.04	
4/18/2014	4443.36		0.23	4444.210
5/14/2014	4443.75		0.01	4444.895
6/12/2014	4444.33		0.24	4445.310
7/9/2014	4444.53		0.47	4445.174
8/8/2014	4444.32		0.23	4444.342
9/9/2014	4444.44		0.36	4443.819
10/7/2014	4444.55		0.50	4444.033
11/11/2014	4444.21		0.14	4443.846
12/9/2014	4444.05		0.04	4443.573
1/14/2015	4443.73		0.01	4443.228
2/11/2015	4443.71		0.02	4443.176
3/9/2015	4443.5		0.12	4443.230
4/13/2015	4443.63		0.04	4444.013
5/4/2015	4443.87		0.00	4444.445
Average =	4443.8		5.90	5.51
NS = 1 - (F/Fo)	0.07			



**APPENDIX F**  
**MODEL SENSITIVITY ANALYSIS**

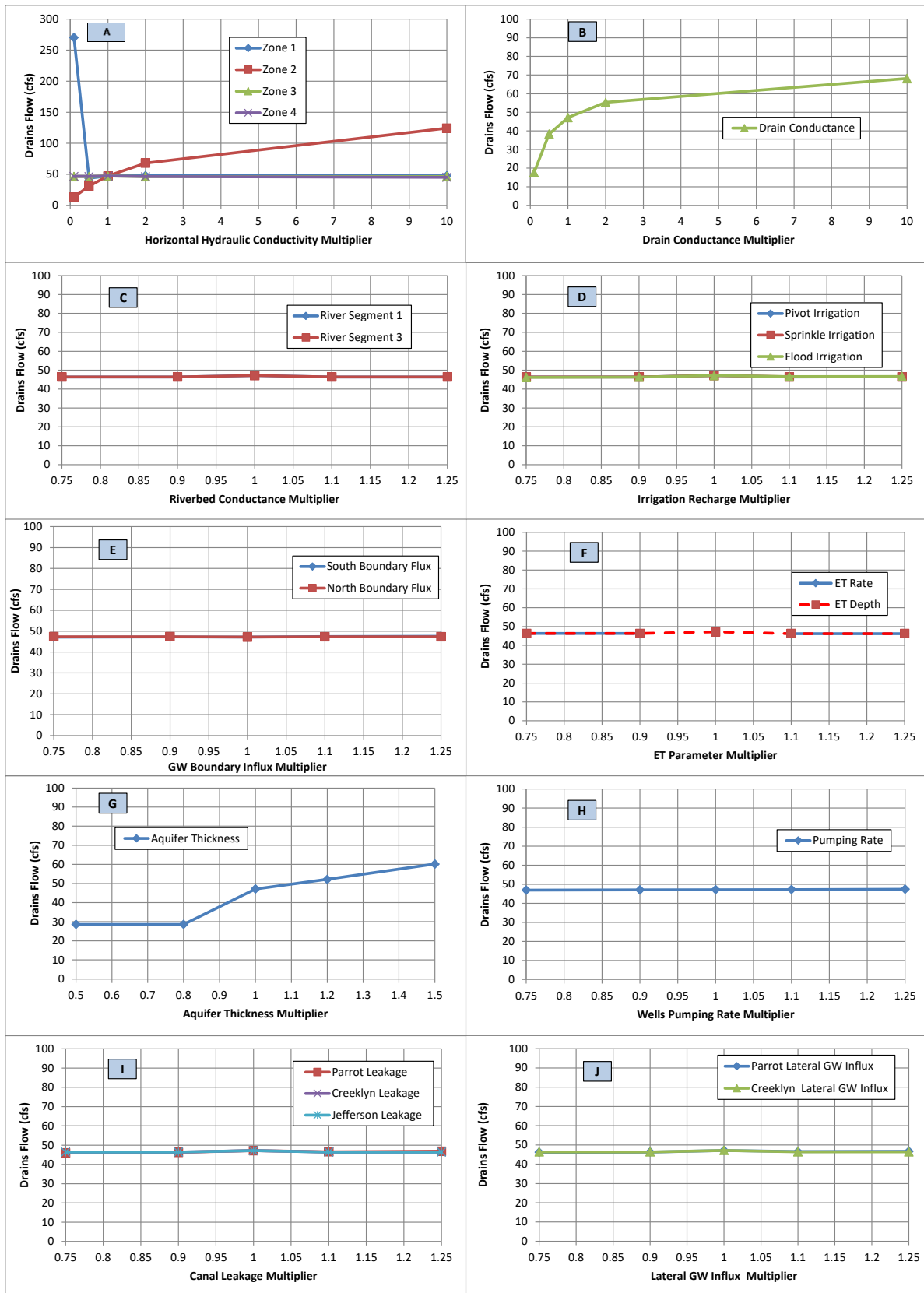


Figure F1. The sensitivity analysis done for the groundwater-fed streams (drains) indicates that the discharge is most sensitive to zone 2 hydraulic conductivity, drain bed conductance, and aquifer thickness.

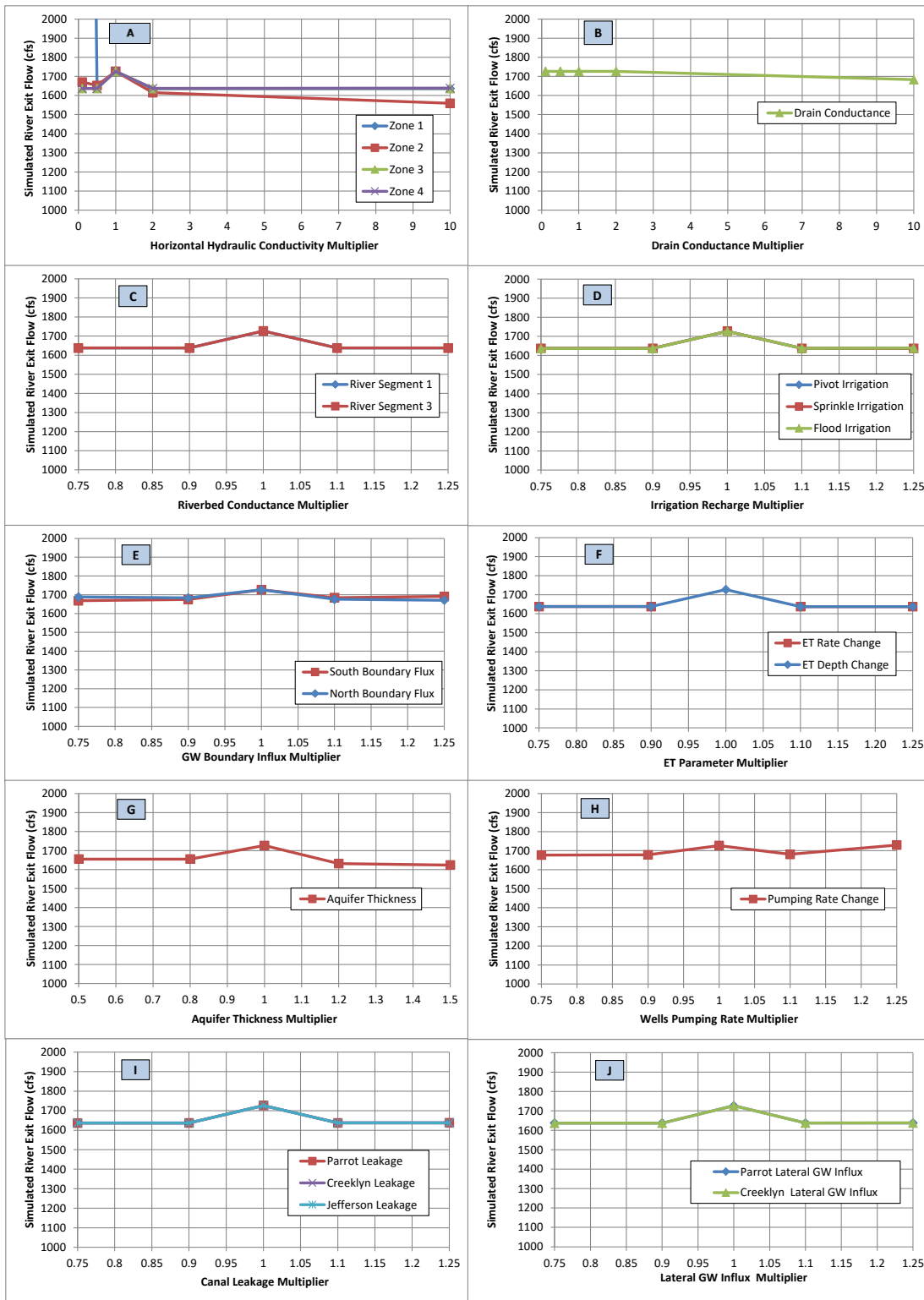


Figure F2. The Jefferson River flow at Corbett's station is sensitive to zone 1 hydraulic conductivity.

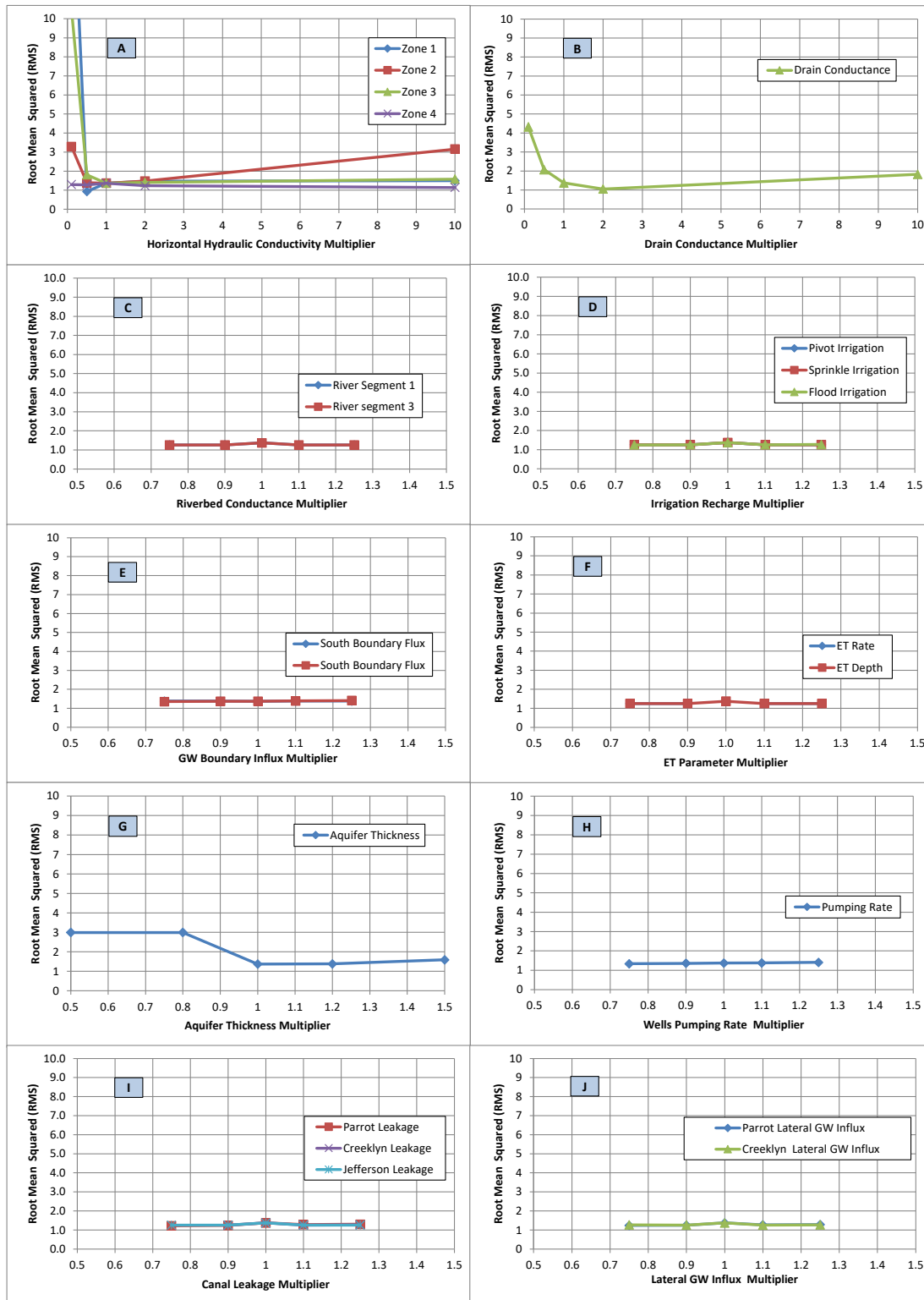


Figure F3. The model sensitivity analysis show that the calibration statistic RMS is most sensitive to hydraulic conductivity in zones 1, 2, and 3, drain bed conductance for Parson’s Slough and Willow Spring, and aquifer thickness.

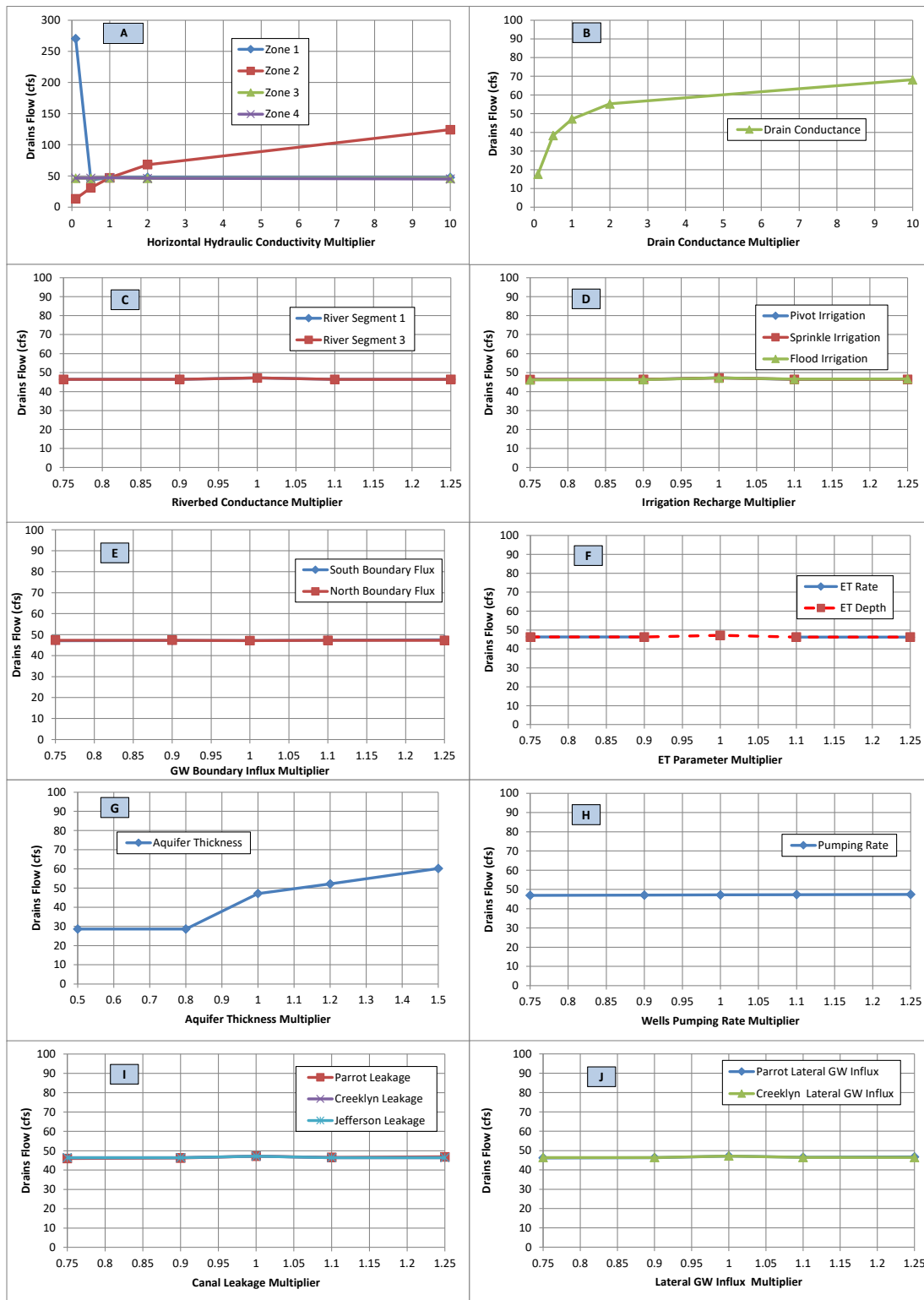


Figure F4. The model sensitivity analysis show that calibration statistics RSS is most sensitive to hydraulic conductivity (zones 1 & 2), drain bed conductance at Parson’s Slough and Willow Springs, and aquifer thickness.

